INFORMATION TO USERS

This manuscript has been reproduced from the microfilm master. UMI films the text directly from the original or copy submitted. Thus, some thesis and dissertation copies are in typewriter face, while others may be from any type of computer printer.

The quality of this reproduction is dependent upon the quality of the copy submitted. Broken or indistinct print, colored or poor quality illustrations and photographs, print bleedthrough, substandard margins, and improper alignment can adversely affect reproduction.

In the unlikely event that the author did not send UMI a complete manuscript and there are missing pages, these will be noted. Also, if unauthorized copyright material had to be removed, a note will indicate the deletion.

Oversize materials (e.g., maps, drawings, charts) are reproduced by sectioning the original, beginning at the upper left-hand corner and continuing from left to right in equal sections with small overlaps.

Photographs included in the original manuscript have been reproduced xerographically in this copy. Higher quality 6" x 9" black and white photographic prints are available for any photographs or illustrations appearing in this copy for an additional charge. Contact UMI directly to order.

ProQuest Information and Learning
300 North Zeeb Road, Ann Arbor, MI 48106-1346 USA
800-521-0600

Molecular and genetic characterization of *rf2*, a mitochondrial aldehyde dehydrogenase gene required for male fertility in maize (*Zea mays* L.)

by

Xiangqin Cui

A dissertation submitted to the graduate faculty

in partial fulfillment of the requirements for the degree of

DOCTOR OF PHILOSOPHY

Major: Genetics

Major Professor: Patrick S. Schnable

Iowa State University

Ames, Iowa

2001

Bell & Howell Information and Learning Company
300 North Zeeb Road
P.O. Box 1346
Ann Arbor, MI 48106-1346

Graduate College

Iowa State University

This is to certify that the Doctoral dissertation of

Xiangqin Cui

has met the dissertation requirements of Iowa State University

Signature was redacted for privacy.

Major professor

Signature was redacted for privacy.

For the Major Program

Signature was redacted for privacy.

For the Graduate College

TABLE OF CONTENTS

CHAPTER 1. GENERAL INTRODUCTION

General Introduction

Maize, commonly known as corn, is a major agricultural crop (Dowswell et al., 1996; Salvador, 1997). Hybrid seeds have played an important role in increasing corn yields during the 20th century (Bauman et al., 1986). The production of hybrid seed often involves the hand emasculation of female parents, which is a labor-intensive process. In the late 1960's, this process was largely (85%) replaced by using the T-cytoplasm male sterility (cms-T) system to induce male sterility in the female parents of commercial hybrids (Ullstrup, 1972). However, plants that carry T cytoplasm are highly susceptible to two fungal strains, *Mycosphaerella zeae-maydis* and race T of *Cochiliobolus heterostrophus*. The latter was directly responsible for the loss of 710 million bushels of corn in the United States during the southern corn leaf blight epidemic in 1970 (Tatum, 1971; Hooker, 1972; Ullstrup, 1972; Wise et al., 1999a).

Since the epidemic, extensive research has been conducted on the cms-T system to address the underlying mechanism of male sterility and fungus susceptibility. It has been demonstrated that both male sterility and fungal susceptibility are due to a T-cytoplasm-specific protein, URF13. URF13 is encoded by the T-cytoplasm mitochondrial genome and accumulates in the mitochondria inner membrane, where it increases membrane permeability (reviewed by Pring and Lonsdale, 1989; Levings, 1990, 1993; Williams and Levings, 1992; Dewey and Korth, 1994; Wise et al., 1999a).

The cms-T system has two unlinked nuclear restorer genes, *rf1* and *rf2*. They work in concert to revert the phenotype of T-cytoplasm-induced male sterility; however, they do not diminish the susceptibility of T-cytoplasm maize to the disease-causing fungi (Duvick, 1965; Ullstrup, 1972). The functional *Rf1* allele is able to alter the accumulation of T-*urf13* transcripts and reduce the accumulation of URF13 by 80% (Forde and Leaver, 1980; Dewey et al., 1986; Dewey et al., 1987; Kennell et al., 1987; Wise et al., 1996). In contrast, the *Rf2* gene does not affect the accumulation of URF13, although it is necessary for the restoration of T-cytoplasm male sterility (Forde and Leaver, 1980; Dewey et al., 1987). Unlike *rf1*, most maize inbred lines have a functional *Rf2* allele (Duvick, 1965; Wise et al., 1999a). Due to its unique behavior, research on the *rf2* gene will not only improve the understanding of cms-T related male sterility and its restoration, but also contribute to the knowledge of nuclear and mitochondrial genome interactions as well as anther development in general.

Dissertation Organization

This dissertation is organized into six chapters. Chapter 1 is a general introduction to the current body of knowledge on the cms-T system and its restorers. Chapters 2, 3, 4 and 5 are papers that have been published or submitted to scientific journals as a result of the dissertation research.

Chapter 2 describes the cloning and sequence analysis of the *rf2* gene. Hypotheses on the mechanism of *rf2* function were formed based on the high degree of sequence similarity between RF2 and mammalian mitochondria aldehyde dehydrogenases. This paper is the

result of contributions from multiple authors. My contributions include the isolation and sequence analysis of the *rf2* cDNA and the mRNA accumulation survey of the mutant alleles.

Chapter 3 describes the genetic and biochemical characterizations of *rf2* and its encoded protein, RF2. This study demonstrates that RF2 is indeed a mitochondrial aldehyde dehydrogenase and that its activity is involved in anther development, even in plants that carry normal cytoplasm. The expression and biochemical analyses of RF2 were conducted by Feng Liu in the Schnable laboratory. The genetic characterization of *rf2* and the analyses of the *rf2-R213* allele arose from my dissertation research.

Chapter 4 describes experiments testing whether the RF2 protein acts in the fermentation pathway. Three genes coding for the rate-limiting enzyme of this pathway, PDC, were knocked out. Mutants from *pdc3* were extensively characterized for their effects on anaerobic tolerance and male fertility. Assistance for sequencing the *pdc* genes and genetic crossing was received from other authors.

Chapter 5 describes the characterization of the *Mu* suppression, which is associated with some of the *rf2* mutant alleles when the *Mu* activity is low in the genome. All data in this paper except the sequencing of the *rf2* genomic clones were directly derived from my dissertation research.

Literature Review

Maize anther development and male sterility

Maize is a monoecious plant. Its male flowers develop in the tassel on the apex of the plant (Kiesselbach, 1999). Each tassel branch has hundreds of spikelets and each spikelet

consists of an upper and lower floret. Three anthers develop in each floret, while the pistil is degenerated in the early developmental stage. Although the upper and lower florets have the same structure, anthers in the lower floret develop approximately three days later than anthers in the upper floret of the same spikelet (Hsu and Peterson, 1991). A maize anther has four chambers, named loculi. Numerous pollen grains develop in each locule. An anther is composed of wall tissues and sporogenous tissue. The anther wall contains four layers of cells listed here from outermost to innermost: epidermis, endothecium, middle layer, and tapetum. The inner-most tapetal layer is a specialized cell layer that contains darkly staining uni- and bi-nucleate cells and provides nutrients for the development of pollen (Pacini et al., 1985; Chapman, 1987; Horner et al., 1993).

The formation of male gametes is a precisely regulated sequential process. It begins with a group of cells in the center of a locule. Depending on genetic background and environmental condition, approximately seven weeks after planting, these cells undergo reduction divisions to become gametes. The gametes then progress through early-, mid-, and late-microspore stages to become young pollen, which then matures into pollen to be released when the tassel sheds (Palmer et al., 1992).

Any disruption in the regulation or structure of anther and pollen development can potentially prevent the production of mature pollen, which results in male sterility (Horner and Palmer, 1995). Mutants that only affect male fertility but not female fertility are known as male sterile (ms) mutants. Ms mutants have been obtained in many plant species (reviewed by Gottschalk and Kaul, 1974; Kaul, 1988). In maize, a large collection of ms mutants have been identified and various stages and tissues during anther development are affected among these mutants. Therefore, these mutants are valuable materials for studying

the anther and pollen development in maize (Albertsen and Phillips, 1981; Chaubal et al., 2000).

Cytoplasm Male Sterility

One category of male sterility is controlled by genetic factors located in the cytoplasm; therefore, it is referred to as cytoplasmic male sterility (cms) (Mackenzie et al., 1994; Levings and Vasil, 1995; Schnable and Wise, 1998). Cytoplasmic male sterility was first reported in flax (*Linum usitatissimum* L.) in 1921 (Bateson and Gairdner, 1921). Since then, cms has been observed in over 150 plant species (Laser and Lersten, 1972), including agriculturally important crops such as maize, rice, sorghum, and soybean. In all the characterized cases, cms is related to novel open reading frames (ORFs) created by recombination in the mitochondrial genome (Schnable and Wise, 1998). Interestingly, most of the well-characterized cms systems have nuclear restorer genes, which can correct the defects caused by the cytoplasm mutation and restore male fertility. Most of the characterized restorer genes function by altering the accumulation of novel ORF-related transcripts, such as the *Rfp1* and *Rfp2* restorers in canola (Singh et al., 1996), the *Rf-1* restorer in rice (Iwabuchi et al., 1993), the *Rf3* restorer in sorghum (Tang et al., 1996), and the *Fr2* restorer in bean (Abad et al., 1995). However, the *Fr* gene in bean functions through deleting the novel ORF from the mitochondrial genome (He et al., 1995). Some restoration functions are also related to the post-transcriptional RNA editing in mitochondria. For example, the presence of *Rf4* restorer in sorghum is correlated with the high level of RNA editing at *atp6* (Pring et al., 1999).

In maize, cytoplasmic male sterility was first identified by Rhoades in 1931. Since then, numerous studies have focused on the three major cms systems: S (USDA), C (Charrua), and T (Texas) (Laughnan and Gabay-Laughnan, 1983). These three cms systems can be distinguished from each other and from normal (N) cytoplasm by their mitochondrial transcription profiles and nuclear restorer genes (Duvick, 1965; Beckett, 1971; Gracen and Grogen, 1974). Cms-S mitochondria have two transcripts, *orf355* and *orf77*, that are absent in normal mitochondria. A dominant nuclear restorer gene, *Rf3*, alters the accumulation of these two transcripts (Laughnan and Gabay, 1975; Zabala et al., 1997, Wen and Chase, 1999). The cms-C system also has chimeric open reading frames in its mitochondrial genome (Dewey et al., 1991). This system has three nuclear restorers, *Rf4*, *Rf5*, and *Rf6* (Josephson et al., 1978; Kheyr-Pour et al., 1981). *Rf4* can restore cms-C by itself, but *Rf5* and *Rf6* work in concert (Vidakovic, 1988). The cms-T system is probably the best characterized among all cms systems in any plant species due to its wide application in the production of hybrid seeds and its direct relationship to the southern corn leaf blight in 1970 (Ullstrup, 1972).

T-cytoplasm male sterility

In 1944, a single male sterile plant arose from a Texas maize variety, Golden June. When this plant was crossed by inbred line Tx203, all the resulting progeny were male sterile, which suggested the male sterility phenotype originated from cytoplasm of the female parent (Rogers and Edwardson, 1952). Due to its Texas origin, this cytoplasmic male sterility is referred to as T (Texas) cytoplasmic male sterility. A plant that carries T

cytoplasm develops a normal tassel, except that anthers arrest early in pollen development and then degenerate. Therefore, no anthers exert from cms-T tassels. The cms-T system is the most stable system among the three maize cms systems in that its phenotype is only minimally affected by environmental conditions (Wych, 1988). When anthers from T-cytoplasm male sterile plants were compared with those from N-cytoplasm fertile plants, no noticeable differences were observed at the level of resolution afforded by the light microscope until the early microspore stage during anther development. At this stage, the tapetal layer of cms-T anthers became thicker and stained with methylene blue-azure A combination less intensely than that of N-cytoplasm anthers. Later, the tapetal cells were filled with more vacuoles and degenerated by the late-microspore stage. In contrast, N-cytoplasm tapetal cells remained darkly staining and had few vacuoles until the late microspore stage, when the whole tapetal layer was compressed into a thin band (Warmke and Lee, 1977). When anthers were observed at electron microscopy level, the mitochondria in the tapetal cells from T-cytoplasm plants appeared to have disorganized cristae and lightly staining matrix in the earlier tetrad stage. There was no difference between other organelles of tapetal cells in T- and N- cytoplasm plants until very late stages in pollen development (Warmke and Lee, 1977). It was also observed that mitochondria numbers in tapetal cells increased 40 fold compared to those in other cells between precallose and tetrad stages during anther development in both T- and N- cytoplasm plants (Warmke and Lee, 1978). These results indicate that mitochondria play a critical role during microsporogenesis, and suggest that the mitochondrial malfunction is the cause of male sterility in cms-T.

The cms-T system was widely used to generate male-sterile female parents to replace the labor-intensive hand emasculation in the hybrid seed production in the late 1960's. T

cytoplasm was transferred into desirable inbred lines to produce male sterile female parents, while nuclear restorer genes were transferred into desirable male parents. The resulting F1 commercial hybrid seeds were male fertile because of the presence of restorers, even though they carried T cytoplasm (Rogers and Edwardson, 1952; Wise et al., 1999a). By the end of 1969, 85% of US commercial hybrid corn contained T cytoplasm (Ullstrup, 1972). However, T-cytoplasm plants exhibit high susceptibility to two fungal strains, *Mycosphaerella zeae-maydis* (asexual stage: *Phyllosticta maydis*) and race T of *Cochiliobolus heterostrophus* [asexual stage: *Bipolaris maydis* (Nisikado &Miyake) Shoemaker = *Helminthosporium maydis* (Nisikado &Miyake)] (Mercado and Lantican, 1961; Villareal and Lantican, 1965). These two strains cause severe lesions in the leaf, ear and stalk of T-cytoplasm plants, resulting in premature plant death (Scheifele et al., 1970; Ullstrup, 1972). Race T of *C. heterostrophus* was the direct causative agent of the 1970's southern corn leaf blight epidemic, during which approximately 710 billion bushes of corn were lost in the US (Ullstrup, 1972). It was later demonstrated that these two fungus strains produce linear long chain β-polyketols, termed PM-toxin and T-toxin (Kono and Daly, 1979; Kono et al., 1980, 1985; Daly and Knoche, 1982). These two host-specific pathotoxins interact specifically with T-cytoplasm plants to cause susceptibility to these two fungus strains (Hooker et al., 1970; Comstock et al., 1973; Yoder, 1973). Further studies on T-toxin and PM-toxin indicate that they interact with the mitochondria of T cytoplasm and cause swelling of the mitochondria, loss of matrix density, uncoupling of the oxidative phosphorylation, inhibition of malate oxidation, and stimulation of NADH and succinate oxidation (Miller and Koeppe, 1971; Gengenbach et al., 1973; Peterson et al., 1975; Aldrich et al., 1977). These effects are all caused by the increased permeability of the mitochondrial

inner membrane (Gregory et al., 1979; Mathews et al., 1979; Bervillé, 1984; Holden and Sze, 1984, 1987). A synthetic insecticide, methomyl, was found to induce the same lesions on T-cytoplasm plants, although it has a quite different structure from T-toxin and PM-toxin (Humaydan and Scott, 1977). Therefore, it has been used for identifying T-cytoplasm plants.

Multiple approaches were explored to identify the genetic factor for T-cytoplasm male sterility and sensitivity to fungal toxins. In an attempt to separate male sterility from toxin sensitivity, cell cultures were produced from T-cytoplasm tissues. When toxin-resistant cells isolated from media containing T-toxin were regenerated into adult plants, they were all male fertile (Gengenbach and Green, 1975; Gengenbach et al., 1977; Brettell et al., 1979, 1980). In addition, male-fertile and toxin-resistant revertants were also obtained in the absence of fungal toxin (Brettell et al., 1980; Dixon and Leaver, 1982). These results strongly indicate that male sterility and toxin sensitivity originate from the same factor. Meanwhile, the cytoplasmic genomes (mitochondrial and chloroplastic) of T and N cytoplasms were compared. The only differences identified were in the mitochondrial genome (Gengenbach et al., 1973; Levings and Pring, 1976; Gregory et al., 1978; Pring and Levings, 1978). To identify the specific region in the mitochondrial genome related to male sterility and toxin sensitivity, DNA clones from T-cytoplasm mitochondrial genome were hybridized with RNA transcripts from T- and N-cytoplasm mitochondria, to screen for clones that exhibited differences. A fragment of one clone, 2H3, hybridized to T-, but not N-cytoplasm mitochondrial RNA. This fragment of 2H3 contained two open reading frames, T-*urf13* and *orf221*, both of which were present in T cytoplasm but absent in N cytoplasm (Dewey et al., 1986). When the toxin-resistant and male-fertile revertants isolated from tissue culture were analyzed with T-*urf13* and *orf221*, it became apparent that 19 of 20 events

had lost both of these two open reading frames by recombination (Gengenbach et al., 1981; Kemble et al., 1982; Umbeck and Gengenbach, 1983; Fauron et al., 1987). The remaining revertant, T-4, had generated a five-basepair insertion, which caused a frame shift in T-*urf13* and truncated the URF13 protein from 113 to 74 amino acids, while *orf221* was not altered (Wise et al., 1987a). This result demonstrated that T-*urf13* (and not *orf221*) is the genetic factor that conditions male sterility and toxin sensitivity. Antibodies generated using synthetic polypeptides that were designed based on the T-*urf13* sequence detected a 13-kD mitochondrial protein, URF13 (Dewey et al., 1987; Wise et al., 1987b). This confirmed the earlier observation that a 13-kD protein accumulated only in T cytoplasm when the mitochondrial protein profiles were compared between T and N cytoplasms (Forde et al., 1978; Forde and Leaver, 1980).

Other evidence that URF13 is the causal factor of toxin sensitivity was derived from the expression of URF13 in other organisms. *E. coli* strains expressing URF13 were found to be sensitive to T-toxin. Ionic leakage was observed in the presence of T-toxin when URF13 expression was induced. Interestingly, cells expressing URF13 had growth defects, even in the absence of fungal toxin (Dewey et al., 1988). T-toxin or PM-toxin sensitivity was also observed when URF13 was expressed in yeast (Huang et al., 1990; Glab et al., 1990), tobacco (von Allmen et al., 1991; Chaumont et al., 1995), and insect cells (Korth and Levings, 1993).

Immunolocalization using URF13 antibodies revealed that the URF13 protein is localized in the mitochondrial inner membrane (Hack et al., 1991). Cross-linking and terminus-specific-antibody binding experiments suggested that the URF13 protein exists as both oligomers and multimers, and all the URF13 molecules are in the same orientation

(Korth et al., 1991). Deletion and site-directed mutagenesis experiments demonstrated that the N terminal 83 amino acids of URF13 are necessary for T-toxin sensitivity, which explains the T-toxin insensitivity of the 74-amino-acid URF13 protein from T-4 (Braun et al., 1989). The structure of URF13 was determined by topological studies. URF13 has three trans-membrane α-helices; only helix II participates in forming a pore in a homotetramer (Rhoads et al., 1994; Siedow et al., 1995; Rhoads et al., 1995). Binding and site-directed mutagenesis indicated that mutation or cross-linking of Asp39 on helix II abolished the sensitivity to T-toxin, PM-toxin and methomyl, which suggests that Asp39 is the binding site of T-toxin, PM-toxin and methomyl (Braun et al., 1990; Kaspi and Siedow, 1993).

Restorers of cms-T

Two nuclear restorer genes, *rf1* and *rf2*, were initially identified for the cms-T system. Both genes are required for fertility restoration (Duvick, 1956, 1965). Few maize inbred lines carry the functional *Rf1* allele, while the functional *Rf2* allele is present in most inbred lines (Duvick, 1965; Wise et al., 1999a). The *rf1* gene was mapped to chromosome 3L, 11 cM from *tassel seed 4* (*ts4*) (Duvick et al., 1961). The *rf2* gene was mapped to chromosome 9L, 5 cM from the *waxy* (*wx1*) gene (Snyder and Duvick, 1969). High resolution mapping of these two genes was conducted using RFLP markers (Wise and Schnable, 1994). Two additional nuclear restorer genes for cms-T were recently identified, *Rf8* and *Rf**. These two restorers can partially replace *Rf1* (Dill et al., 1997; Wise et al., 1999b), but they are more influenced by environment (Dill et al., 1997; Wise et al., 1999b). Identification of *Rf8* and *Rf** confirmed earlier speculation that nuclear genetic background, in addition to the function

of *Rf1*, affects the transcript accumulation of T-*urf13* based on the comparisons among different inbred lines carrying T cytoplasm (Kennell et al., 1987; Rocheford et al., 1992).

T cytoplasm accumulates five T-*urf13* transcripts, 2.0-kb, 1.8-kb, 1.5-kb, 1.0-kb and 0.8-kb. The presence of a functional *Rf1* gene in the nuclear genome generates additional 1.6-kb and 0.6-kb transcripts (Dewey et al., 1986; Kennell et al., 1987; Kennell and Pring, 1989; Wise et al., 1996). In addition, the URF13 protein accumulation is reduced by 80% in the presence of *Rf1* (Forde and Leaver, 1980; Dewey et al., 1987). The mitochondria from *Rf1*-restored T-cytoplasm plants are less sensitive to T-toxin than those from male sterile T-cytoplasm plants (Barratt and Flavell, 1975), although the susceptibility to the two fungi is not obviously affected (Payne and Yoder 1978; Ullstrup, 1972). The presence of *Rf8* or *Rf** in the nuclear genome also alters the accumulation of T-*urf13* transcripts in the mitochondria. Additional 1.42-kb and 0.42-kb or 1.4-kb and 0.4-kb T-*urf13* transcripts are present in the *Rf8*- or *Rf**- restored T-cytoplasm plants, respectively (Dill et al., 1997; Wise et al., 1999b). The mechanisms by which additional T-*urf13* transcripts arise in the presence of the restorers, *Rf1*, *Rf8* and *Rf**, are not clear. One hypothesis is that these restorer genes encode endonucleases that recognize and cleave specific sites in the mitochondrial transcripts. Support for this hypothesis comes from the consensus sequence CNACNNU located right proceeding the 5' ends of some restorer-dependent transcripts in maize and sorghum (Tang et al., 1996; Dill et al., 1997). This consensus sequence may serve as the recognition site for the endonucleases encoded by the restorers. Cloning of the *rf1* gene is underway (Wise et al., 1996).

Characterization of *rf2*

The *rf2* gene was identified and mapped to chromosome 9 (Snyder and Duvick, 1969; Wise and Schnable, 1994). It is different from most nuclear restorers in that it does not affect the accumulation of URF13 in the mitochondria, although it is absolutely necessary for the restoration of cms-T (Forde and Leaver, 1980; Dewey et al., 1987). Most maize lines carry a functional copy of the *rf2* gene, although they have never been exposed to T cytoplasm (Duvick, 1965; Wise et al., 1999a). This indicates that *rf2* gene plays an important physiological role in maize independent of being a cms-T restorer. To better understand the function of *rf2*, transposon insertion mutants were generated for the gene cloning via transposon tagging (Schnable and Wise, 1994). The cloning and characterization of *rf2* is presented in this dissertation.

Literature Cited

Abad AR, Mehrtens BJ, Mackenzie SA (1995) Specific expression in reproductive tissues and fate of a mitochondrial sterility-associated protein in cytoplasmic male-sterile bean. Plant Cell 7: 271-85

Albertsen MC, Phillips RL (1981) Developmental cytology of 13 male sterile loci in maize. Canadian Journal of Genetics and Cytology 23: 195–208

Aldrich HC, Gracen VE, York D, Earle ED, Yoder OC (1977) Ultrastructural effects of *Helminthosporium maydis* race T toxin on mitochondria of corn roots and protoplasts. Tissue Cell 9: 167-77

Barratt DHP, Flavell RB (1975) Alterations in mitochondria associated with cytoplasmic and nuclear genes concerned with male-sterility in maize. Theor. Appl. Genet. 45: 315-321

Bateson, W, Gairdner AE (1921) Male-sterility in flax, subject to two types of segregation. J. Genet. 11: 269-275

Bauman LF, Crane PL (1986) Hybrid corn-history, development and selection considerations. National Corn Handbook. Cooperative extension Service, Iowa State University, Ames, Iowa.

Beckett JB (1971) Classification of male-sterile cytoplasms in maize (*Zea mays* L.). Crop Science 11: 724-727

Bervillé A, Ghazi A, Charbonnier M, Bonavent J-F (1984) Effects of methomyl and *Helminthosporium maydis* toxin on matrix volume, proton motive force, and NAD accumulation in maize (*Zea mays* L.) mitochondria. Plant Physiol. 76: 508-517

Braun CJ, Siedow JN, Williams ME, Levings CS III (1989) Mutations in the maize mitochondrial T-*urf13* gene eliminate sensitivity to a fungal pathotoxin. Proc. Natl. Acad. Sci. USA 86: 4435-9

Braun CJ, Siedow JN, Williams ME, Levings CS III (1990) Fungal toxins bind to the URF13 protein in maize mitochondria and *Escherichia coli*. Plant Cell 2: 153-161

Brettell RIS, Goddard BVD, Ingram DS (1979) Selection of Tcms-cytoplasm maize tissue cultures resistant to *Drechslera maydis* T-toxin. Maydica 24: 203-213

Brettell RIS, Thomas E, Ingram DS (1980) Reversion of Texas male sterile cytoplasm maize in culture to give fertile, T-toxin resistant plants. Theor. Appl. Genet. 58: 55-58

Chapman GP (1987) The tapetum. International Review of Cytology 107: 111–125

Chaubal R, Zanella C, Trimnell MR, Fox TW, Albertsen MC, Bedinger P (2000) Two male-sterile mutants of *Zea Mays* (Poaceae) with an extra cell division in the anther wall. Am. J. Bot. 87: 1193-1201

Chaumont F, Bernier B, Buxant R, Williams ME, Levings CS III, Boutry M (1995) Targeting the maize T-*urf13* product into tobacco mitochondria confers methomyl sensitivity to mitochondrial respiration. Proc. Natl. Acad. Sci. USA 92: 1167-71

Comstock JC Martinson CA, Gengenbach BG (1973) Host specificity of a toxin from *Phyllosticta maydis* for Texas cytoplasmically male-sterile maize. Phytopathology 63: 1357-1361

Daly JM, Knoche HW (1982) The chemistry and biology of pathotoxins exhibiting host-selectivity. In DS Ingram, PH Williams eds, Advances in Plant Pathology, Academic Press, New York, pp. 83-138

Dewey RE, Korth KL (1994) VI.2 Molecular Aspects of Cytoplasmic Male Sterility in Maize. In YPS Bajaj ed. Biotechnology in Agriculture and Forestry. Vol. 25. Berlin Heidelberg, Springer-Verlag. pp. 402-416

Dewey RE, Levings CS III, Timothy DH (1986) Novel recombinations in the maize mitochondrial genome produce a unique transcriptional unit in the Texas male-sterile cytoplasm. Cell 44: 439-49

Dewey RE, Siedow JN, Timothy DH, Levings CS III (1988) A 13-kilodalton maize mitochondrial protein in *E. coli* confers sensitivity to *Bipolaris maydis* toxin. Science 239: 293-295

Dewey RE, Timothy DH, Levings CS III (1987) A mitochondrial protein associated with cytoplasmic male sterility in the T cytoplasm of maize. Proc. Natl. Acad. Sci. USA 84: 5374-5378

Dewey RE, Timothy DH, Levings CS III (1991) Chimeric mitochondrial genes expressed in the C male-sterile cytoplasm of maize. Curr. Genet. 20: 475-82

Dill CL, Wise RP, Schnable PS (1997) *Rf8* and *Rf** mediate unique T-*urf13*-transcript accumulation, revealing a conserved motif associated with RNA processing and restoration of pollen fertility in T-cytoplasm maize. Genetics 147: 1367-79

Dixon LK, Leaver CJ (1982) Mitochondrial sensitivity to *Drechsllera maydis* T-toxin and the synthesis of a variant mitochondrial polypeptide in plants derived from maize tissue cultures with Texas male-sterile cytoplasm. Theor. Appl. Genet. 63: 75-80

Dowswell CR., Paliwal RL, Cantrell RP (1996) Maize in the Third World. Boulder, CO: Westview Press

Duvick DN (1956) Allelism and comparative genetics of fertility restoration of cytoplasmically pollen sterile maize. Genetics 41: 544-565

Duvick DN, Snyder RJ, Anderson EG (1961) The chromosomal location of *Rf1*, a restorer gene for cytoplasmic pollen sterile maize. Genetics 46: 1245-1252

Duvick DN (1965) Cytoplasmic pollen sterility in corn. In EW Caspari, JM Thoday, Eds, Advances in Genetics Vol. 13. Academic Press, New York, pp. 1-56

Duvick DN (1969) Chromosomal Location of *Rf2*, a restorer gene for cytoplasmic pollen sterile maize. Crop Science 9: 156-157

Fauron CM-R, Abbott AG, Brettell RIS, Gesteland RF (1987) Maize mitochondrial DNA rearrangements between the normal type, the Texas male sterile cytoplasm, and a fertile revertant cms-T regenerated plant. Curr. Genet. 11: 339-346

Forde BG, Leaver CJ (1980) Nuclear and cytoplasmic genes controlling synthesis of variant mitochondrial polypeptides in male-sterile maize. Proc. Natl. Acad. Sci. USA 77: 418-422

Forde BG, Oliver RJC, Leaver CJ (1978) Variation in mitochondrial translation products associated with male-sterile cytoplasms in maize. Proc. Natl. Acad. Sci. USA 75: 3841-3845

Gengenbach BG, Green CE (1975) Selection of T-cytoplasm maize callus cultures resistant to *helminthosporium maydis* race T pathotoxin. Crop Sci. 15: 645-649

Gengenbach BG, Miller RJ, Koeppe DE, Arntzen CJ (1973) The effect of toxin from *Helminthosporium maydis* (race T) on isolated corn mitochondria: Swelling. Can. J. Bot. 51: 2119-2125

Gengenbach BG, Green CE, Donovan CM (1977) Inheritance of selected pathotoxin resistance in maize plants regenerated from cell cultures. Proc. Natl. Acad. Sci. USA 74: 5113-5117

Gengenbach BG, Connelly JA, Pring DR, Conde MF (1981) Mitochondrial DNA variation in maize plants regenerated during tissue culture selection. Theor. Appl. Genet. 59: 161-167

Glab N, Wise RP, Pring DR, Jacq C, Slonimski P (1990) Expression in *Saccharomyces cerevisiae* of a gene associated with cytoplasmic male sterility from maize: respiratory dysfunction and uncoupling of yeast mitochondria. Mol. Gen. Genet. 223: 24-32

Gottschalk W, Kaul MLH (1974) The genetic control of microsporogenesis in higher plants. Nucleus 17: 133–166

Gracen, VE, Grogen CO (1974) Diversity and suitability for hybrid production of different sources of cytoplasmic male sterility in maize. Agron. J. 66: 654-657

Gregory P, Mathews DE, Gregory P, Gracen VE (1979) *Helmintbosporium maydis* race T toxin induces leakage of NAD^+ from T cytoplasm corn mitochondria. Plant Physiol. 63: 1149-1153

Gregory P, Matthews DE, York DW, Earle E, Gracen VE (1978) Southern corn leaf blight disease: Studies on mitochondrial biochemistry and ultrastructure. Mycopathologia 66: 105-112

Hack E, Lin C, Yang H, Horner HT (1991) T-URF13 protein from mitochondria of Texas male-sterile maize (*Zea mays* L.). Plant Physiol. 95: 861-870

He S, Lyznik A, Mackenzie S (1995) Pollen fertility restoration by nuclear gene *Fr* in CMS bean: nuclear-directed alteration of a mitochondrial population. Genetics 139: 955-62

Holden MJ, Sze H (1984) *Helminthosporium maydis* T toxin increased membrane permeability to Ca^{2+} in susceptible corn mitochondria. Plant Physiol. 75: 235-237

Holden MJ, Sze H (1987) Dissipation of the membrane potential in susceptible corn mitochondria by the toxin of *Helminthosporium maydis*, race T, and toxin analogs. Plant Physiol. 84: 670-676

Hooker AL (1972) Southern corn leaf light of corn-Present status and future prospects. J. Environ. Qual. 1: 244-249

Hooker AL, smith DR, Lim SM, Beckett JB (1970) Reaction of corn seedlings with male-sterile cytoplasm to *helminthosporium maydis*. Plant Dis. Reptr. 54: 708-712

Horner HT, Palmer RG (1995) Mechanisms of genic male sterility. Crop Science 35: 1527-1535

Horner HT, Hall VL, Vargas-Olvera MA (1993) Isolation, sorting, and characterization of uni- and bi-nucleate tapetal protoplasts from anthers of normal and Texas cytoplasmic male-sterile *Zea mays* L. Protoplasma 173: 48-57

Hsu SU, Peterson PA (1991) The upper and lower florets of spikelets in maize. J. Genet. & Breed. 45: 215-222

Huang J, Lee SH, Lin C, Medici R, Hack E, Myers AM (1990) Expression in yeast of the T-*urf13* protein from Texas male-sterile maize mitochondria confers sensitivity to methomyl and to Texas-cytoplasm-specific fungal toxins. EMBO J. 9: 339-347

Humaydan HS, Scott EW (1977) Methomyl insecticide selective phytotoxicity on sweet corn hybrids and inbreds having the Texas male sterile cytoplasm. Hortscience 12: 312-313

Iwabuchi M, Kyozuka J, Shimamoto K (1993) Processing followed by complete editing of an altered mitochondrial atp6 RNA restores fertility of cytoplasmic male sterile rice. EMBO J. 12: 1437-46

Josephson LM, Morgan TE, Arnold, JM (1978) Genetics and inheritance of fertility restoration of male-sterile cytoplasms in corn. Proc. 33rd Ann. Corn Sorghum Res. Conf. 33: 48-59

Kaspi CI, Siedow JN (1993) Cross-linking of the cms-T maize mitochondrial pore-forming protein URF13 by N,N'-dicyclohexylcarbodiimide and its effect on URF13 sensitivity to fungal toxins. J. Biol. Chem. 268: 5828-5833

Kaul MLH (1988) Male sterility in higher plants. Springer-Verlag, Berlin, Germany

Kemble RJ, Flavell RB, Brettell RIS (1982) Mitochondrial DNA analysis of fertile and sterile maize plants derived from tissue culture with the Texas male sterile cytoplasm. Theor. Appl. Genet. 62: 213-217

Kennell JC, Pring DR (1989) Initiation and processing of *atp6*, *T-urf13* and ORF221 transcripts from mitochondria of T cytoplasm maize. Mol. Gen. Genet. 216: 16-24

Kennell JC, Wise RP, Pring DR (1987) Influence of nuclear background on transcription of a maize mitochondrial region associated with Texas male sterile cytoplasm. Mol. Gen. Genet. 210: 399-406

Kheyr-Pour A, Gracen VE, Everett HL (1981) Genetics of fertility restoration in the C-group of cytoplasmic male sterility in maize. Genetics 98: 379-88

Kiesselbach TA (1999) The structure and reproduction of corn. 50th anniversary edition, Cold Spring Harbor Laboratory Press, Cold Spring Harbor, New York, pp. 38-50

Kono Y, Daly JM (1979) Characterization of the host-specific pathotoxin produced by *Helminthosporium maydis*, race T, affecting corn with Texas male sterile cytoplasm. Bioorg. Chem. 8: 391-397

Kono Y, Takeuchi S, Kawarada A, Daly JM, Knoche HW (1980) Structure of the host-specific pathotoxins produced by *Helminthosporium maydis*, race T. Tetrahedron Lett. 21: 1537-1540

Kono Y, Suzuki Y, Takeuchi S, Knoche HW, Daly JM (1985) Studies on the host-specific pathotoxins produced by *H. maydis* race T and *P. maydis*: Absolute configuration of PM-toxins and HMT-toxins. Agric. Biol. Chem. 49: 559-562

Korth KL, Levings CS III. (1993) Baculovirus expression of the maize mitochondrial protein URF13 confers insecticidal activity in cell cultures and larvae. Proc. Natl. Acad. Sci. USA. 90: 3388-3392

Korth KL, Kaspi CI, Siedow JN, Levings CS III (1991) URF13, a maize mitochondrial pore-forming protein, is oligomeric and has a mixed orientation in *Escherichia coli* plasma membranes. Proc. Natl. Acad. Sci. USA 88: 10865-10869

Laughnan JR, Gabay S (1975) An episomal basis for instability of S male sterility in maize and some implications for plant breeding. In CW Birky Jr, PS Perlman, TJ Byers eds, Genetics and the Biogenesis of Cell Organelles, Columbus: Ohio State Unv. Press, pp. 330-49

Laughnan JR, Gabay-Laughnan S (1983) Cytoplasmic male sterility in maize. Annu. Rev. Genet. 17: 27-48

Laser KD, Lersten NR (1972) Anatomy and cytology of microsporogenesis in cytoplasmic male sterile angiosperms. Bot. Rev. 38: 425-454

Levings CS III (1990) The Texas cytoplasm of maize: Cytoplasmic male sterility and disease susceptibility. Science 250: 942-947

Levings CS III (1993) Thoughts on cytoplasmic male sterility in *cms*-T maize. Plant Cell 5: 1285-1290

Levings CS III, Pring DR (1976) Restriction endonuclease analysis of mitochondrial DNA from normal and Texas cytoplasmic male-sterile maize. Science 193: 158-160

Levings CS III, Vasil IK (1995) The Molecular Biology of Plant Mitochondria, Kluwer Academic publishers, The Netherlands.

Mackenzie SA, Shichuan H, Lyznik A (1994) The elusive plant mitochondrion as a genetic system. Plant Physiol. 105: 775-780

Mathews DE, Gregory P, Gracen VE (1979) *Helminthosporium maydis* race T toxin induces leakage of NAD^+ from T cytoplasm corn mitochondria. Plant Physiol. 63: 1149-1153

Mercado AC Jr, Lantican RM (1961) The susceptibility of cytoplasmic male sterile lines of corn to *Helminthosporium maydis* Nish &Miy. Philipp. Agric. 45: 235-243

Miller RJ, Koeppe DE (1971) Southern corn leaf blight: Susceptible and resistant mitochondria. Science 173: 67-69

Pacini E, Franchi GG, Hesse M (1985) The tapetum: its form, function, and possible phylogeny in Embryophyta. Plant Systematics and Evolution 149: 155–185

Palmer RG, Albertsen MC, Horner HT, Skorupska H (1992) Male sterility in soybean and maize: Developmental comparisons. Nucleus 35: 1-18

Payne GA, Yoder OC (1978) Effect of the nuclear genome of corn on the sensitivity to *Helminthosporium maydis* race T-toxin and on susceptibility to *H. maydis* race T. Phytopathology 68: 331-337

Peterson PA, Flavell RB, Barratt DHP (1975) Altered mitochondrial membrane activities associated with cytoplasmically-inherited disease sensitivity in maize. Theor. Appl. Genet. 45: 309-314

Pring DR, Levings CS III (1978) Heterogeneity of maize cytoplasmic genomes among male-sterile cytoplasms. Genetics 89: 121-136

Pring DR, Lonsdale DM (1989) Cytoplasmic male sterility and maternal inheritance of disease susceptibility in maize. Annu. Rev. Phytopathol. 27: 483-502

Pring DR, Tang HV, Howad W, Kempken F (1999) A unique two-gene gametophytic male sterility system in sorghum involving a possible role of RNA editing in fertility restoration. J Hered. 90: 386-93

Rhoades MM (1931) Cytoplasmic inheritance of male sterility in *Zea mays*. Science 73: 340-341

Rhoads DM, Kaspi CI, Levings CS III, Siedow JN (1994) N,N'-dicyclohexylcarbodiimide cross-linking suggests a central core of helices II in oligomers of URF13, the pore-forming T-toxin receptor of *cms*-T maize mitochondria. Proc. Natl. Acad. Sci. USA 91: 8253-8257

Rhoads DM, Levings CS III, Siedow JN (1995) URF13, a ligand-gated, pore-forming receptor for T-toxin in the inner membrane of cms-T mitochondria. J. Bioenerg. Biomembr. 27: 437-45

Rocheford TR, Kennell JC, Pring DR (1992) Genetic analysis of nuclear control of T-*urf13/orf221* transcription in T cytoplasm maize. Theor. Appl. Genet. 84: 891-898

Rogers JS, Edwardson JR (1952) The utilization of cytoplasmic male-sterile inbreds in the production of corn hybrids. Agron. J. 44: 8-13

Salvador R J (1997) Maize. In the Encyclopedia of Mexico: Culture, History and Society. Fitzroy Dearborn Publishers, Chicago.

Scheifele GL, Whitehead W, Rowe C (1970) Increase susceptibility to southern leaf spot (*Helminthosporium maydis*) in inbred lines and hybrids of maize with Texas male-sterile cytoplasm. Plant Dis. Rep. 54: 501-503

Schnable PS, Wise RP (1994) Recovery of heritable, transposon-induced, mutant alleles of the *rf2* nuclear restorer of T-cytoplasm maize. Genetics 136: 1171-1185

Schnable PS, Wise RP (1998) The molecular basis of cytoplasmic male sterility and fertility restoration. Trends in Plant Science 3: 175-180

Siedow JN, Rhoads DM, Ward GC, Levings CS III (1995) The relationship between the mitochondrial gene T-*urf13* and fungal pathotoxin sensitivity in maize. Biochim. Biophys. Acta. 1271: 235-240

Singh M, Hamel N, Menassa R, Li XQ, Young B, Jean M, Landry BS, Brown GG (1996) Nuclear genes associated with a single *Brassica* CMS restorer locus influence transcripts of three different mitochondrial gene regions. Genetics 143: 505-516

Snyder RJ, Duvick DN (1969) Chromosomal location of *Rf2*, a restorer gene for cytoplasmic pollen sterile maize. Crop. Sci. 9: 156-157

Tang HV, Pring DR, Shaw LC, Salazar RA, Muza FR, Yan B, Schertz KF (1996) Transcript processing internal to a mitochondrial open reading frame is correlated with fertility restoration in male-sterile sorghum. Plant J. 10: 123-33

Tatum LA (1971) The southern corn leaf blight epidemic. Science 171: 1113-1116

Ullstrup AJ (1972) The impacts of the southern corn leaf blight epidemics of 1970-1971. Annu. Rev. Phytopathol. 10: 37-51

Umbeck PF, Gengenbach BG (1983) Reversion of male-sterile T-cytoplasm maize to male fertility in tissue culture. Crop Sci. 23: 584-588

Vidakovic M (1988) Genetics of fertility restoration in cytoplasmic male sterility of the C-type (cms-C) in maize (*Zea mays* L.). Maydica 33: 51-64

Villareal RL, Lantican RM (1965) The cytoplasmic inheritance of susceptibility to *Helminthosporium* leaf spot in corn. Philipp. Agric. 49: 294-300

von Allmen JM, Rottmann WH, Gengenbach BG, Harvey AJ, Lonsdale DM (1991) Transfer of methomyl and Hm T-toxin sensitivity from T-cytoplasm maize to tobacco. Mol. Gen. Genet. 229: 405-412

Warmke HE, Lee S-LJ (1977) Mitochondrial degeneration in Texas cytoplasmic male-sterile corn anthers. J. Hered. 68: 213-222

Warmke HE, Lee S-LJ (1978) Pollen abortion in T cytoplasmic male-sterile corn (Zea mays): a suggested mechanism. Science 200: 561-563

Wen L, Chase CD (1999) Pleiotropic effects of a nuclear restorer-of-fertility locus on mitochondrial transcripts in male-fertile and S male-sterile maize. Curr Genet. 35: 521-526

Williams ME, Levings CS III (1992) Molecular biology of cytoplasmic male sterility. In J. Janick ed, Plant Breeding Reviews, Vol. 10. Wiley, New York. pp. 23-51

Wise RP, Dill CL, Schnable PS (1996) Mutator-induced mutations of the *rf1* nuclear fertility restorer of T-cytoplasm maize alter the accumulation of *T-urf13* mitochondrial transcripts. Genetics 143: 1383-1394

Wise RP, Schnable PS (1994) Mapping complementary genes in maize: positioning the *rf1* and *rf2* nuclear-fertility restorer loci of Texas (T) cytoplasm relative to RFLP and visible markers. Theor. Appl. Genet. 88: 785-795

Wise RP, Bronson CR, Schnable PS, Horner HT (1999a) The genetics, pathology, and molecular biology of T-cytoplasm male sterility in maize. Adv. Agron. 65: 79-130

Wise RP, Gobelman-Werner K, Pei D, Dill CL, Schnable PS (1999b) Mitochondrial transcript processing and restoration of male fertility in T-cytoplasm maize. J. Hered. 90: 380-385

Wise RP, Pring DR, Gengenbach BG (1987a) Mutation to male fertility and toxin insensitivity in Texas (T)-cytoplasm maize is associated with a frameshift in a mitochondrial open reading frame. Proc. Natl. Acad. Sci. USA 84: 2858-2862

Wise RP, Fliss AE, Pring DR, Gengenbach BG (1987b) *urf13*-T of T cytoplasm maize mitochondria encodes a 13-kD polypeptide. Plant Mol. Biol. 9: 121-126

Wych RD (1988) Production of hybrid seed corn. In: GF Sprague and JW Dudley eds, Corn and Corn Improvement. 3rd ed. ASA Monograph 18. Amer. Soc. Agronomy, Madison, WI. pp. 565-607

Yoder OC (1973) A selective toxin produced by *Phyllosticta maydis*. Phytopathology 63: 1361-1366

Zabala G, Gabay-Laughnan S, Laughnan JR (1997) The nuclear gene *Rf3* affects the expression of the mitochondrial chimeric sequence R implicated in S-type male sterility in maize. Genetics 147: 847-860

CHAPTER 2. THE *rf2* NUCLEAR RESTORER GENE OF MALE-STERILE, T-CYTOPLASM MAIZE

A paper published in Science [a]

Xiangqin Cui,[b] Roger P. Wise,[c] and Patrick S. Schnable[d]

Abstract

The male-sterile, T cytoplasm (cmsT) of maize serves as a model for the nuclear restoration of cytoplasmic male sterility. The *rf2* gene, one of two nuclear genes required for fertility restoration in cmsT maize, was cloned. The protein predicted by the *rf2* sequence is a putative aldehyde dehydrogenase, which suggests several mechanisms that might explain *Rf2*-mediated fertility restoration of cmsT. Aldehyde dehydrogenase may be involved in the detoxification of acetaldehyde produced via ethanolic fermentation during pollen development, may play a role in energy metabolism, or may interact with URF13, the mitochondrial protein associated with male sterility in cmsT maize.

---

[a] Reprinted with permission of Science, 1996, 272: 1334-1336.

[b] Department of Zoology & Genetics, Iowa State University, Ames, IA 50011.

[c] Field Crops Research, USDA-Agricultural Research Service and Department of Plant Pathology, Iowa State University, Ames, IA 50011.

[d] Departments of Agronomy and Zoology & Genetics, Iowa State University, Ames, IA 50011.

Results and Discussion

Cytoplasmic male sterility (cms) is a maternally inherited inability to produce functional pollen. It has been observed in over 150 plant species (1) and is often associated with the expression of novel mitochondrial open-reading frames (2). In many cms systems, restoration of male fertility can occur in the presence of specific nuclear genes (3). These fertility-restorer genes are thought to block or compensate for cytoplasmic dysfunctions that are phenotypically expressed during pollen development. Efforts to characterize the molecular mechanisms by which these events occur have been hampered by the absence of cloned nuclear restorer genes.

The T cytoplasm of maize serves as a model for cms and fertility restoration. Restoration of fertility to cmsT maize requires the combined action of dominant alleles of two nuclear restorer genes, *rf1* and *rf2* (4). Until the 1970 epidemic of southern corn leaf blight, cmsT was used to produce approximately 85% of the hybrid seed in the United States (5). T-cytoplasm maize is highly sensitive to the host-selective pathotoxin, HmT, produced by *Cochliobolus heterostrophus* Drechsler race T (6). The mitochondrial gene, T-*urf13*, which is present in T cytoplasm, but absent in N cytoplasm, is responsible for male sterility and toxin sensitivity (7). T-*urf13* encodes a 13-kD mitochondrial polypeptide (URF13) (8, 9).

Even in the absence of pathogens, URF13 appears to have a slight deleterious effect on maize cells (10), presumably as consequence of subtle perturbations in mitochondrial

function. However, under these conditions, the only striking phenotype conditioned by URF13 is male sterility, which occurs as a consequence of a degeneration of the tapetal layer of anthers (11). The selective nature of this degeneration is paradoxical, because URF13 is expressed in many, if not all, maize tissues (12). It is possible that there is a tapetum-specific compound (Factor X) that is a necessary prerequisite for URF13-induced toxicity (13). Alternatively, tissue-specific degeneration could occur if tissues differ in their requirements for mitochondrial function (14). The accumulation of toxic URF13 is reduced approximately 80% in plants carrying *Rf1* (8, 15), presumably as a consequence of its ability to alter the accumulation and nature of T-*urf13* transcripts (16). In contrast, *Rf2* does not affect URF13 accumulation (8) and nothing is known about its essential role in fertility restoration.

To clone this nuclear fertility restorer gene, we employed a transposon tagging strategy to isolate *rf2* mutant (*rf2-m*) alleles (17). Genetic crosses were performed such that rare progeny plants that carried newly generated transposon tagged *rf2* alleles were male sterile. Seven *rf2-m* mutant alleles were isolated via a screen of approximately 178,300 plants. Six of these mutant alleles were derived from *Mutator* transposon stocks and may therefore have arisen by the insertion of *Mu* transposons. In an effort to identify such a transposon inserted within the *rf2* gene, we subjected DNA samples from test-cross progeny families (each of which involved a different *rf2-m* allele) to DNA gel-blot analysis using probes specific to individual classes of *Mu* transposons. In one such family derived from the cross T cytoplasm *rf2-m8122/Rf2-Ky21* X *rf2-ref/rf2-ref*, all 56 male-sterile progeny carried

a 3.4-kb, *Mu1*-containing, *Eco*RI-*Hin*dIII DNA fragment that was absent in all 49 male-fertile siblings (Fig. 1). This result demonstrated that this DNA fragment was closely linked to, or part of, the *rf2* locus. This 3.4-kb DNA fragment was cloned as the plasmid pF#9 (Fig. 1C). The identity of this DNA fragment was established by allelic cross-referencing experiments. In such experiments (Fig. 2), the putative *rf2* clone revealed DNA polymorphisms between each of four progenitor alleles (18) and their corresponding *rf2-m* derivatives (Fig. 2). Because mutations at the *rf2* locus coincided with DNA sequence rearrangements in the region detected by DD1, we conclude that DD1 cross-hybridizes to DNA fragments containing the *rf2* locus.

Using DD1 as a probe, we isolated a 1.2-kb partial *Rf2* cDNA clone from a cDNA library prepared from RNA isolated from immature tassels of the inbred line W22. Subsequently, we isolated a 2.2-kb *Rf2* cDNA clone from a cDNA library prepared from RNA isolated from seedlings of the inbred line B73 (19). The latter *Rf2* cDNA detects a 2.3-kb transcript in RNA isolated from immature tassels (20) of the *Rf2*-containing inbred line Ky21 (Fig. 3). Although this transcript also accumulated to at least normal levels in the tassels of plants homozygous for the *rf2-ref* allele, it was not detectable in total RNA isolated from tassels homozygous for *rf2-m8904*, *rf2-m9323*, and *rf2-m9437*, and is barely detectable in RNA isolated from tassels homozygous for *rf2-m8110* and *rf2-m8122* (Fig. 3).

This 2.2-kb cDNA appears to be near full-length because its size corresponds well with that of the *Rf2* transcript (Fig. 3). Additionally, the sequence (21) contains in-frame stop codons 5' of two methionine residues, and the cDNA encodes a putative mitochondrial

targeting signal (Fig. 4). Computer-based homology searches of GenBank and other databases using various derivatives of the Blast algorithm (22) revealed substantial similarity (approximately 60% identity and 75% similarity) between the predicted *Rf2*-encoded protein and mammalian mitochondrial aldehyde dehydrogenases (ALDH) which catalyze the oxidation of a broad range of aldehydes to acids (Fig. 4). The two catalytic domains present in ALDHs are conserved in the RF2 protein. Although several ALDH's have been partially purified from plants (23), their role in plant metabolism has not been clarified. In yeast, *Drosophila*, and mammals, the enzymes alcohol dehydrogenase (ADH) and ALDH function together to oxidize ethanol through acetaldehyde to acetate. It is this NADH (reduced form of nicotinamide adenine dinucleotide)-producing pathway that allows these organisms to survive under aerobic conditions on diets where ethanol constitutes the sole carbon and energy source. Hence, one possible role for ALDH in plants is the detoxification of ethanol and acetaldehyde following brief periods of fermentation.

Our working hypothesis is that the RF2 protein has a function independent of its role as a nuclear restorer in cmsT maize (17). According to this hypothesis, the RF2 protein has been recruited in T-cytoplasm maize to ameliorate the mitochondrial lesion associated with T-*urf13* expression. Assuming the *rf2* gene encodes an ALDH, we have developed two hypotheses for the mechanism by which this could occur.

According to the "Metabolic Hypothesis", the normal metabolic role of ALDH becomes essential in T-cytoplasm cells due to URF13-mediated alterations of mitochondrial function. For example, the energy produced by ALDH-catalyzed α-oxidation of fatty acids

could become essential if T-cytoplasm tapetum cells have an energy deficit. Alternatively, the potential role of ALDH in scavenging and detoxifying acetaldehyde could become essential if URF13 alters mitochondrial function such that additional pyruvate is shunted into aerobic fermentation (24).

The "Interaction Hypothesis" suggests that the RF2 protein interacts directly or indirectly with URF13 and thereby diminishes its deleterious effects. Because of the broad specificities of ALDHs (25), and their diverse metabolic functions (26), the RF2 protein could act by modifying: (i) some component or components of the inner mitochondrial membrane or (ii) "Factor X". For example, an ALDH-catalyzed oxidation of an aldehyde component of the mitochondrial membrane could alter the binding of URF13 to that membrane. Alternatively, if Factor X is an aldehyde, it could be inactivated through oxidation. Either of these events could alter the toxicity associated with the accumulation of URF13 in the mitochondria without affecting URF13 accumulation (consistent with the behavior of *Rf2*).

References and Notes

1. K. D. Laser and N. R. Lersten, *Bot. Rev.* **38**, 425 (1972).

2. S. Mackenzie, H. Shichuan, A. Lyznik, *Plant Physiol.* **105**, 775 (1994).

3. M. R. Hanson and M. F. Conde, *Int. Rev. Cytol.* **94**, 213 (1985).

4. J. R. Laughnan and S. Gabay-Laughnan, *Annu. Rev. Genet.* **17**, 27 (1983).

5. A. J. Ullstrup, *Annu. Rev. Phytopath.* **10**, 37 (1972); D. R. Pring and D. M. Lonsdale, *Annu. Rev. Phytopathol.* **27**, 483 (1989).

6. J. C. Comstock, C. A. Martinson, B. G. Gengenbach, *Phytopathology* **63**, 1357 (1973); O. C. Yoder, *Phytopathology*. **63**, 1361 (1973); A. L. Hooker, D. R. Smith, S. M. Lim, J. B. Beckett, *Plant Dis. Rep.* **54**, 708 (1970).

7. C. S. Levings III, *Plant Cell* **5**, 1285 (1993).

8. R. E. Dewey, D. H. Timothy, C. S. Levings III, *Proc. Natl. Acad. Sci. U.S.A.* **84**, 5374 (1987);

9. R. P. Wise, A. E. Fliss, D. R. Pring, B. G. Gengenbach, *Plant Mol. Biol.* **9**, 121 (1987); K. L. Korth, C. I. Kaspi, J. N. Siedow, C. S. Levings III, *Proc. Natl. Acad. Sci. U.S.A.* **88**, 10865 (1991).

10. D. R. Pring, B. G. Gengenbach, R. P. Wise, *Phil. Trans. Roy. Soc. Lond. Ser. B.* **319**, 187 (1988); D. N. Duvick, *Adv. Genet.* **13**, 1 (1965).

11. H. E. Warmke and S.-L. J. Lee, *J. Hered.* **68**, 213 (1977).

12. E. Hack, C. Lin, H. Yang, H.T. Horner, *Plant Physiol.* **95**, 861 (1991).

13. R. Flavell, *Plant Sci. Lett.* **3**, 259 (1974).

14. D. C. Wallace, *Trends Genet.* **5**, 9 (1989).

15. B. G. Forde and C. J. Leaver, *Proc. Natl. Acad. Sci. U.S.A.* **77**, 418 (1980).

16. R. E. Dewey, C. S. Levings III, D. H. Timothy, *Cell* **44**, 439 (1986); J. C. Kennell, R. P. Wise, D. R. Pring, *Mol. Gen. Genet.* **210**, 399 (1987); J. C. Kennell and D. R. Pring,

Mol. Gen. Genet. **216**, 16 (1989); R. P. Wise, C. L. Dill, P. S. Schnable, *Genetics*, in press.

17. P. S. Schnable, R. P. Wise, *Genetics* **136**, 1171 (1994).

18. On the basis of their pedigrees, five of the *rf2-m* alleles isolated via the *Mutator* transposon tagging experiment (*rf2-m8110*, *rf2-m8122*, *rf2-m9323*, *rf2-m9390*, and *rf2-m9437*) would be expected to have been derived from *Rf2-Q66*, *Rf2-Q67*, *Rf2-B77*, or *Rf2-B79*. Their wild-type progenitor alleles were determined by comparing the restriction fragment length polymorphism (RFLP) fingerprints through the use of 3' *sus1* and *umc153* markers that flank the *rf2* locus [R. P. Wise and P. S. Schnable, *Theor. Appl. Genet.* **88**, 785 (1994)] and *rf2* intron sequences of DNA samples carrying mutant alleles to those carrying the potential progenitor alleles.

19. The inbreds W22 and B73 carry *Rf2* alleles. The 1.2-kb and 2.2-kb *Rf2* cDNAs were isolated from the 2ts library prepared by the Steve Dellaporta laboratory [A. Delong, A. Calderon-Urrea, S. L. Dellaporta, *Cell* **74**, 757 (1993)] and from a library prepared by Alice Barkan, respectively (A. Barkan, personal communication).

20. Total RNA was isolated from immature tassels according to the method of Dean et al. [*EMBO J.* **4**, 3055 (1985)]. About 10 μg of total RNA was loaded in each lane of the RNA gel [H. Lehrach et al. *Biochemistry* **16**, 4743 (1977)]. RNAs were transferred onto a Magna Charge nylon membrane (Micron Separations Inc.) and hybridized with an *rf2* cDNA probe at 68°C. RNA loading was quantified by stripping and

rehybridizing the membrane to a tubulin cDNA probe (*tub1*) [R. Villemur et al., J. Mol. Biol. **227**, 81 (1992)].

21. Each strand of the 1.2- and 2.2-kb cDNAs was sequenced at least once at the ISU Nucleic Acid Facility.

22. S. F. Altschul, W. Gish, W. Miller, E. W. Myers, D. J. Lipman, *Mol. Biol.* **215**, 403 (1990).

23. H. Asker and D. D. Davies, *Phytochem* **24**, 689 (1985).

24. M. Bucher, R. Brandle, C. Kuhlemeier, *EMBO J.* **13**, 2755 (1994); M. Bucher, K, A, Brander, S, Sbicego, T, Mandel, C, Kuhlemeier, *Plant Mol. Biol.* **28**, 739 (1995)

25. W. Ambroziak and R. Pietruszko, in *Enzymology and Molecular Biology of Carbonyl Metabolism,* H. Weiner, D. W. Crabb, and T. G. Flynn, Eds. (Plenum Press, New York, c1993), pp. 5-15.

26. W. B. Jakoby and D. M. Ziegler, *J. Biol. Chem.* **265**, 20715 (1990); J. M. L. Tasayco and G. D. Prestwich, *Archives of Biochem. Biophys.* **278**, 444 (1990).

27 K. Nakai and M. Kanehisa, *Genomics* **14**, 897 (1992).

28. We thank W. J. Chen, C. L. Dill, K. Gobelman-Werner, S. Heinen, and P. F. Zhang for technical assistance, A. Barkan and S. Dellaporta for gifts of cDNA libraries, V. Chandler for *Mu* probes, J. Imsande, C. Kuhlemeier, C. Leaver, S. Levings, B. Nikolau, and D. Pring for stimulating discussions and/or for sharing results prior to publication. X.C. is a student in the Iowa State University Interdepartmental Genetics graduate program. This research was supported by USDA-NRI competitive

grants AMD 9201761 and AMD 9400901 to P.S.S. and R.P.W and by Hatch Act and State of Iowa funds. Journal Paper No. J-16653 of the Iowa Agriculture and Home Economics Experiment Station, Ames, IA 50011, Project Nos. 2447 and 3152.

Figure Legends

Fig. 1. (**A**) *Mu1* copy number reduction and Co-segregation analysis of male-sterile (*rf2-m8122/rf2-ref*) and male-fertile siblings (*Rf2-Ky21/rf2-ref*) from a test cross. The *Mu1*-hybridizing, 3.4-kb *Eco*RI-*Hin*dIII DNA fragment is present in all 56 male-fertile siblings carrying *rf2-m8122*, but absent in all 49 male-sterile siblings not carrying *rf2-m8122*. Lanes are indicated as follows: OE is the male-sterile plant from the mutant screen in which the *rf2-m8122* allele was first identified (17); GGP, GP and P refer to the great-grandparent, grandparent, and parent, respectively, of the segregating family (each of these ancestors had the genotype *rf2-m8122/Rf2*); and S and F refer to male-sterile and male-fertile siblings, respectively. The *rf2-ref* allele is the reference allele carried by the inbred line Wf9. (**B**) Cosegregation of sterility with an RFLP detected by DD1. The DNA blot from panel A was stripped and then reprobed with the 846-bp *Dra*I fragment adjacent to the *Mu1* transposon in pF#9 (probe DD1 in Panel C). The resulting hybridization pattern established that DD1 is a low-copy sequence in the maize genome. Although not visible in this panel, probe DD1 also hybridized weakly to a second genomic fragment. (**C**) Restriction map of the DNA

insert of pF#9 (24). Abbreviations for restriction enzyme sites: E, *Eco*RI; B, *Bgl*II; D, *Dra*I; P, *Pst*I; H, *Hin*dIII.

Fig. 2. Allelic cross-referencing experiments. The DD1 fragment of pF#9 (Fig. 1C) was hybridized to gel blots containing DNA isolated from plants that carried four independent *rf2* mutants and their respective wild-type progenitor alleles. *rf2-m8110* and *rf2-m9390* are derived from the wild-type allele *Rf2-Q67*; *rf2-m8122* and *rf2-m9323* are derived from *Rf2-Q66* (18). (**A**) *Eco*RI; (**B**) *Hin*dIII.

Fig. 3. Gel blot containing RNA prepared from immature tassels homozygous for the indicated *rf2* alleles (20). All plants were T-cytoplasm and derived from the Ky21 inbred background (after four to five backcrosses), except the one used in the first lane, which was an N-cytoplasm, Ky21 plant. RNAs were hybridized with the 2.2-kb *rf2* cDNA (**A**) or the maize tubulin cDNA, *tub1* (**B**).

Fig 4. Sequence alignment of the predicted RF2 protein (GenBank accession number U43082) with bovine (GenBank accession number P20000) and human (GenBank accession number P05091) mitochondrial ALDH (27). Solid circles indicate positions of the two possible translation initiation codons of *rf2*. Mitochondrial targeting signals (Box I) predicted by the PSORT algorithm (27) and the Glu (Box II) and Cys (Box III) catalytic domains of ALDH identified by the Motifs algorithm of the GCG sequence analysis software package

are indicated. The insertion site of the *Mu* transposon that generated the *rf2-m8122* allele is indicated by a solid triangle. Identical and similar amino acid residues are indicated by black and gray backgrounds, respectively. There is a single nucleotide polymorphism between the *Rf2-B73* and *Rf2-W22* alleles; this G to C transversion results in the substitution of an asparagine for a lysine residue at position 427.

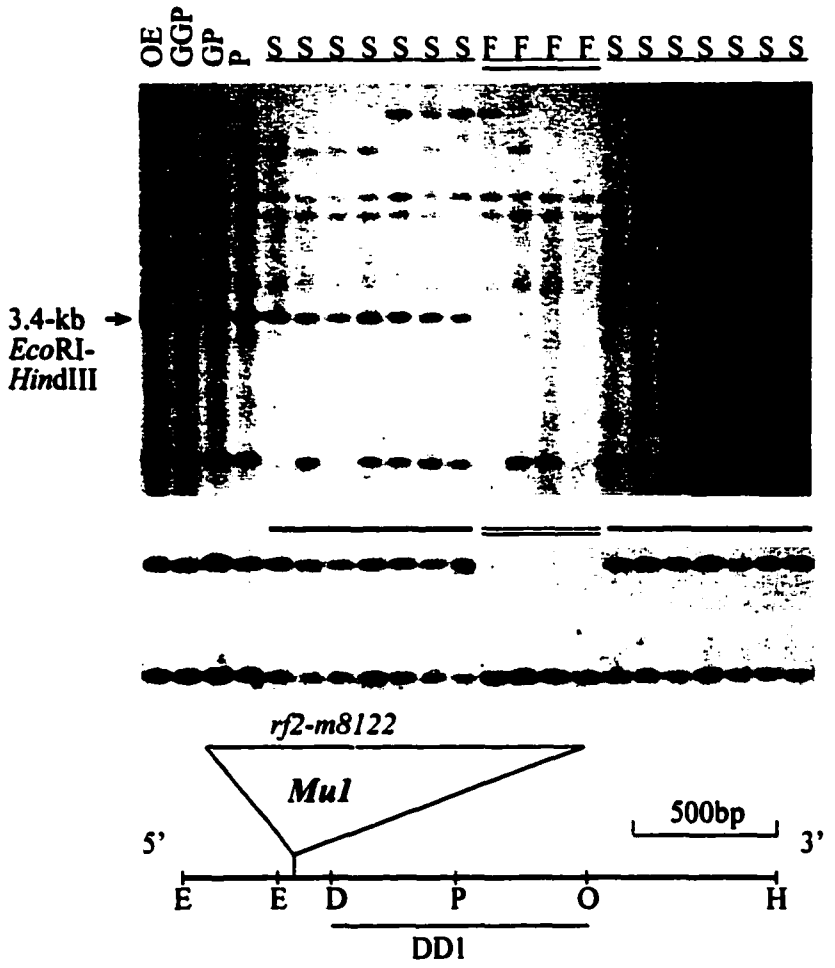

Cui et al., Fig. 2

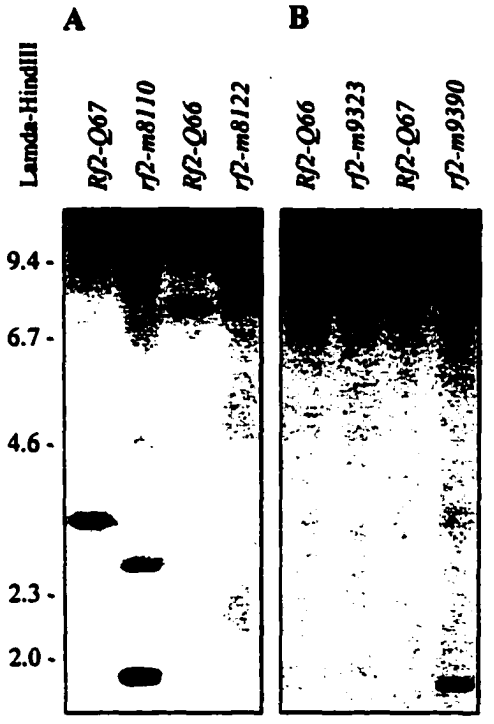

Cui et al., Fig. 2

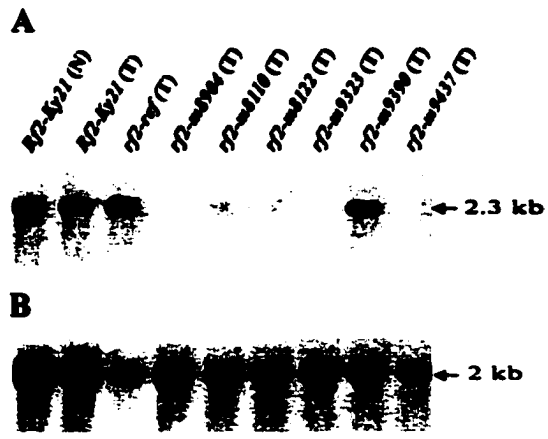

Cui et al., Fig. 3.

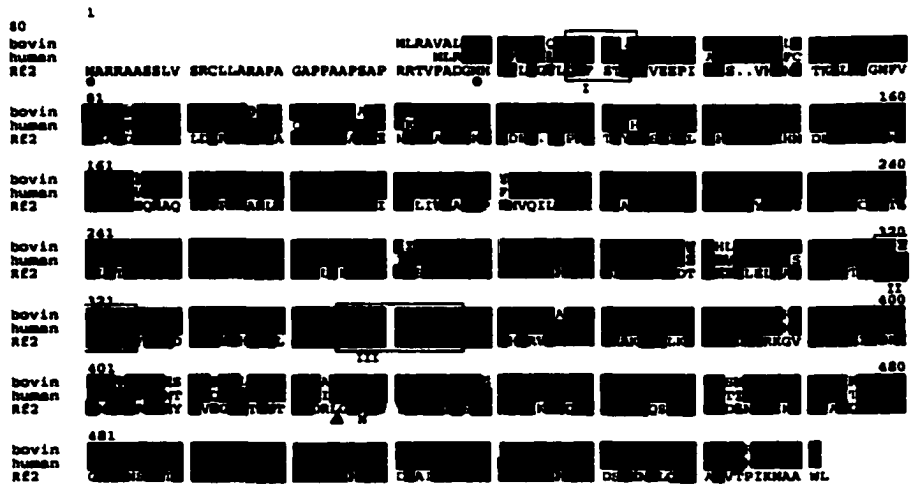

Cui et al., Fig. 4.

CHAPTER 3. MITOCHONDRIAL ALDEHYDE DEHYDROGENASE ACTIVITY IS REQUIRED FOR MALE FERTILITY IN MAIZE

A paper accepted by Plant Cell

Feng Liu,[a,b,1] Xiangqin Cui,[a,b,1] Harry T. Horner,[c] Henry Weiner,[d] and Patrick S. Schnable[a,b,e,f]

Abstract

Some plant cytoplasms express novel mitochondrial genes that cause male sterility. Nuclear genes that disrupt the accumulation of the corresponding mitochondrial gene products can restore fertility to such plants. The Texas (T) cytoplasm mitochondrial genome of maize expresses a novel protein, URF13, that is necessary for T cytoplasm-induced male sterility. Working in concert, functional alleles of two nuclear genes, *rf1* and *rf2*, can restore fertility to T cytoplasm plants. *Rf1* alleles, but not *Rf2* alleles, reduce the accumulation of URF13.

---

[a] Department of Zoology and Genetics, Iowa State University, Ames, Iowa 50011

[b] Interdepartmental Genetics Program, Iowa State University, Ames, Iowa 50011

[c] Department of Botany, Iowa State University, Ames, Iowa 50011

[d] Department of Biochemistry, Purdue University, West Lafayette, Indiana 47907-1153

[e] Department of Agronomy, Iowa State University, Ames, Iowa 50011

[f] Center for Plant Genomics, Iowa State University, Ames, Iowa 50011

[1] These authors contributed equally to this work.

T cytoplasm plants. *Rf1* alleles, but not *Rf2* alleles, reduce the accumulation of URF13. Hence, *Rf2* differs from typical nuclear restorers in that it does not alter the accumulation of the mitochondrial protein necessary for T cytoplasm-induced male sterility. This study established that the *rf2* gene encodes a soluble protein that accumulates in the mitochondrial matrix. Three independent lines of evidence establish that the RF2 protein is an aldehyde dehydrogenase. The finding that T cytoplasm plants that are homozygous for the *rf2-R213* allele are male sterile but accumulate normal amounts of RF2 protein that lacks normal mitochondrial aldehyde dehydrogenase (mtALDH) activity provides strong evidence that *rf2*-encoded mtALDH activity is required to restore male fertility to T cytoplasm maize. Detailed genetic analyses have established that the *rf2* gene also is required for anther development in normal cytoplasm maize. Hence, it appears that the *rf2* gene was recruited recently to function as a nuclear restorer. ALDHs typically have very broad substrate specificities. Indeed, the RF2 protein is capable of oxidizing at least three aldehydes. Hence, the specific metabolic pathway(s) within which the *rf2*-encoded mtALDH acts remains to be discovered.

Introduction

Maternally inherited cytoplasmic male sterility (CMS) occurs in many plant species and is widely used to facilitate the production of hybrid seed because it eliminates the need for emasculation by hand. Mitochondrial defects account for all instances in which the nature of the lesion responsible for CMS has been identified (reviewed by Mackenzie et al., 1994;

defects can be avoided or overcome by the action of nuclear genes, termed nuclear restorers. However, the specific mechanisms by which restoration can occur are only poorly understood.

The male-sterile Texas (T) cytoplasm (cms-T) was used to produce approximately 85% of U.S. hybrid maize seed until the 1970 epidemic of southern corn leaf blight (Ullstrup, 1972; Pring and Lonsdale, 1989). cms-T maize is highly sensitive to a host-selective toxin (T toxin) produced by race T of *Cochliobolus heterostrophus*, the causal organism of southern corn leaf blight (Hooker et al., 1970; Comstock and Scheffer, 1973; Yoder, 1973). The genomes of T cytoplasm mitochondria contain a unique mitochondrial gene, *urf13*, that encodes the URF13 protein. URF13 accumulates in the inner membrane of the mitochondria (Forde and Leaver, 1980; Dewey et al., 1986; Wise et al., 1987a; Hack et al., 1991; Korth et al., 1991; Levings and Siedow, 1992) and is believed to be responsible for both the sensitivity to T toxin and the male sterility of cms-T maize (reviewed by Levings, 1990, 1993; Wise et al., 1999). The URF13 protein accumulates in many tissues of cms-T maize plants. However, in the absence of T toxin, the only severely affected tissue is the tapetal cell layer of the anthers, which undergoes a premature degeneration at the early microspore stage, resulting in pollen abortion (Warmke and Lee, 1977).

The combined action of two dominant alleles of two nuclear genes, *rf1* and *rf2*, restores the male fertility of cms-T maize (reviewed by Wise et al., 1999). Neither of these restorers alters the sensitivity of cms-T maize to T toxin. The function of the *rf1* gene in restoration

relates to its ability to modify the expression of *urf13*, thereby reducing the accumulation of URF13 (Dewey et al., 1987; Kennell and Pring, 1989).

As a first step toward determining its function in fertility restoration, the *rf2* gene was cloned via transposon tagging (Cui et al., 1996). The *rf2*-encoded protein, RF2, contains a predicted mitochondrial targeting sequence and exhibits approximately 60% identity and 75% similarity to class II mammalian mitochondrial aldehyde dehydrogenases (mtALDHs). ALDHs are a family of $NAD(P)^+$-dependent enzymes that catalyze the oxidation of numerous aldehydes (reviewed by Lindahl, 1992; Yoshida et al., 1998). A large number of ALDHs have been characterized in mammals, yeast, insects, and bacteria (reviewed by Perozich et al., 1999). In mammals and yeast, the class I (a cytosolic form) and class II (a mitochondrial form) isozymes have been particularly well characterized (Lindahl, 1992; Wang et al., 1998). According to recently revised nomenclature (Vasiliou et al., 1999), the *rf2* gene is equivalent to ALDH2B1. Only a few studies of plant class II mtALDHs have been reported (Asker and Davies, 1985; Osakovskii et al., 1992; op den Camp and Kuhlemeier, 1997). Although plant betaine ALDHs have been subjected to fairly intensive study (Vojtechova et al., 1997), these enzymes are only distantly related to class II mtALDHs.

The primary functions of ALDHs are believed to be the detoxification of ethanol-derived acetaldehyde and the oxidization of aldehydes derived from polyamine syntheses (Lindahl and Petersen, 1991). Based on the presence of indoleacetaldehyde dehydrogenase activity in cell-free extracts from mung bean seedlings (Wightman and Cohen, 1968), it has been suggested that ALDHs may be involved in the production of the plant hormone indole-3-

acetyl acetate (Marumo, 1986). However, this biochemical reaction also can be catalyzed by an aldehyde oxidase (Rajagopal, 1971).

Most maize inbred lines carry functional *Rf2* alleles, even though they have never been exposed to T cytoplasm. This suggests that the RF2 protein has an important physiological role other than restoring male fertility to plants that carry T cytoplasm (Schnable and Wise, 1994). In this report, we demonstrate that the RF2 protein is, as predicted (Cui et al., 1996), a mtALDH that accumulates in most organs. In addition, we demonstrate that this mtALDH activity is required for normal anther development not only in T cytoplasm maize but also in normal (N) cytoplasm maize.

Results

RF2 Accumulation in Maize

The *rf2* cDNA was cloned into the expression vector pET-30b, and the resulting plasmid, pLB333, was expressed in *E. coli*. The His-tagged recombinant RF2 protein was purified to homogeneity and used as an antigen to inject rabbits. Affinity-purified anti-RF2 polyclonal antibodies were used for immunoblot analyses. These analyses revealed that the RF2 protein accumulates in most organs examined, including seedling and mature leaves, mesocotyls, roots, tassels, ears, and stems (Figure 1A). However, the levels of RF2 accumulation varied among these organs, and it was not detectable in mature dried kernels (data not shown). A weak reaction signal can be detected in protein preparations from some, but not all, tissues from plants homozygous for the *rf2-m8904* allele, suggesting either that this allele is not

completely null or that the purified antibody can recognize a closely related protein. There is no significant difference in the accumulation of RF2 protein between seedlings that carry N or T cytoplasm (Figure 1B), nor is there a significant difference in RF2 protein accumulation between seedlings homozygous for *rf1* or *Rf1* (data not shown). The inbred line R213 is homozygous for the *rf2* reference allele (*rf2-R213*). Even though this allele does not restore male fertility to T cytoplasm plants, the inbred line R213 accumulates RF2 protein at levels indistinguishable from those seen in the inbred line Ky21 (Figure 1B).

RF2 Is a Mitochondrial Protein

Various computational analyses (Nakai, 1991) of the predicted RF2 protein suggest that it is targeted to mitochondria. To determine the subcellular localization of the RF2 protein, chloroplastic, microsomal, cytosolic, and mitochondrial fractions were prepared by differential centrifugation or by Percoll density centrifugation. Chlorophyll content and catalase, alcohol dehydrogenase, and cytochrome *c* oxidase activities were used as markers for these four fractions. These assays demonstrated that the mitochondrial fraction was not significantly contaminated by proteins from other organelles or the cytosol (Table 1). Immunoblot analyses revealed that the RF2 protein is present primarily in the mitochondrial fraction (Figures 2A and 2B). Furthermore, when isolated mitochondria were incubated with papain, in the presence of Triton X-100 the RF2 protein was digested, and in the absence of Triton X-100 the RF2 protein was resistant to papain digestion (Figure 2C). This result indicates that the RF2 protein is located within the mitochondrion and not simply associated

with its outer surface. Purified mitochondria were further fractionated into soluble and insoluble fractions. Cytochrome *c* oxidase (Errede et al., 1967) and malate dehydrogenase (Rocha and Ting, 1970) activities were used as markers for mitochondria membrane and matrix proteins, respectively. More than 98% of the cytochrome *c* oxidase activity was found in the insoluble fraction, whereas malate dehydrogenase activity was found exclusively in the soluble fraction. These results indicate that the insoluble fraction contains mitochondrial membrane proteins and that it has no detectable level of contamination by matrix proteins. Similarly, the soluble fraction contains mitochondrial matrix proteins and is not significantly contaminated by mitochondrial membrane proteins. Immunoblot analyses of these soluble and insoluble mitochondrial fractions revealed that RF2 is a matrix protein (Figure 2D).

Assuming that the translation of the RF2 protein begins at the first methionine codon in the cDNA, its predicted molecular mass would be 59.4 kD. However, the RF2 protein contains a predicted mitochondrial targeting sequence (MARRAASSLVSRCLLARAPAGAPPAAPSAPRRTVPADGMHRLLPGVLQRFS) whose predicted cleavage site is Leu^{42} or Ser^{51} (underlined). If the predicted mitochondrial targeting sequence is cleaved at one of these sites, the molecular mass of the mitochondrial RF2 protein would be 55.3 or 54.1 kD, respectively. On the basis of SDS-PAGE analysis, the RF2 protein isolated from mitochondria was estimated to be 53.2 kD (data not shown). This sizing by PAGE indicates that the RF2 protein is translated as a precursor that is processed after import into the matrix space. These data are consistent with either Leu^{42} or

Ser^{51} being the cleavage site, because SDS-PAGE analysis cannot provide the level of resolution required to determine the actual cleavage site. Hence, it will be necessary to conduct N-terminal sequencing to determine the actual cleavage site.

Immunolocalization experiments revealed that the accumulation of the RF2 protein is substantially greater in the cells of the tapetum than in other cell layers of the anther wall during the premeiosis stage (Figure 3). This result is consistent with the massive accumulation of mitochondria that occurs in the tapetal cells between the premeiotic and tetrad stages of microsporogenesis (Warmke and Lee, 1978). This result also suggests that during the premeiosis stage the amount of RF2 protein per mitochondrion may be higher in tapetal cells than other cells. This hypothesis is based on the observation that little RF2 signal was observed in pollen mother cells even though the number of mitochondria per unit volume in pollen mother cells is about two-fold greater than that in tapetal cells during this stage (Warmke and Lee, 1978).

Recombinant RF2 Exhibits ALDH Activity

The predicted RF2 protein exhibits a high level of sequence similarity to ALDHs; however, the His-tagged recombinant RF2 protein produced by pLB333 did not exhibit ALDH activity (data not shown). This construct included a His tag, an S tag, and the predicted maize mitochondrial targeting sequence, any of which might interfere with ALDH activity. Hence, the *rf2* cDNA was cloned into another expression vector, pET-17b, which does not include a His tag or an S tag, in such a way that the putative maize mitochondrial

targeting sequence was removed and only two vector-derived amino acids were added in the N terminus of the RF2 protein. The resulting plasmid, pMAP11, was transformed into the *E. coli* strain BL21(DE3). Expression of RF2 was induced by isopropylthio-β-galactoside (IPTG) and examined via immunoblot analysis. Although most of the recombinant RF2 protein produced by these cells accumulated in inclusion bodies, the soluble fraction of the crude cellular extract accumulated levels of RF2 protein detectable via immunoblot analyses (data not shown).

This soluble fraction was subjected to assays for ALDH activity in which the reduction of NAD^+ to NADH was monitored with a fluorescence spectrophotometer at 460 nm. Acetaldehye and glycolaldehyde were selected for these initial enzyme assays because acetaldehyde is a substrate in the fermentation pathway, which we have hypothesized may be involved in fertility restoration (Cui et al., 1996). Glycolaldehyde is structurally similar to lactaldehyde, which is not commercially available. Lactaldehyde is the in vivo substrate for the aldehyde dehydrogenase that is mutated in the JA111(DE3) strain of *E. coli*. When acetaldehyde was used as a substrate, ALDH activity was detected in extracts from BL21(DE3)pMAP11 (Figure 4). Control assays using extracts from BL21(DE3)pET-17b showed no ALDH activity (Figure 4). When glycolaldehyde was used as a substrate, ALDH activity was detected in extracts from both BL21(DE3)pMAP11 and BL21(DE3)pET-17b cells. This finding indicates that the BL21(DE3) strain contains endogenous glycolaldehyde dehydrogenase activity. However, the level of glycolaldehyde dehydrogenase activity was substantially greater in extracts from BL21(DE3)pMAP11 cells (Figure 4). These data

demonstrate that the RF2 protein has both acetaldehyde and glycolaldehyde dehydrogenase activities.

The *rf2* Gene Can Complement an *E. coli* ALDH Mutant

The *E. coli* strain 3 (Caballero et al., 1983) can grow on media in which 1,2-propanediol is the sole carbon source. To use this carbon source, strain 3 must first oxidize 1,2-propanediol to L-lactaldehyde, which is then further oxidized to L-lactate by an ALDH. L-Lactate is subsequently converted to pyruvate, which can enter central metabolism (Boronat and Aguilar, 1979). *E. coli* strain JA111 differs from strain 3 in that it carries a mutation in the *ald* gene that encodes an ALDH capable of oxidizing L-lactaldehyde to L-lactate. Hence, unlike strain 3, strain JA111 is unable to grow on media in which 1,2-propanediol is the sole carbon source (Hidalgo et al., 1991).

To determine whether *rf2* can complement the *ald* mutant, JA111 was first lysogenized with λDE3, which carries the T7 RNA polymerase gene. This was done because *rf2* expression is under the control of the T7 promoter in pMAP11. The resulting strain JA111(DE3) exhibited the same inability to grow on media in which 1,2-propanediol is the sole carbon source as JA111 (Figure 5). Subsequently, the plasmids pMAP11, pET-17b, and pALD9 (a plasmid that carries the *E. coli ald* gene and that can complement the *ald*-deficient mutant of JA111) were transformed into JA111(DE3). The ability of JA111(DE3)pMAP11 to express RF2 was tested using immunoblot analysis and ALDH activity assays (data not shown). All of the strains grew normally on glucose media, but only JA111(DE3)pALD9

and JA111(DE3)pMAP11 were able to grow on 1,2-propanediol media (Figure 5). This result indicates that the recombinant RF2 protein exhibits L-lactaldehyde dehydrogenase activity.

It should be noted that the complementation analyses described above were performed in the absence of IPTG induction. This was because *E. coli* strain JA111(DE3)pMAP11 failed to grow on 1,2-propanediol media when induced with all tested levels of IPTG (0.5, 1.0, and 1.5 mM). In contrast, *E. coli* cells that expressed the endogenous *ald* gene from the pALD9 construct grew on 1,2-propanediol media under all tested levels of IPTG. Both cells could grow on glucose media containing various levels of IPTG. The reason for this discrepancy is not known.

ALDH Activity in Maize Mitochondrial Extracts

To compare the enzyme activity of recombinant RF2 protein to that of the native RF2 protein, ALDH assays were performed on protein extracts from maize mitochondria prepared from immature unpollinated ears of the inbred line Ky21 (which is homozygous for the functional *Rf2-Ky21* allele) and a near-isogenic line homozygous for *rf2-m8904*. When acetaldehyde was used as a substrate, mtALDH activity was approximately four-fold to five-fold greater in wild-type Ky21 plants than in mutant plants. When glycolaldehyde was used as a substrate, wild-type plants exhibited 16- to 34-fold greater levels of ALDH activity than mutants (Table 2, Figures 6A and 6B). These results demonstrate that, like the recombinant RF2 protein, the native RF2 protein exhibits acetaldehyde and glycolaldehyde dehydrogenase

activities. The levels of ALDH activity were not significantly different in mitochondrial extracts from N and T cytoplasm plants (Table 2), which is consistent with the fact that the accumulation of RF2 protein does not differ between these genotypes (Figure 1). ALDH assays of submitochondrial fractions revealed that ALDH activity is confined to the mitochondrial matrix (data not shown), which is consistent with the results of immunoblot analyses (Figure 2D).

Molecular Lesion in the *rf2-R213* Allele

The inbred line R213 carries a mutant allele of *rf2* (*rf2-R213*) that is not capable of restoring male fertility to T cytoplasm maize. Surprisingly, this inbred line accumulates RF2 protein (Figure 1B) of the same size and at the same level as does the inbred line Ky21, which carries a functional *Rf2* allele. In addition, mitochondrial extracts from R213 exhibit a small amount of ALDH activity (data not shown). In contrast, a stock that is homozygous for *rf2-R213* but near isogenic with Ky21 accumulates *rf2* mRNA (Cui et al., 1996) and RF2 protein (data not shown) but does not exhibit ALDH activity (Figure 6C). Hence, it appears that the *rf2-R213* allele does not code for a functional ALDH.

To identify the molecular lesion in the *rf2-R213* allele, the coding region of this allele was amplified via reverse transcription–polymerase chain reaction (PCR) and sequenced. Sequence analysis revealed that the *rf2-R213* allele (GenBank accession number AF269064) has four single nucleotide polymorphisms (SNPs) relative to the wild-type *rf2-B73* allele (GenBank accession number U43082). These polymorphisms introduce three amino acid

substitutions (one SNP is a silent third position substitution). The RF2 protein structure was predicted using SWISS-MODEL (http://www.expasy.ch/swissmod; Guex and Peitsch, 1997) using as a template bovine mtALDH (Protein Data Bank number 1AG8), which exhibits 62% identity and 70% similarity to RF2. The Asn^{400}-to-Lys and the Ile^{522}-to-Met substitutions in the *rf2-R213* allele are both located at the periphery of the RF2 protein structure (Figure 7), whereas the Pro^{323}-to-Ser substitution is located in the substrate binding pocket (Liu et al., 1997; Steinmetz et al., 1997) and in the conserved catalytic Glu^{317} domain predicted by the Motifs function of the Genetics Computer Group (Madison, WI) package. The Asn^{400}-to-Lys substitution mimics the functional bovine mtALDH, and the Ile^{522}-to-Met substitution is conservative. In contrast, the mutation of Pro^{323}-to-Ser is likely to greatly affect the protein structure. Hence, this substitution is most likely to be responsible for the loss of ALDH activity in the *rf2-R213* allele.

The *rf2* Gene Is Required for Normal Anther Development in N Cytoplasm Maize

Most maize inbred lines carry functional *Rf2* alleles, even though they have never been exposed to T cytoplasm. This suggests that the RF2 protein has an important physiological role other than restoring male fertility to plants that carry T cytoplasm (Schnable and Wise, 1994). To characterize this physiological role of the *rf2* gene, the effects on anther development of two independent transposon insertion mutant alleles, *rf2-m8904* and *rf2-m9323*, were characterized. These characterizations were performed on plants homozygous for these two alleles that were derived from three and four generations, respectively, of

backcrossing to the inbred line N cytoplasm Ky21. The tassels of the backcrossed *rf2-m* plants exert anthers and shed functional pollen. However, various degrees of anther arrest (Figure 8) were observed in plants homozygous for these two alleles compared with the near-isogenic N cytoplasm Ky21 plants (Figure 8A). Arrested anthers were smaller than those at the same developmental stage in wild-type N cytoplasm Ky21 plants (data not shown) and failed to shed pollen. Arrested anthers were distributed evenly within affected tassels.

A maize spikelet consists of an upper and a lower floret, each of which contains three anthers. Anthers in the lower floret progress through development approximately 3 days after those in the upper floret of the same spikelet (Hsu and Peterson, 1991). When sections of spikelets from N cytoplasm *rf2-m* plants were observed microscopically, various defects were observed, from slightly affected microspores to completely degenerated microspores and shriveled locules. As expected based on the gross examination of spikelets, these defects are observed mainly in the anthers from lower florets (Figure 9).

To demonstrate that the anther arrest phenotype is caused by loss of *Rf2* function, plants from a segregating population, resulting from the test cross (N) *wx rf2-m8904/wx rf2-m8904* × *wx rf2-m8904/Wx Rf2-Ky21* were observed for anther arrest. Plants were categorized into five classes according to the severity of anther arrest (Figure 8). Among the progeny of this test cross, the anther arrest phenotype is well correlated with the waxy kernel phenotype, which serves as a marker for *rf2* (data not shown). To further characterize the relationship between anther arrest and the *rf2* mutation, some plants from the N, 'N', A, and AA categories (see Methods for a description of the categories) were genotyped at the *rf2* locus

via restriction fragment length polymorphism (RFLP) analysis using the *rf2* cDNA as a probe (98 6503-06 in Table 3). The ambiguous category 'A' (Figure 8C) was not genotyped. All 38 plants from the N and 'N' categories were heterozygous *rf2-m8904/Rf2-Ky21*, and all 23 plants from the A and AA categories were homozygous for the *rf2-m8904* allele. Similar results were obtained from a population segregating for the other tested *rf2* mutant allele, *rf2-m9323*. However, in this case, two exceptions were observed. Both exceptional plants were homozygous for *rf2-m9323* but did not exhibit anther arrest (98 6509-10 in Table 3). These results indicate that either (1) the *rf2* mutation is the cause of the anther arrest phenotype and the two exceptions in the population segregating for *rf2-m9323* represent instances of incomplete penetrance or indicate the presence of a suppressing factor, or (2) the genetic factor that causes anther arrest is not *rf2* but is closely linked to *rf2*.

Two independent revertant (*Rf2'*) alleles derived from the excision of the nonautonomous transposon insertion from the *rf2-m8904* allele were used to distinguish between these two possibilities. Both of these revertant alleles, *Rf2'1036W103* and *Rf2'1036W110*, confer male fertility to plants that carry T cytoplasm. Because these two revertant alleles would be expected to have exactly the same haplotype in the vicinity of the *rf2* locus as the *rf2-m8904* mutant from which they arose, these alleles represent useful reagents for determining whether the anther arrest phenotype is controlled by *rf2* or a closely linked gene.

Observation of 29 progeny from the cross (N) *rf2-m8904/rf2-m8904* × *Rf2'1036W103/Rf2'1036W103* revealed that all exhibited normal anther development. This revertant allele also was used to generate a segregating population from the test cross (N) *wx*

rf2-m8904/wx rf2-m8904 × *Wx rf2-R213/wx Rf2'1036W103*. All of the 9 resulting progeny that carried the revertant allele were normal, and 10 of 12 of the progeny that carried *rf2-m8904/rf2-R213* exhibited the anther arrest phenotype (99 6655-56 in Table 3). Similar results were obtained with the *Rf2'1036W110* revertant allele (99 6657-58 in Table 3). Hence, these data demonstrate that *Rf2* function is required to prevent anther arrest in N cytoplasm plants.

Partial ALDH Activity Causes Anther Arrest in T Cytoplasm

Because the lack of *rf2*-encoded mtALDH activity causes complete male sterility in T cytoplasm plants but only partial anther arrest in N cytoplasm plants, we hypothesized that the full development of anthers in T cytoplasm plants requires more RF2 activity than that in N cytoplasm plants. To test this hypothesis, suppressible *rf2 Mu* insertion alleles *rf2-m9437*, *rf2-m9390*, and *rf2-m8110* were used to observe the phenotype associated with low, but not null, levels of RF2. *Mu* suppression is the loss of a *Mu*-induced allele's capacity to condition a mutant phenotype in the absence of excisional loss of the associated *Mu* transposons (Martienssen et al., 1989). Many maize *Mu*-induced mutant alleles, such as *hcf106*::*Mu1*, exhibit *Mu* suppression (Martienssen et al., 1989, 1990; Barkan and Martienssen, 1991). *Mu* suppression occurs in the absence of high activity of the autonomous *Mu* transposon *MuDR* (Lowe et al., 1992; Greene et al., 1994; Martienssen and Baron, 1994).

The suppressible *rf2* alleles fail to condition male sterility in T cytoplasm plants in the absence of *MuDR* (X. Cui, A.P. Hsia, D.A. Ashlock, R.P. Wise, and P.S. Schnable, submitted manuscript). Various degrees of *Mu* suppression can be obtained from these suppressible alleles when *Mu* activity is at intermediate levels. Plants that carry partially suppressed *rf2-m* alleles exert various numbers of anthers (from a few to almost all), some of which shed pollen (Figures 8G, 8H, and 8I). Analysis of individual spikelets revealed that exerted anthers are always derived from the upper florets, whereas the anthers in most lower florets are arrested in their development. The *rf2*-mediated anther arrest that occurs in these partially suppressed T cytoplasm plants closely resembles the arrest that occurs in N cytoplasm plants completely lacking RF2 activity. Therefore, the full development of anthers in T cytoplasm plants requires more RF2 activity than in N-cytoplasm plants. Similarly, the full development of anthers in lower florets requires more RF2 activity than in upper florets.

Discussion

CMS systems play important roles in the production of hybrid seed. In addition, they serve as useful models for the study of mitochondrial mutations and nucleus–mitochondria interactions (Mackenzie et al., 1994). Despite the considerable effort that has been directed toward understanding CMS systems, the *rf2* gene remains the only nuclear restorer of CMS to be cloned from any species. As such, it represents a unique resource for the study of the molecular mechanisms associated with fertility restoration.

CMS systems often are associated with the presence of novel mitochondrial open reading frames (Schnable and Wise, 1998). In at least some cases, it is known that the gene products associated with these open reading frames cause male sterility (Gengenbach et al., 1981; Kemble et al., 1982; Umbeck and Gengenbach, 1983; Fauron et al., 1987; Wise et al., 1987b; He et al., 1996). Hence, nuclear genes that disrupt the normal accumulation of these gene products can function as nuclear restorers. Examples of this type of nuclear restorer include the *Fr* gene, which is capable of directing the loss of the CMS-associated *pvs* sequence from the *Phaseolus vulgaris* mitochondrial genome (MacKenzie and Chase 1990), and the *rf1* gene, which reduces the accumulation of the cms-T–associated URF13 protein (Dewey et al., 1987; Kennell and Pring, 1989). In contrast, even though the *rf2* gene is a nuclear restorer of cms-T, it does not affect the accumulation of URF13. Hence, the analysis of the *rf2* gene has defined another general mechanism by which nuclear genes can function as restorers. Instead of affecting the accumulation of CMS-associated gene products, "compensatory restorers," such as *rf2*, provide "work around" solutions that compensate for the metabolic dysfunctions caused by CMS-associated gene products.

The *rf2* Gene Encodes a mtALDH

The first two steps toward defining the mechanism by which *rf2* compensates for the as-yet-undefined metabolic disruptions induced by URF13 were to determine the enzymatic function and the localization of the RF2 protein. The sequence-based prediction that the *rf2* gene encodes an ALDH (Cui et al., 1996) was tested via three independent approaches. First,

it was established that recombinant RF2 protein has acetaldehyde and glycolaldehyde dehydrogenase activities. Second, the *rf2* gene was shown to complement an *E. coli* mutant that requires L-lactaldehyde dehydrogenase activity. Third, protein extracts of mitochondria purified from wild-type maize plants were found to contain more acetaldehyde and glycolaldehyde dehydrogenase activities than similar extracts from *rf2* mutant plants. Hence, we conclude that the *rf2* gene encodes an ALDH.

The accumulation of the RF2 protein to high levels in the tapetal layer of anthers is consistent with the observation that premature degeneration of the tapetum occurs in unrestored cms-T plants (Wamke and Lee, 1977). Subcellular and suborganellar fractionation experiments established that the RF2 protein accumulates in the mitochondrial matrix and thereby have confirmed and extended the sequence-based predictions of Cui et al. (1996).

mtALDH Activity Is Required for Fertility Restoration of cms-T Maize

The results described above establish that the *rf2* gene encodes a mtALDH. However, it is formally possible that some feature of the RF2 protein, other than its ALDH activity, is responsible for its ability to function as a restorer. For example, the ALDH-derived ω-crystallin lacks ALDH activity and functions as a structural protein in the lens of squid and octopus (Zinovieva et al., 1993). Analysis of a spontaneous *rf2* mutant allele provided data to test this hypothesis. Plants homozygous for *rf2-R213* accumulate mRNA (Cui et al., 1996) and protein (Figure 1B) of the same sizes and in the same amounts as do nonmutant plants. However, the protein encoded by this allele does not exhibit ALDH activity (Figure

6). Sequence analysis of *rf2-R213* defined a single amino acid substitution, Pro^{323} to Ser, that is likely to be responsible for the loss of ALDH activity. Hence, these data strongly support the view that the *rf2* gene functions as a restorer of fertility by virtue of its ability to encode ALDH activity.

The Metabolic Role of *rf2*-Encoded mtALDH

One of the challenges of the postgenomic era is how to assign enzymatic functions to thousands of newly identified proteins. In many instances, it is possible to obtain clues regarding the functions of these proteins on the basis of sequence similarities and high throughput functional assays (Martzen et al., 1999). However, once an enzymatic function has been established, there remains the even more difficult "postpostgenomic" challenge of defining the precise metabolic roles of the enzymatic functions within an organism. This challenge exists because orthologous proteins can have different metabolic functions among organisms and the same protein can have different functions within an organism.

Because mtALDHs typically have many potential substrates (Klyosov, 1996), the task of determining the specific aldehyde(s) that must be oxidized during fertility restoration is particularly challenging. Although the three-dimensional structure of the RF2 protein has been predicted via modeling using the known structure of a mammalian class II mtALDH as a template (Steinmetz et al., 1997), this information does not provide information regarding the metabolically important substrate(s) of this enzyme. Biochemical approaches to defining this substrate are complicated by the fact that mutants of the *rf2* gene exert their effects on male

fertility (at least in T cytoplasm maize) in only a single internal cell layer of the anther (i.e., the tapetum).

One function of mtALDHs in mammals is the detoxification of ethanol-derived acetaldehyde. It has been established that enzymes involved in fermentation (i.e., pyruvate decarboxylase [EC 4.1.1.1], alcohol dehydrogenase [EC 1.1.1.1], and aldehyde dehydrogenase [EC 1.2.1.3]) are expressed during microspore development (reviewed by Tadege et al., 1999); this study established that the RF2 protein exhibits acetaldehyde dehydrogenase activity. Hence, we are currently using a genetic approach to test the hypothesis that the metabolically significant substrate of RF2 is acetaldehyde.

However, diverse aldehydes are produced via numerous metabolic pathways, including the peroxidation of membrane lipids that can result from oxidative stress (Siu and Draper, 1982); glycine biosynthesis (Davies, 1959); the catabolism of threonine (Styrvold et al., 1986), phenylalanine (Ferrandez et al., 1997), and tyrosine (Ferrandez et al., 1997); vitamin A metabolism (McCaffery and Drager 1993); and indole-3-acetyl acetate biosynthesis (Marumo, 1986). Other biogenic aldehydes and retinaldehydes also are possible substrates of RF2. In mammalian systems, trace amounts of such products are capable of affecting gene action (Sladek et al., 1989; Lindahl, 1992). Hence, in parallel with testing specific hypotheses, we are also conducting genetic screens for suppressors and enhancers of *rf2* mutants with the expectation that the nature of the genes identified via these screens will provide clues regarding the specific biochemical pathway(s) in which the *rf2*-encoded mtALDH functions during fertility restoration.

The *rf2* Gene Has a Function Independent of Its Role in Restoration

Most of the examined maize inbred lines (15 of 17) carry functional alleles of the *rf2* gene (Wise et al., 1999). The two exceptions, R213 and Wf9, carry the same mutant *rf2* allele, because R213 was derived from Wf9 (D. Duvick, personal communication). Because most inbred lines have never (or have only recently) been exposed to T cytoplasm, it has been hypothesized that the *rf2* gene must have been selected during evolution for a function other than fertility restoration (Schnable and Wise, 1994). According to this hypothesis, the *rf2* gene was recruited only recently to serve as a nuclear restorer. However, the nature of this other (presumed) function was not predicted, because *rf2* was not known to confer any phenotype in maize that does not carry T cytoplasm.

The detailed analyses reported here establish that the *rf2* gene plays a significant developmental role, even in plants that do not carry T cytoplasm. Specifically, this gene is required for normal anther development in plants that carry N cytoplasm. The recruitment of the *rf2* gene to serve as a nuclear restorer demonstrates the ability of plant genomes to respond to novel metabolic disturbances.

Because the *rf2* gene has been recruited only recently to serve its new function as a restorer of CMS, it is not surprising that the levels of *rf2* mRNA (Cui et al., 1996), RF2 protein, and *rf2*-encoded ALDH activity are not higher in T cytoplasm than in N cytoplasm maize (Figures 1 and 6). However, this latter observation also indicates that *rf2*-encoded levels of ALDH activity are high enough in N cytoplasm plants to accommodate the

enzymatic function(s) required for restoration of T cytoplasm plants. This is true even though an analysis of suppressible *rf2* alleles suggests that higher levels of *rf2* expression are required for anther development in T cytoplasm that in N cytoplasm maize. However, it should be noted that although *rf2* mutants affect anther development in plants that carry either N or T cytoplasm, the metabolic role that the RF2 protein plays during the restoration of cms-T may differ from the role that it plays during anther development in N cytoplasm maize.

Although the upper floret develops several days earlier than the lower floret from the same spikelet (Hsu and Peterson, 1991), the two florets do not exhibit visually detectable differences in their developmental programs. However, because this study revealed that *rf2* mutations preferentially affect the lower florets in plants that carry either T or N cytoplasm, we hypothesize that even at the same developmental stage upper and lower florets will exhibit different patterns of gene expression.

Methods

Maize Strains and *rf2* Alleles

The inbred maize (*Zea mays*) line Ky21 is homozygous for functional alleles of the *rf1* (*Rf1-Ky21*) and *rf2* (*Rf2-Ky21*) loci. The inbred line R213 is fixed for *Rf1* and *rf2*. Because R213 was derived from a cross between Ky21 and Wf9 (*rf1-Wf9*, *rf2-Wf9*) (D. Duvick, Pioneer Hi-bred International, Inc., personal communication), the *Rf1* allele carried by R213 must be *Rf1-Ky21*. Similarly, the *rf2* allele in R213 must be identical to *rf2-Wf9*. However, to

be consistent with previous nomenclature, this allele is referred to as *rf2-R213*. A Texas (T) cytoplasm version of Ky21 was generated by backcrossing a T cytoplasm version of the inbred line R213 to Ky21 for seven generations. Restriction fragment length polymorphism (RFLP) analysis established that the resulting line is homozygous for *Rf1-Ky21* and *Rf2-Ky21*. The T cytoplasm versions of Ky21 homozygous for the *rf2-m* or *rf2-R213* mutant alleles were generated by backcrossing each allele to Ky21 for at least three generations. All lines used in this study carry the *Rf1-Ky21* allele.

The *rf2-m* alleles were derived from *Mutator* or *Spm/En* transposon tagging experiments (Schnable and Wise, 1994). The progenitor alleles of *rf2-m8122*, *rf2-m9323*, *rf2-m9390*, and *rf2-m8110* have been described (Cui et al., 1996). Based on sequence comparisons, the progenitor allele of *rf2-m9437* (GenBank accession number AF318138) is *Rf2-B79* (GenBank accession number AF318135). The progenitor allele of *rf2-m8904* (GenBank accession numbers AF318130, AF318131, and AF318132) has not yet been identified. However, it is not *Rf2-B79*, *Rf2-Q66* (GenBank accession number AF318133), *Rf2-Q67* (GenBank accession number AF318134), or *Rf2-B77* (GenBank accession numbers AF318136 and AF318137). When originally isolated, the *rf2-m8904* allele conferred a stable male-sterile phenotype. However, it appears to contain a transposon insertion. This conclusion is based on the observation that the allele can produce functional revertant alleles (*Rf2'*) that contain an RFLP relative to *rf2-m8904* (see below).

Genetic analyses established that the *rf2-m8904* allele does not contain an autonomous *Spm/En* transposon insertion (Schnable and Wise, 1994). However, some crosses (e.g., 95

1902-21/2945) between stocks that carried *rf2-m8904* and related stocks derived from the *Spm/En* tagging population yielded progeny that produced tassels with male-fertile sectors, presumably because they were chimeric for revertant *Rf2'* alleles. Pollen from revertant sectors was used to pollinate T cytoplasm R213 plants. Some of the resulting progeny were male fertile and self-pollinated. Plants that were homozygous for two revertant alleles, *Rf2'1036W103* (GenBank accession numbers AF318139, AF318140, and AF318141) and *Rf2'1036W110* (GenBank accession numbers AF318142, AF318143, and AF318144), were identified by RFLP analysis. The 1.2-kb partial *rf2* cDNA probe (Cui et al., 1996) detected two distinct HindIII fragments of approximately 9 and 10 kb in DNA from plants homozygous for *rf2-m8904* but only a single 10-kb fragment in DNA from plants homozygous for the revertant alleles. In contrast, the six introns (844 bp) of these alleles that have been sequenced are identical to the corresponding introns of *rf2-m8904*, even though 28 single nucleotide polymorphisms (SNPs) were identified between these alleles and the *Rf2-B73* allele (GenBank accession number AF215823). Hence, it appears that *Rf2'1036W103* and *Rf2'1036W110* arose from *rf2-m8904* via the excision of a nonautonomous transposon that was activated by the introduction of an autonomous transposon via the cross described above.

Genotype and Phenotype Determinations

Immature ears or young leaves were collected from plants to be genotyped. DNA was extracted from ears according to a procedure described by Dellaporta et al. (1983). Ten

micrograms of DNA was digested with KpnI at 37°C for 3 hr and separated on a 0.8% agarose gel. DNA gel blot analyses (Sambrook et al., 1989) were conducted on these DNA samples using as a probe the full length *rf2* cDNA isolated from prf27311 (Cui et al., 1996) labeled with ^{32}P.

Male fertility and anther arrest phenotypes were scored in the morning for several days during the period of pollen shed. Plants were scored for male fertility according to the scale of Schnable and Wise (1994). The degrees of anther arrest were categorized into five classes (N, 'N', 'A', A, and AA). The N category is equivalent to the phenotype displayed by Ky21 (Figure 8A); 'N' category plants have very few arrested anthers (Figure 8B); 'A' category plants have some arrested anthers but fewer than half of the lower florets contain arrested anthers (Figure 8C); most of the lower florets in A category plants contain arrested anthers (Figure 8D); and most anthers in most of the lower florets in AA category plants are arrested (Figure 8E).

Expression of the RF2 Protein in *Escherichia coli*

Polymerase chain reaction (PCR) was performed using primers rf2-B2 (5′-AAGATCTGATGCACAGGCTGTTGCCA-3′) and rf2-xq (5′-CCAACTTTCCAGGCATACATCA-3′) to amplify a portion of the *rf2* cDNA (nucleotides 368 to 918) from plasmid prf27311 that contains the 2.2-kb full length *rf2* cDNA (Cui et al., 1996). The 5′ primer (rf2-B2) was synthesized such that it contained an extra BglII site; the

3′ primer (rf2-xq) was downstream of an internal NdeI site. A three-fragment ligation was conducted using the 367-bp BglII–NdeI PCR product, the 1493-bp NdeI–KpnI fragment from prf27311, and the BglII–KpnI fragment of the expression vector pET-30b (Novagen, Madison, WI). The resulting plasmid was termed pLB333. Plasmid pMAP11 was generated in a similar fashion except that the 5′ primer (rf2-lp1, 5′-GTCTAGAACCGCAGCAGCAGTAGAGG-3′) carried an NheI site, the PCR product included nucleotides 407 to 918 from prf27311, and the cloning vector was NheI–KpnI-digested pET-17b.

Both plasmids were transformed into the *E. coli* strain BL21(DE3) for expression. Transformed cells were incubated at 37°C overnight, transferred to 200 mL of fresh medium (1.6% tryptone, 1.0% yeast extract, and 0.5% NaCl) the next morning, and incubated in a 37°C shaker. Once the OD_{600} reached 0.8 to 1.0, 1 mM isopropylthio-β-galactoside (IPTG) was added and incubation was continued for another 3 hr or until the OD_{600} reached 1.5.

Antibody Preparation and Purification

RF2 protein that had been expressed from pLB333 as a fusion protein containing six histidines (His tag), and the S tag was purified by Ni^{2+} affinity chromatography under denaturing conditions using the protocol described in the sixth edition of the Novagen pET system manual. The eluted fraction was dialyzed sequentially against TEN buffer (100 mM Tris, pH 8.0, 10 mM EDTA, and 50 mM NaCl) containing 3, 1, or 0.5 M urea. Finally, this

fraction was dialyzed twice against TEN buffer without urea. The dialysis tubing containing RF2 protein was embedded in ground sucrose overnight, and then its contents were passed through a Sephadex G-75 column equilibrated with 50 mM Tris, pH 8.0, and 0.1 M NaCl. Aliquots of fractions of the flow through were subjected to SDS-PAGE and then transferred to nitrocellulose membranes. The RF2-containing fractions could be recognized because they contained detectable levels of S tag peptide, which was detected according to the manufacturer's instructions (Novagen). Fractions that contained the S tag (and hence the RF2 protein) were pooled. SDS-PAGE analysis of the pooled fractions revealed only a single Coomassie Brilliant Blue R 250–stainable protein of about the size expected for the recombinant RF2 protein (i.e., 57 kD).

The recombinant RF2 protein was concentrated to 1 mg/mL using a Millipore (Bedford, MA) spin column (Centriplus 30) and then used as an antigen to inject rabbits. Two weeks after the second injection, antisera were collected and used directly or further purified according to Dumbroff and Gepstein (1993) with the following modifications. Maize tassels with the genotype *rf2-m8904/rf2-m8904* Ky21 were ground in TBS buffer (25 mM Tris, pH 7.5, and 150 mM NaCl) supplemented with 1 mM phenylmethylsulfonyl fluoride (Sigma, St. Louis, MO), 5 mM EDTA, and 1 μg/mL E-64 (Sigma), filtered through four layers of cheesecloth, and spun at 12,000*g* for 10 min. An 8- × 8-cm^2 piece of nitrocellulose membrane was incubated at room temperature on a shaker for 3 hr in the resulting supernatant, which contained 100 mg of protein extracted from the *rf2-m8904/rf2-m8904* tassels. The membrane was washed in TBS four times and rinsed in PBS (0.8% NaCl, 0.02% KCl, 0.14% Na_2HPO_4,

and 0.024% KH_2PO_4, pH 7.2). The bound protein was fixed to the membrane by treatment with 0.2% glutaraldehyde in PBS for 1 hr and subsequently washed sequentially in PBS and TBS. One milliliter of antiserum was added to 10 mL of TBS and incubated with the membrane overnight at 4°C. The solution was collected and loaded onto a protein A–agarose column and washed with 10 volumes of TBS. Antibodies were eluted from the column using 0.1 M glycine, pH 3.0, neutralized with 1.0 M Tris, pH 8.0, passed through a PBS-equilibrated Sephadex G-25 spin column, divided into aliquots, and stored at –20°C.

Immunolocalization

Maize anthers at the premeiotic stage were dissected and fixed at 4°C for 6 hr in 2% glutaraldehyde, 3% paraformaldehyde, and 0.1 M sodium cacodylate, pH 7.0. The fixed anthers were dehydrated in 25, 50, 75, 80, 90, 95, and 100% (twice) ethanol for 20 min each and then infiltrated with ethanol:LR White (Electron Microscopy Sciences, Fort Washington, PA) (1:3), ethanol:LR White (1:1), ethanol:LR White (3:1), and LR White (twice) for 30 min each (modified from Parthasarathy, 1994). The embedded anthers were left in a 60°C oven overnight and then cross-sectioned into 1-μm-thick sections. These sections were mounted on polylysine-treated slides, blocked with 5% dry milk in TBS, and incubated with purified anti-RF2 polyclonal antibodies (final concentration, 36.5 μg/mL) at 37°C for 3 hr. Slides were washed with TBS three times for 10 min each and then incubated with 10-nm gold-labeled goat anti-rabbit IgG secondary antibodies (1:3000; Sigma) at 37°C for 3 hr. The gold

particles were enhanced using a silver enhancing kit (SE-100; Sigma) and viewed and photographed with a phase contrast light microscope.

Light Microscopy

Maize spikelets and anthers at various stages were fixed in 50% ethanol, 5% acetic acid, and 3.7% formaldehyde at room temperature for 24 hr. Fixed tissues were dehydrated, infiltrated, and embedded in paraffin (Sylvester and Ruzin, 1994). Cross-sections of 10 to 20 μm were deparaffined and stained with toluidine blue for observation via bright-field microscopy.

Sequencing

DNA sequencing was performed at the Iowa State University DNA Sequencing and Synthesis Facility on an automated sequencer (ABI 373A; Applied Biosystems, Foster City, CA). Sequence assembling and analyses were performed using the Wisconsin GCG software package, version 10.0-Unix, from the Genetics Computer Group. Polymorphisms detected between *rf2-R213* cDNA and wild-type *Rf2-B73* were confirmed by sequencing polymorphic regions obtained by PCR amplification of the *rf2-R213* allele from genomic DNA of the inbred line R213.

E. coli Complementation

E. coli strain JA111 was lysogenized with a recombinant λDE3 phage (Novagen) according to the manufacturer's instructions. The resulting strain was designated JA111(DE3) and carried a T7 RNA polymerase gene under the control of the lacUV5 promoter. Plasmid pALD9 carries an E. coli aldehyde dehydrogenase that complements the E. coli ald-deficient mutant JA111 (Hidalgo et al., 1991). Plasmids pALD9, pMAP11, and pET-17b were each transformed into JA111(DE3) by electroporation. Two pMAP11 transformants (pMAP11-1 and pMAP11-2) and one pET-17b transformant were selected for further analysis. Each E. coli culture was streaked in duplicate on basal medium (Boronat and Aguilar, 1979) supplemented with either 40 mM glucose or 40 mM 1,2-propanediol as the sole carbon source and incubated at 37°C. Cells grown on glucose were scored after 24 hr of incubation, whereas cells grown on 1,2-propanediol were scored after 3 days.

Cell Fractionation and Mitochondria Preparation

Mitochondria to be used in the subcellular localization experiment were purified from 4-day-old etiolated Ky21 seedlings via Percoll gradient centrifugation (Jackson and Moore, 1979). Chloroplasts were prepared from 7-day-old green maize Ky21 seedlings according to Leegood and Walker (1983). Chlorophyll (Leegood and Walker, 1983), catalase (Vigil, 1983), alcohol dehydrogenase (Freeling and Schwartz, 1973; Quail, 1979), and cytochrome *c* oxidase (Errede et al., 1967) were used as markers in chloroplastic, microsomal, cytosolic, and mitochondrial fractions, respectively. For the catalase assay, fractions were passed through a

Sephadex G-15 spin column equilibrated with 0.1 M phosphate buffer, pH 7.0, before the enzyme assay.

Mitochondria for other purposes were prepared from either etiolated maize seedlings or unpollinated ears according to the method of Payne et al. (1980) and then further purified by sucrose cushion centrifugation (Jackson and Moore, 1979). The proteinase protection assay of mitochondria was conducted according to Huang et al. (1990), except that papain was used instead of proteinase K.

To isolate the membrane and soluble fractions from mitochondria, purified mitochondria were resuspended in 20 mM 3-(*N*-morpholino)-propanesulfonic acid, pH 7.5, and 1 mM DTT to yield a 0.2 mg/mL protein solution and sonicated three times for 10 sec each using a Fisher model 60 sonicator set at 15 W. The solution was then spun at 100,000*g* for 2 hr. The supernatant contained the soluble mitochondrial proteins. The pellet was resuspended and washed once with 20 mM 3-(*N*-morpholino)-propanesulfonic acid, pH 7.5, and 1 mM DTT and centrifuged as described above. The resulting pellet was collected and resuspended in the buffer described above.

Preparation of Protein Extracts, SDS-PAGE, and Immunoblot Analysis

E. coli protein was prepared according to the sixth edition of the Novagen pET system manual. Total maize protein was prepared by grinding tissue in 2 to 4 volumes of 0.1 M Tris, pH 8.0, 0.1 M NaCl, 5 mM EDTA, 1 mM phenylmethylsulfonyl fluoride, 0.1% Triton X-100, and 1% insoluble polyvinylpyrrolidone and then centrifuging the resulting material at

14,000g for 20 min. The supernatant was subjected to SDS-PAGE according to Sambrook et al. (1989). Separated proteins were transferred to a nitrocellulose membrane using a semidry electrophoretic transfer cell (Bio-Rad, Hercules, CA) at 20 V for 2 hr. Membranes were blocked using 3% BSA in TBS and incubated with purified anti-RF2 antibodies at room temperature for 3 hr, washed with TBS and 0.05% Tween 20 three times for 10 min each, and then incubated with anti-rabbit IgG alkaline phosphatase secondary antibody (1:30,000 dilution; Sigma) for 1 hr. The result was visualized by staining with nitroblue tetrazolium/5-bromo-4-chloro-3-indolyl phosphate (Sigma).

ALDH Assays

For *E. coli* aldehyde dehydrogenase (ALDH) assays (modified from op den Camp and Kuhlemeier, 1997), cells were washed with water and resuspended in 0.1 volume of the original cell cultures of 0.1 M Hepes, pH 7.4, 1 mM EDTA, 2 mM DTT, and 0.1% Triton X-100, treated with lysozyme (0.1 mg/mL) on ice for 20 min, and sonicated three times for 10 sec each using a Fisher model 60 sonicator at maximum output. Between sonication treatments, the cellular extract was cooled in an ice water bath. The lysate was centrifuged at 14,000*g* for 20 min. The resulting supernatant was used as a crude enzyme extract.

For maize mitochondrial ALDH assays, mitochondria were prepared from maize seedlings or unpollinated ears according to Payne et al. (1980). The resulting mitochondrial pellet was resuspended in 0.1 M Hepes, pH 7.4, 1 mM EDTA, 2 mM DTT, and 0.1%

Triton X-100, sonicated, and centrifuged as described above. The resulting supernatant served as a crude enzyme extract.

For each ALDH assay, 200 μg of *E. coli* protein extract or 180 μg of mitochondrial protein extract was added to a reaction mixture containing 1.5 mM NAD (Sigma) and 0.1 M sodium pyrophosphate buffer, pH 8.5, and the total volume was adjusted to 1.0 mL with water. After 30 sec of prereaction, aldehyde (17 μM acetaldehyde or 20 μM glycolaldehyde) was added to the mixture, which was excited at 360 nm, and the emission fluorescence of NADH was recorded at 460 nm at 10-sec intervals for up to 2 min on a model F-2000 fluorescence spectrophotometer (Hitachi, Tokyo, Japan). ALDH activity was expressed as nanomoles of NADH production per minute per milligram of protein.

Reverse Transcription–PCR of *rf2-R213*

RNA from immature tassels (still in the whorl) from the inbred line R213 was extracted according to Dean et al. (1985). First strand DNA synthesis was conducted from 5 μg of RNA using a 3′ rapid amplification of cDNA ends kit (Gibco BRL, Rockville, MD) and *rf2*-specific primers (rf2-xq, 5′-CCAACTTTCCAGGCATACATCA-3′; and RF2C2, 5′-CCAGGCTAGGGCAAATCTTAT-3′). The resulting DNA was used as a template in subsequent PCR reactions with various *rf2* primer combinations that covered the entire *rf2* coding sequence. Both strands of the PCR products were sequenced completely.

Acknowledgments

We thank Juan Aguilar (Department of Biochemistry, School of Pharmacy, University of Barcelona, Spain) for the gift of the *ald*-deficient *E. coli* strain JA111 and the plasmid pALD9 and Robert Thornburg (Department of Biochemistry, Biophysics, and Molecular Biology, Iowa State University) for providing access to the fluorescence spectrophotometer. We also thank Miwa Kojima for illustrating the maize spikelet. This research was supported in part by competitive grants from the United States Department of Agriculture National Research Initiative program to P.S.S. (9801805 and 0001478) and from the Human Frontiers in Science Program (RG0067) to Cris Kuhlemeier (Institute of Plant Physiology, University of Berne, Berne, Switzerland) and P.S.S. This is journal paper number 18706 of the Iowa Agriculture and Home Economics Experiment Station (Ames, IA), project number 3554, supported by Hatch Act and State of Iowa funds.

Literature Cited

Asker, H., and Davies, D.D. (1985). Mitochondrial aldehyde dehydrogenase from plants. Phytochemistry **24,** 689-693.

Barkan, A., and Martienssen, R.A. (1991). Inactivation of maize transposon *Mu* suppresses a mutant phenotype by activating an outward-reading promoter near the end of *Mu1*. Proc. Natl. Acad. Sci. USA **88,** 3502-3506.

Boronat, A., and Aguilar, J. (1979). Rhamnose-induced propanediol oxidoreductase in *Escherichia coli*: Purification, properties, and comparison with the fucose-induced enzyme. J. Bacteriol. **140,** 320-326.

Caballero, E., Baldoma, L., Ros, J., Boronat, A., and Aguilar, J. (1983). Identification of lactaldehyde dehydrogenase and glycolaldehyde dehydrogenase as functions of the same protein in *Escherichia coli*. J. Biol. Chem. **258,** 7788-7792.

Comstock, J.C., and Scheffer, R.P. (1973). Role of host-selective toxin in colonization of corn leaves by *Helminthosporium carbonum*. Phytopathology **63,** 24-29.

Cui, X., Wise, R.P., and Schnable, P.S. (1996). The *rf2* nuclear restorer gene of male-sterile T-cytoplasm maize. Science **272,** 1334-1336.

Davies, D.D. (1959). The purification and properties of glycolaldehyde dehydrogenase. J. Exp. Bot. **11,** 289-295.

Dean, C., Van Den Elzen, P., Tamaki, S., Dunsmuir, P., and Bedbrook, J. (1985). Differential expression of the eight genes of the petunia ribulose bisphosphate carboxylase small subunit multi-gene family. EMBO J. **4,** 3055-3061.

Dellaporta, S.L., Wood, J., and Hicks, J.B. (1983). A plant DNA minipreparation: Version 2. Plant Mol. Biol. Rep. **1,** 19-22.

Dewey, R.E., Levings, C.S., III, and Timothy, D.H. (1986). Novel recombinations in the maize mitochondrial genome produce a unique transcriptional unit in the Texas male-sterile cytoplasm. Cell **44,** 439-449.

Dewey, R.E., Timothy, D.H., and Levings, C.S., III (1987). A mitochondrial protein associated with cytoplasmic male sterility in the T cytoplasm of maize. Proc. Natl. Acad. Sci. USA **84,** 5374-5378.

Dumbroff, E.B., and Gepstein, S. (1993). Immunological methods for assessing protein expression in plants. In Methods in Plant Molecular Biology and Biotechnology, B.R. Glick and J.E. Thompson, eds (Boca Raton, FL: CRC Press), pp. 207-241.

Errede, B., Kamen, M.D., and Hatefi, Y. (1967). Preparation and properties of complex IV (ferrocytochrome c:oxidoreductase EC 1.9.3.1). Methods Enzymol. **10,** 41-48.

Fauron, C.M.-R., Abbott, A.G., Brettell, R.I.S., and Gesteland, R.F. (1987). Maize mitochondrial DNA rearrangements between the normal type, the Texas male sterile cytoplasm, and a fertile revertant cms-T regenerated plant. Curr. Genet. **11,** 339-346.

Ferrandez, A., Prieto, M.A., Garcia, J.L., and Diaz, E. (1997). Molecular characterization of PadA, a phenylacetaldehyde dehydrogenase from *Escherichia coli*. FEBS Lett. **406,** 23-27.

Forde, B.G., and Leaver, C.J. (1980). Nuclear and cytoplasmic genes controlling synthesis of variant mitochondrial polypeptides in male sterile maize. Proc. Natl. Acad. Sci. USA **77,** 418-422.

Freeling, M., and Schwartz, D. (1973). Genetic relationships between the multiple alcohol dehydrogenases of maize. Biochem. Genet. **8**, 27-36.

Gengenbach, B.G, Connelly, J.A., Pring, D.R., and Conde, M.F. (1981). Mitochondrial DNA variation in maize plants regenerated during tissue culture selection. Theor. Appl. Genet. **59**, 161-167.

Greene, B., Walko, R., and Hake, S. (1994). *Mutator* insertions in an intron of the maize *knotted1* gene result in dominant suppressible mutations. Genetics **138**, 1275-1285.

Guex, N., and Peitsch, M.C. (1997). SWISS-MODEL and the Swiss-PdbViewer: An environment for comparative protein modeling. Electrophoresis **18**, 2714-2723.

Hack, E., Lin, C., Yang, H., and Horner, H.T. (1991). T-URF13 protein from mitochondria of Texas male-sterile maize (*Zea mays* L.). Plant Physiol. **95**, 861-870.

He, S., Abad, A.R., Gelvin, S.B., and Mackenzie, S.A. (1996). A cytoplasmic male sterility-associated mitochondrial protein causes pollen disruption in transgenic tobacco. Proc. Natl. Acad. Sci. USA **93**, 11763-11768.

Hidalgo, E., Chen, Y.-M., Lin, E.C.C., and Aguilar, J. (1991). Molecular cloning and DNA sequencing of the *Escherichia coli* K-12 ald gene encoding aldehyde dehydrogenase. J. Bacteriol. **173**, 6118-6123.

Hooker, A.L., Smith, D.R., Jim, S.R., and Beckett, J.B. (1970). Reaction of corn seedlings with male-sterile cytoplasm to *Helminthosporium maydis*. Plant Dis. Rep. **54**, 708-712.

Hsu, S.U., and Peterson, P.A. (1991). The upper and lower florets of spikelets in maize. J. Genet. Breed. **45**, 215-222.

Huang, J., Lee, S.-H., Lin, C., Medici, R., Hack, E., and Myers, A.M. (1990). Expression in yeast of the T-URF13 protein from Texas male-sterile maize mitochondria confers sensitivity to methomyl and to Texas-cytoplasm-specific fungal toxins. EMBO J. **9**, 339-347.

Jackson, C., and Moore, A.L. (1979). Isolation of intact higher-plant mitochondria. In Plant Organelles, Methodological Surveys (B): Biochemistry, Vol. 9, E. Reid, ed (Chichester, UK: Ellis Horwood), pp. 1-12.

Kemble, R.J., Flavell, R.B., and Brettell, R.I.S. (1982). Mitochondrial DNA analysis of fertile and sterile maize plants derived from tissue culture with the Texas male sterile cytoplasm. Theor. Appl. Genet. **62,** 213-217.

Kennell, J.C., and Pring, D.R. (1989). Initiation and processing of atp6, T-urf13 and ORF221 transcripts from mitochondria of T cytoplasm maize. Mol. Gen. Genet. **216,** 16-24.

Kiesselbach, T.A. (1980). The Structure and Reproduction of Corn. (Cold Spring Harbor, NY: Cold Spring Harbor Laboratory Press), p. 43.

Klyosov, A.A. (1996). Kinetics and specificity of human liver aldehyde dehydrogenase toward aliphatic, aromatic, and fused polycyclic aldehydes. Biochemistry **35,** 4457-4467.

Koradi, R., Billeter, M., and Wüthrich, K. (1996). MOLMOL: A program for display and analysis of macromolecular structures. J. Mol. Graphics **14,** 51-55.

Korth, K.L., Kaspi, C.I., Seidow, J.N., and Levings, C.S., III (1991). URF13, a maize mitochondrial pore-forming protein, is oligomeric and has a mixed orientation in *Escherichia coli* plasma membranes. Proc. Natl. Acad. Sci. USA **88,** 10865-10869.

Leegood, R.C., and Walker, D.A. (1983). Chloroplast. In Isolation of Membranes and Organelles from Plant Cells, J.L. Hall and A.L. Moore, eds (London: Academic Press), pp. 185-210.

Levings, C.S., III (1990). The Texas cytoplasm of maize: Cytoplasmic male sterility and disease susceptibility. Science **250,** 942-947.

Levings, C.S., III (1993). Thoughts on cytoplasmic male sterility in cms-T maize. Plant Cell **5,** 1285-1290.

Levings, C.S., III, and Siedow, J.N. (1992). Molecular basis of disease susceptibility in the Texas cytoplasm of maize. Plant Mol. Biol. **19,** 135-147.

Lindahl, R. (1992). Aldehyde dehydrogenases and their role in carcinogenesis. Crit. Rev. Biochem. Mol. Biol. **27,** 283-335.

Lindahl, R., and Petersen, D.R. (1991). Lipid aldehyde oxidation as a physiological role for class 3 aldehyde dehydrogenases. Biochem. Pharmacol. **41,** 1583-1587.

Liu, Z.J., Sun, Y.J., Rose, J., Chung, Y.J., Hsiao, C.D., Chang, W.R., Kuo, I., Perozich, J., Lindahl, R., Hempel, J., and Wang, B.C. (1997). The first structure of an aldehyde

dehydrogenase reveals novel interactions between NAD and the Rossmann fold. Nat. Struct. Biol. **4**, 317-326.

Lowe, B., Mathern, J., and Hake, S. (1992). Active *Mutator* elements suppress the Knotted phenotype and increase recombination at the *Kn1-0* tandem duplication. Genetics **132**, 813-822.

Mackenzie, S., and Chase, C.D. (1990). Fertility restoration is associated with loss of a portion of the mitochondrial genome in cytoplasmic male-sterile common bean. Plant Cell **2**, 905-912.

Mackenzie, S., Shichuan, H., and Lyznik, A. (1994). The elusive plant mitochondrion as a genetic system. Plant Physiol. **105**, 775-780.

Martienssen, R., and Baron, A. (1994). Coordinate suppression of mutations caused by Robertson's *Mutator* transposons in maize. Genetics **136**, 1157-1170.

Martienssen, R.A., Barkan, A., Freeling, M., and Taylor, W.C. (1989). Molecular cloning of a maize gene involved in photosynthetic membrane organization that is regulated by Robertson's *Mutator*. EMBO J. **8**, 1633-1639.

Martienssen, R., Barkan, A., Taylor, W.C., and Freeling, M. (1990). Somatically heritable switches in the DNA modification of *Mu* transposable elements monitored with a suppressible mutant in maize. Genes Dev. **4**, 331-343.

Martzen, M.R., McCraith, S.M., Spinelli, S.L., Torres, F.M., Fields, S., Grayhack, E.J., and Phizicky, E.M. (1999). A biochemical genomics approach for identifying genes by the activity of their products. Science **286**, 1153-1155.

Marumo, S. (1986). Auxins. In Chemistry of Plant Hormones, N. Takahashi, ed (Boca Raton, FL: CRC Press), pp. 9-56.

McCaffery, P., and Drager, U.C. (1993). Retinoic acid synthesis in the developing retina. Adv. Exp. Med. Biol. **328**, 181-190.

Nakai, K. (1991). Predicting various targeting signals in amino acid sequences. Bull. Inst. Chem. Res. Kyoto Univ. **69**, 269-291.

op den Camp, R.G., and Kuhlemeier, C. (1997). Aldehyde dehydrogenase in tobacco pollen. Plant Mol. Biol. **35**, 355-365.

Osakovskii, V.L., Ponomarev, A.G., Bubyakina, V.V., Tatarinova, T.D., Kononova, S.K., Li, N.G., Khokhlachev, A.V., Kovalenko, V.A., Pashkov, V.I., and Yakunina, N.B. (1992). Aldehyde dehydrogenase of mung bean (*Phaseolus aureus*) root mitochondria: Characterization and preparation of monospecific polyclonal antibodies. Biokhimiya **57**, 418-429.

Parthasarathy, M.V. (1994). Transmission electron microscopy: Chemical fixation, freezing methods, and immunolocalization. In The Maize Handbook, M. Freeling and V. Walbot, eds (New York: Springer-Verlag), pp. 118-134.

Payne, G., Kono, Y., and Daly, J.M. (1980). A comparison of purified host specific toxin from *Helminthosporium maydis*, race T, and its acetate derivative on oxidation by mitochondria from susceptible and resistant plants. Plant Physiol. **65**, 785-791.

Perozich, J., Nicholas, H., Wang, B.C., Lindahl, R., and Hempel, J. (1999). Relationships within the aldehyde dehydrogenase extended family. Protein Sci. **8**, 137-146.

Pring, D.R., and Lonsdale, D.M. (1989). Cytoplasmic male sterility and maternal inheritance of disease susceptibility in maize. Annu. Rev. Phytopathol. **27**, 483-502.

Quail, P.H. (1979). Plant cell fractionation. Annu. Rev. Plant Physiol. **30**, 425-484.

Rajagopal, R. (1971). Metabolism of indole-3-acetaldehyde. III. Some characteristics of the aldehyde oxidase of Avena coleoptile. Physiol. Plant. **24**, 272-281.

Rocha, V., and Ting, I.P. (1970). Preparation of cellular plant organelles from spinach leaves. Arch. Biochem. Biophys. **140**, 398-407.

Sambrook, J., Fritsch, E.F., and Maniatis, T. (1989). Molecular Cloning: A Laboratory Manual, 2nd ed. (Cold Spring Harbor, NY: Cold Spring Harbor Laboratory Press).

Schnable, P.S., and Wise, R.P. (1994). Recovery of heritable, transposon-induced, mutant alleles of the *rf2* nuclear restorer of T-cytoplasm maize. Genetics **136**, 1171-1185.

Schnable, P.S., and Wise, R.P. (1998). The molecular basis of cytoplasmic male sterility and fertility restoration. Trends Plant Sci. **3**, 175-180.

Siu, G.M., and Draper, H.H. (1982). Metabolism of malonaldehyde *in vivo* and *in vitro*. Lipids **17**, 349-355.

Sladek, N.E., Manthey, C.L., Maki, P.A., Zhang, Z., and Landkamer, G.J. (1989). Xenobiotic oxidation catalyzed by aldehyde dehydrogenases. Drug. Metab. Rev. **20,** 697-720.

Steinmetz, C.G., Xie, P., Weiner, H., and Hurley, T.D. (1997). Structure of mitochondrial aldehyde dehydrogenase: The genetic component of ethanol aversion. Structure **5,** 701-711.

Styrvold, O.B., Falkenberg, P., Landfald, B., Eshoo, M.W., Bjornsen, T., and Strom, A.R. (1986). Selection, mapping, and characterization of osmoregulatory mutants of *Escherichia coli* blocked in the choline-glycine betaine pathway. J. Bacteriol. **165,** 856-863.

Sylvester, A.W., and Ruzin, S.E. (1994). Light microscopy. I. Dissection and microtechnique. In The Maize Handbook, M. Freeling and V. Walbot, eds (New York: Springer-Verlag), pp. 89-92.

Tadege, M., Dupuis, I., and Kuhlemeier, C. (1999). Ethanolic fermentation: New function for an old pathway. Trends Plant Sci. **4,** 320-325.

Ullstrup, A.J. (1972). The impacts of the southern corn leaf blight epidemics of 1970-1971. [*Helminthosporium turcicum*]. Annu. Rev. Phytopathol. **10,** 37-50.

Umbeck, P.F., and Gengenbach, B.G. (1983). Reversion of male-sterile T-cytoplasm maize to male fertility in tissue culture. Crop Sci. **23,** 584-588.

Vasiliou, V., Bairoch, A., Tipton, K.F., and Nebert, D.W. (1999). Eukaryotic aldehyde dehydrogenase (ALDH) genes: Human polymorphisms, and recommended nomenclature based on divergent evolution and chromosomal mapping. Pharmacogenetics **9,** 421-434.

Vigil, E.L. (1983). Microbodies. In Isolation of Membranes and Organelles from Plant Cells, J.L. Hall and A.L. Moore, eds (London: Academic Press), pp. 211-236.

Vojtechova, M., Hanson, A.D., and Munoz-Clares, R.A. (1997). Betaine-aldehyde dehydrogenase from amaranth leaves efficiently catalyzes the NAD-dependent oxidation of dimethylsulfoniopropionaldehyde to dimethylsulfoniopropionate. Arch. Biochem. Biophys. **337,** 81-88.

Wang, X., Mann, C.J., Bai, Y., Ni, L., and Weiner, H. (1998). Molecular cloning, characterization, and potential roles of cytosolic and mitochondrial aldehyde dehydrogenases in ethanol metabolism in *Saccharomyces cerevisiae*. J. Bacteriol. **180,** 822-830.

Warmke, H.E., and Lee, S.L.J. (1977). Mitochondrial degeneration in Texas cytoplasmic male-sterile corn anthers. J. Hered. **68,** 213-222.

Warmke, H.E., and Lee, S.L.J. (1978). Pollen abortion in T cytoplasmic male-sterile corn (*Zea mays*): A suggested mechanism. Science **200,** 561-563.

Wightman, F., and Cohen, D. (1968). Intermediary steps in the enzymatic conversion of tryptophan to IAA in cell-free systems from mung bean seedlings. In Biochemistry and Physiology of Plant Growth Substances: Proceedings of the 6th International Conference on Plant Growth Substances, F. Wightman and G. Setterfield, eds (Ottawa, Canada: Runge Press), p. 273.

Wise, R.P., and Schnable, P.S. (1994). Mapping complementary genes in maize: Positioning the *rf1* and *rf2* nuclear-fertility restorer loci of Texas (T) cytoplasm relative to RFLP and visible markers. Theor. Appl. Genet. **88,** 785-795.

Wise, R.P., Fliss, A.E., Pring, D.R., and Gengenbach, B.G. (1987a). *urf13-T* of T-cytoplasm maize mitochondria encodes a 13 kD polypeptide. Plant Mol. Biol. **9,** 121-126.

Wise, R.P., Pring, D.R., and Gengenbach, B.G. (1987b). Mutation to male fertility and toxin insensitivity in Texas (T)-cytoplasm maize is associated with a frame shift in a mitochondrial open reading frame. Proc. Natl. Acad. Sci. USA **84,** 2858-2862.

Wise, R.P., Bronson, C.R., Schnable, P.S., and Horner, H.T. (1999). The genetics, pathology, and molecular biology of T-cytoplasm male sterility in maize. Adv. Agron. **65,** 79-130.

Yoder, O.C. (1973). A selective toxin produced by *Phyllosticta maydis*. Phytopathology **63,** 1361-1366.

Yoshida, A., Rzhetsky, A., Hsu, L.C., and Chang, C. (1998). Human aldehyde dehydrogenase gene family. Eur. J. Biochem. **251,** 549-557.

Zinovieva, R.D., Tomarev, S.I., and Piatigorsky, J. (1993). Aldehyde dehydrogenase-derived omega-crystallins of squid and octopus: Specialization for lens expression. J. Biol. Chem. 268, 11449-11455.

Tables

Table 1. Markers for Cell Fractionation[a]

	Chloroplastic Fraction		Microsomal, Cytosolic, and Mitochondrial Fractions			
	Total[b]	Chloroplastic	Total[c]	Microsomal	Cytosolic	Mitochondrial
COX[d]	0.392 ± 0.032[f]	0	0.480 ± 0.018	0.348 ± 0.048	0.072 ± 0.003	2.712 ± 0.084
ADH[d]	ND	ND	0.290 ± 0.013	0.011 ± 0.007	0.526 ± 0.017	0
Catalase[d]	0.742 ± 0.013	0	1.231 ± 0.132	8.743 ± 0.520	0.650 ± 0.100	0.339 ± 0.015
Chlorophyll[e]	2.069 ± 0.126	10.396 ± 0.039	ND	ND	ND	ND

[a] Data represent the average of three measurements from one typical experiment.

[b] The homogenate of green seedlings that was used for the isolation of the chloroplastic fraction.

[c] The homogenate of etiolated seedlings that was used for the isolation of microsomal, cytosolic and mitochondrial fractions.

[d] The enzyme activities are expressed as arbitrary units per minute per milligram of protein. COX, cytochrome c oxidase; ADH, alcohol dehydrogenase.

[e] Chlorophyll concentration is expressed as milligrams of chlorophyll per milligram of protein.

Table 2. Maize mtALDH Assay[a]

	T Cytoplasm		N Cytoplasm	
	Rf2[b]	*rf2-m*[c]	*Rf2*[b]	*rf2-m*[c]
Acetaldehyde (17 μM)	7.03 ± 0.58	1.43 ± 0.08	7.23 ± 0.15	1.87 ± 0.25
Glycolaldehyde (20 μM)	7.73 ± 0.29	0.23 ± 0.13	6.43 ± 0.29	0.40 ± 0.17

[a] Reaction rates are expressed as change in relative fluorescence units (RFU) at 460 nm per minute per milligram of mitochondrial protein. Data represent the average of three measurements.

[b] Inbred line Ky21.

[c] *rf2-m8904/rf2-m8904* backcrossed into Ky21 for three generations.

Table 3. Correlation between Anther Arrest and *rf2* Genotype in Progeny from the Test Cross: (N) *rf2-m/rf2-m* × *rf2-m/Rf2*

Row No.	Genotype [a]	N + 'N' [b]	A + AA [b]
98 6503-06	*rf2-m8904/rf2-m8904*	0	23
	rf2-m8904/Rf2-Ky21	38	0
98 6509-10	*rf2-m9323/rf2-m9323*	2	17
	rf2-m9323/Rf2-Ky21	30	0
99 6655-56	*rf2-m8904/rf2-R213*	2	10
	rf2-m8904/Rf2'1036W103	9	0
99 6657-58	*rf2-m8904/rf2-R213*	2	12
	rf2-m8904/Rf2'1036W110	13	0

[a] Genotypes were established via DNA gel blot analyses using the partial *rf2* cDNA as a probe.

[b] Anther phenotypes were scored in the morning during the period of pollen shedding. Examples of each phenotype are shown in panels A-E, Figure 8.

Figure Legends

Figure 1. Immunoblot Analysis of RF2 Protein Accumulation.

(A) Different organs from mutant and wild-type maize plants. w, *Rf2-Ky21/Rf2-Ky21*; m, *rf2-m8904/rf2-m8904*. Both maize strains carried T cytoplasm and had been backcrossed to the inbred line Ky21 for three generations. Ear, a young unpollinated ear approximately 10 cm long; young tassel, premeiotic stage of microsporogenesis; older tassel, early microspore stage of microsporogenesis; mesocotyl and root, both from 7-day-old seedlings. The lower panel is a duplicated gel stained with Coomassie Blue and serves as a protein loading control.

(B) Seedlings of different cytoplasmic and nuclear backgrounds. Total protein extracts were prepared from 7-day-old seedlings homozygous for the indicated alleles in the indicated cytoplasmic background. *Rf2-Ky21* and *rf2-m8904* are in a Ky21 genetic background, and the *rf2-R213* allele is carried by the inbred line R213 with the indicated cytoplasm. The lower panel is a duplicated gel stained with Coomassie Blue and serves as a protein loading control.

Figure 2. RF2 Protein Accumulates in Mitochondria.

(A) Homogenate (Hg), purified chloroplastic (Ch), microsomal (Ms), cytosolic (Cy), and mitochondrial (Mt) fractions of Ky21 seedlings were subjected to SDS-PAGE and stained with Coomassie Blue.

(B) A duplicate gel was transferred to a nitrocellulose membrane and reacted with affinity-purified anti-RF2 antibodies.

(C) Protein extracts from isolated mitochondria of the inbred line Ky21 were treated with Triton X-100 and papain as indicated, subjected to SDS-PAGE, transferred to a nitrocellulose membrane, and reacted with affinity-purified anti-RF2 antibodies.

(D) Purified mitochondria from Ky21 seedlings were subjected to sonication and centrifugation to isolate the soluble and membrane fractions and then subjected to immunoblot analysis. Mt, purified mitochondria; Inf, insoluble fraction; Sf, soluble fraction.

Figure 3. Immunolocalization of the RF2 Protein.

(A) Diagram of a cross-section of one locule of an anther (from Kiesselbach, 1980). The approximate position of the areas shown in **(B)** and **(C)** is indicated by the box.

(B) Cross-section of a T cytoplasm anther of the inbred line Ky21 that is homozygous for the *Rf2-Ky21* allele incubated with affinity-purified rabbit anti-RF2 antibodies, followed by gold-labeled goat anti-rabbit IgG antibodies and silver enhancement.

(C) Cross-section of an anther from T cytoplasm *rf2-m8904/rf2-m8904* treated as described for **(B)**.

E, epidermis; EL, endothecium; ML, middle layer; T, tapetum; PM, microspore pollen mother cell. Bars in **(B)** and **(C)** = 10 μm.

Figure 4. ALDH Assay of *E. coli*–Expressed Recombinant RF2.

Crude extracts of *E. coli* expressing the RF2 protein were assayed for ALDH activity. RFU 460, relative fluorescence units at 460 nm.

Figure 5. The *rf2* gene can complement an *E. coli ald*-deficient mutant.

(A) Basal medium plus glucose.

(B) Basal medium plus 1,2-propanediol.

–1, JA111; –2, JA111(DE3); +, JA111(DE3)pALD9; Vector, JA111(DE3)pET-17b; RF2-1, JA111(DE3)pMAP11-1; RF2-2, JA111(DE3)pMAP11-2.

Figure 6. Mitochondrial ALDH Assay.

ALDH activity was measured in extracts from mitochondria purified from unpollinated ears produced by T cytoplasm **(A)** or N cytoplasm **(B)** plants or from etiolated seedlings **(C)** of the indicated genotypes. Results from one typical experiment are shown. Data from **(A)** and **(B)** are summarized in Table 2. RFU, relative fluorescence units.

Figure 7. Structure of the RF2 Protein.

This structure was predicted by SWISS-MODEL (Guex and Peitsch, 1997) using bovine mtALDH (Protein Data Bank number 1AG8) as a template. The stereo images were prepared using MOLMOL (Koradi et al., 1996). Residues Glu^{317}, Pro^{323}, Cys^{351}, Asn^{400}, and Ile^{522} in the RF2 sequence are equivalent to amino acid residues Glu^{267}, Pro^{273}, Cys^{301}, Lys^{350}, Ser^{472} in Protein Data Bank number 1AG8, respectively.

Figure 8. Anther Arrest in *rf2* Plants Carrying N or T Cytoplasm.

(A) Normal anther development on a tassel branch from N cytoplasm Ky21.

(B) to **(E)** Various degrees of anther arrest on tassel branches from different plants in a segregating population resulting from the cross (N) *rf2-m9323/rf2-m9323* × *rf2-m9323/Rf2-Ky21*. Arrows identify arrested anthers.

(F) Normal anther development on a tassel branch from a fully suppressed T cytoplasm plant homozygous for *rf2-m9390*.

(G) to **(I)** Various degrees of anther arrest on tassel branches from partially suppressed T cytoplasm plants homozygous for *rf2-m9437*.

(J) Completely sterile tassel branch from an unsuppressed T cytoplasm plant homozygous for *rf2-m9437*.

Figure 9. Microscopic Observation of Anther Arrest.

(A) Illustration of a normal maize spikelet.

(B) A spikelet from an N cytoplasm Ky21 plant.

(C) A spikelet from an N cytoplasm plant homozygous for *rf2-m9323* and near-isogenic with Ky21.

(D) and **(E)** Anthers from the lower florets of N cytoplasm plants homozygous for *rf2-m8904*.

(F) and **(G)** Anthers from the lower florets of N cytoplasm plants homozygous for *rf2-m9323*.

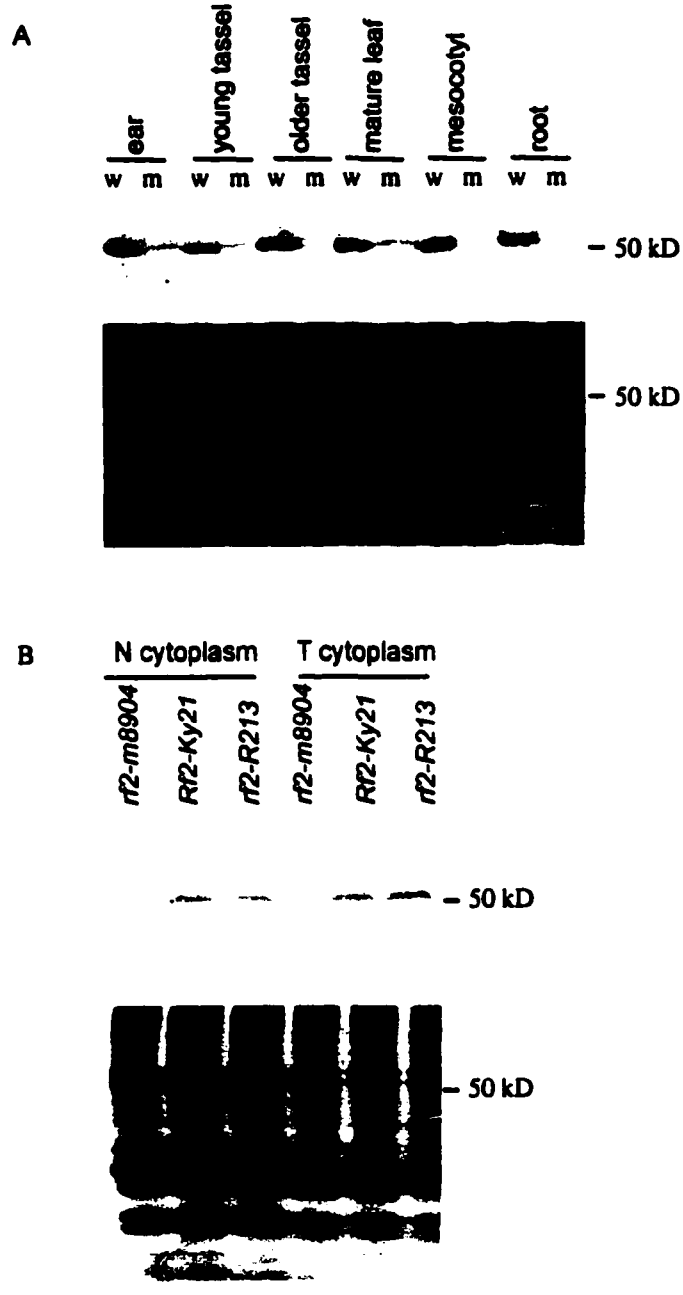

Liu et al., Figure 1.

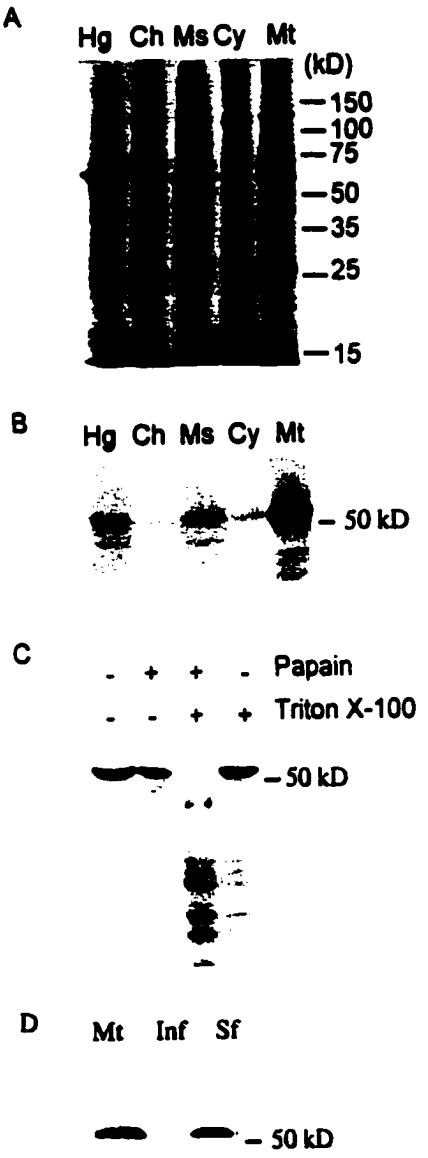

Liu et al., Figure 2.

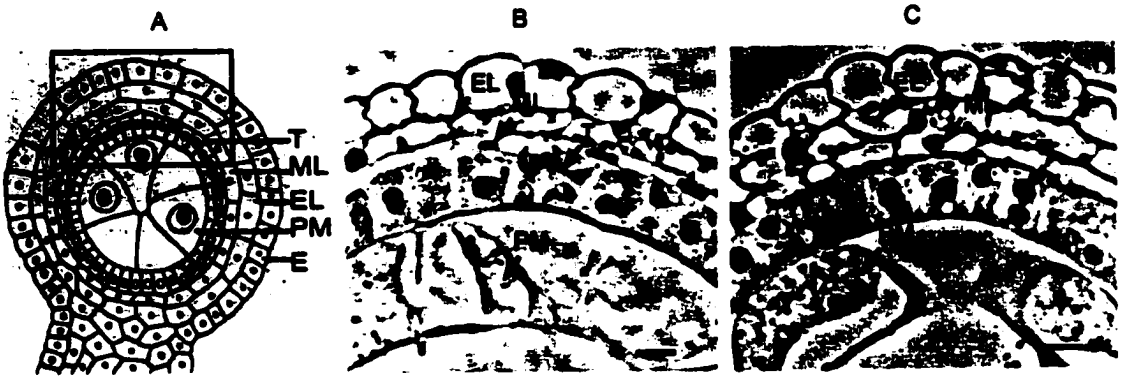

Liu et al., Figure 3.

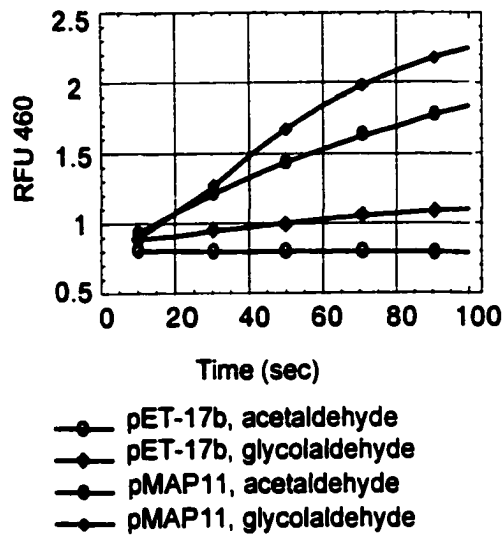

Liu et al., Figure 4

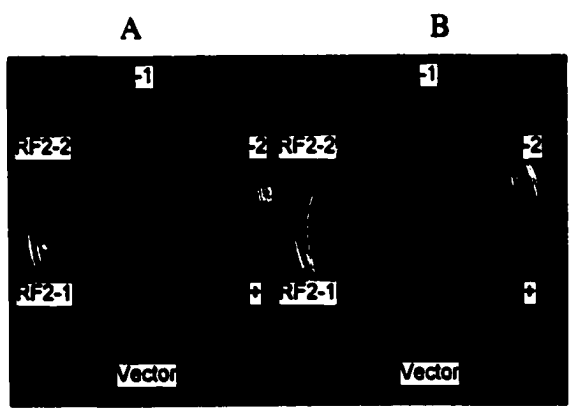

Liu et al., Figure 5.

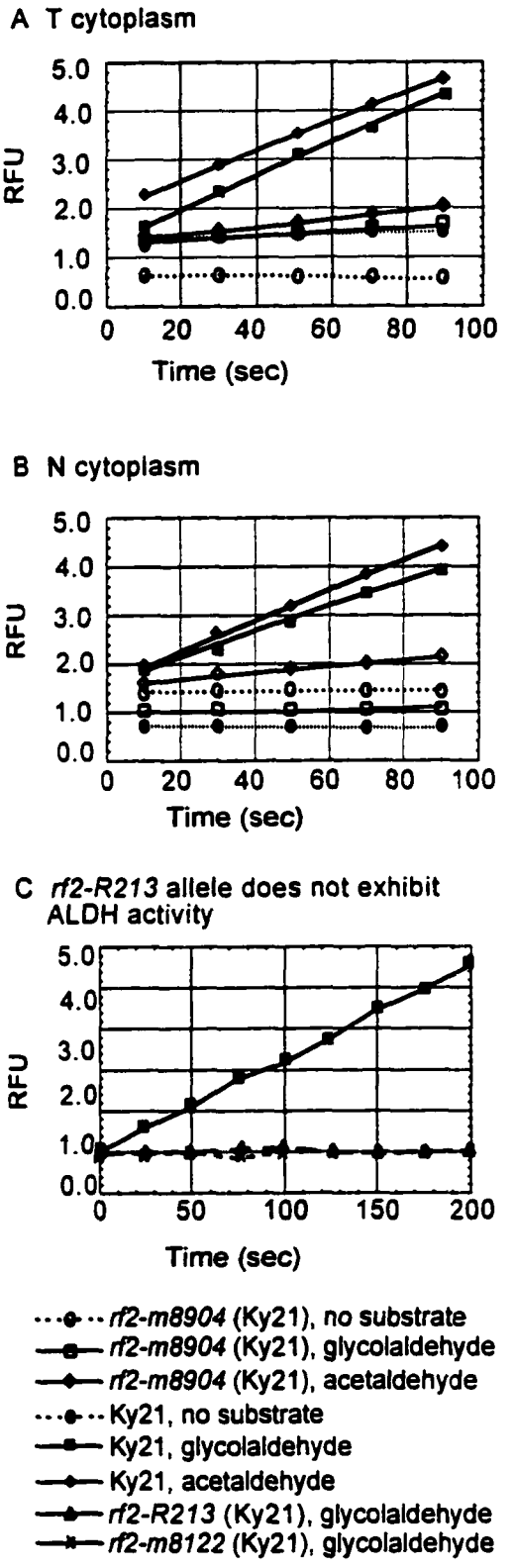

Liu et al., Figure 6

Liu et al., Figure 7

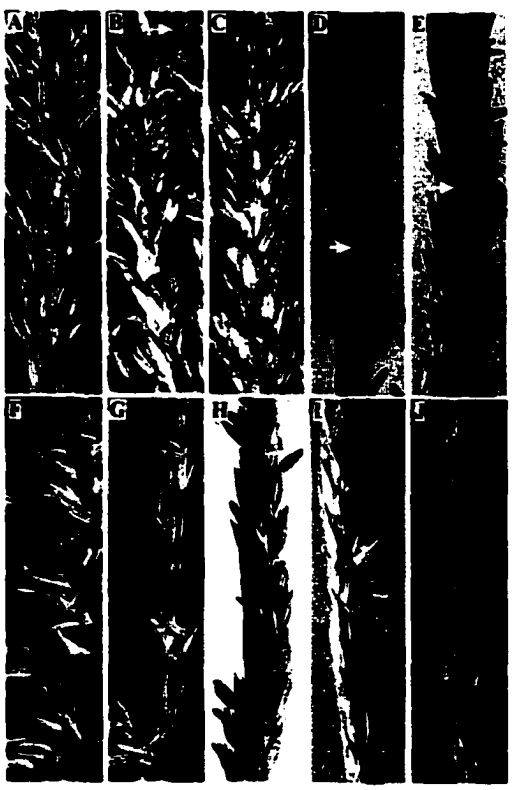

Liu et al., Figure 8

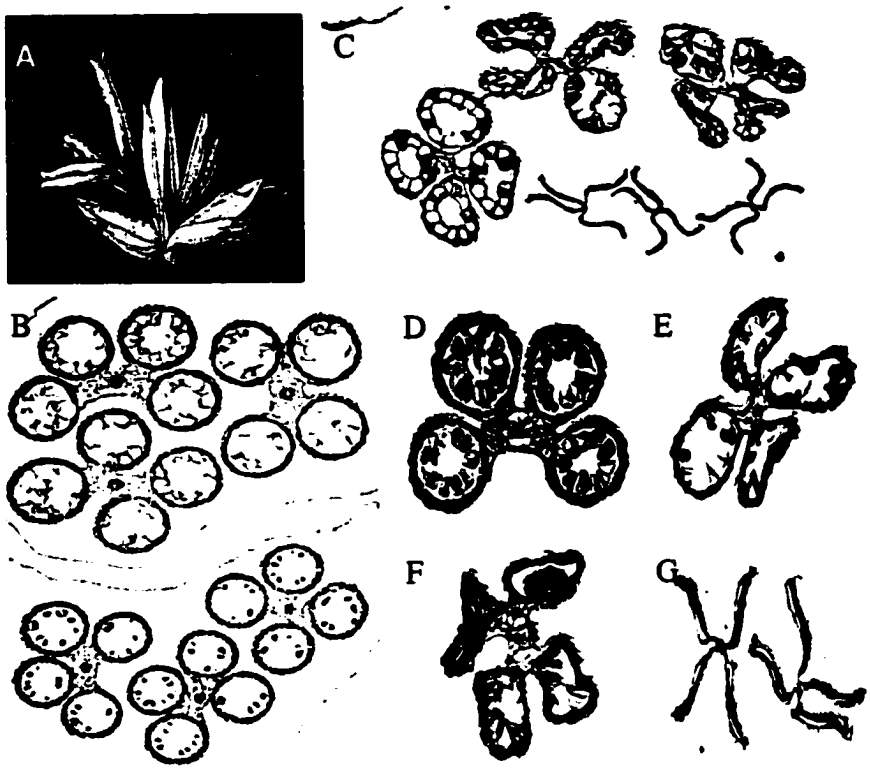

Liu et al., Figure 9

CHAPTER 4. MUTATIONS OF THE MAIZE *pdc3* GENE REDUCE TOLERANCE TO ANAEROBIC STRESSES BUT DO NOT AFFECT MALE FERTILITY

A paper to be submitted to Plant Physiology

Xiangqin Cui,[a,b] Yan Fu,[a,b] Brian E. Scheffler,[c] Carl R. Simmons,[d] Robert B. Meeley,[d] and Patrick S. Schnable[a,b,e,f*]

Abstract

Anaerobic fermentation provides short-term tolerance to the anaerobic stress that plants experience in flooded soils. During anaerobic fermentation, pyruvate is converted to ethanol and NAD^+ is regenerated to allow glycolysis to continue in the absence of oxygen. Pyruvate decarboxylase (PDC) catalyzes the first step in this pathway, the conversion of pyruvate to acetaldehyde. PDC is highly induced by anaerobic stress and is the rate-limiting enzyme in

[a] Department of Zoology and Genetics, Iowa State University, Ames, Iowa 50011

[b] Interdepartmental Genetics Program, Iowa State University, Ames, Iowa 50011

[c] USDA-ARS-NPURU, University, MS 38677

[d] Pioneer Hi-Bred Intl. Inc., Johnston, Iowa 50131

[e] Department of Agronomy, Iowa State University, Ames, Iowa 50011

[f] Center for Plant Genomics, Iowa State University, Ames, Iowa 50011

[*] Corresponding author; e-mail schnable@iastate.edu; fax 515-294-0975

this pathway. However, because *pdc* mutants were not available in any plant species, it has not been possible to obtain direct evidence of the relationship between PDC activity and anaerobic stress tolerance. Biochemical characterizations established that a recombinant protein encoded by the maize *pdc3* gene exhibits PDC activity. A reverse genetic system was used to generate multiple mutant alleles for this gene. These mutants exhibit dramatically reduced levels of tolerance to anaerobic stress. Wild-type seedlings can routinely tolerate more than 72 hours of anaerobic stress. In contrast, seedlings homozygous for *pdc3* mutants are not able to survive 12 hours of anaerobic stress, and most die after six hours. The physiological lesion associated with these mutants is first visible near the coleoptilar node beginning about four hours after the onset of anaerobic stress. Mutant alleles of the *pdc3* gene were also characterized for their relationship to male sterility. The mutation of *pdc3* does not affect male fertility in plants that carry either T or N cytoplasm.

Introduction

When oxygen is limited in plants, the TCA cycle and the electron transport chain are blocked. The product of glycolysis, pyruvate, is reduced to lactate by lactate dehydrogenase (LDH; EC 1.1.1.27) or converted to ethanol by pyruvate decarboxylase (PDC; EC 4.1.1.1) and alcohol dehydrogenase (ADH; EC 1.1.1.1). This second pathway is known as the major pathway of anaerobic fermentation. The production of NAD^+ from either of these pathways allows glycolysis to continue and thereby produce a limited amount of ATP (reviewed by Drew 1997; Sachs 1993). The enzymes involved in these pathways are up-regulated shortly

after the onset of oxygen limitation, while general protein synthesis is dramatically reduced (Kennedy et al., 1992; Sachs 1993; Chritopher and Good, 1996).

Among the enzymes involved in the plant anaerobic fermentation pathway, ADH has been most extensively characterized (reviewed by Freeling and Bennett, 1985). Maize has two genes that encode ADH, *adh1* and *adh2* (Freeling and Schwartz 1973; Gerlach et al., 1982; Dennis et al., 1985). Both are highly induced by anaerobic conditions (Freeling, 1973). Wild-type seedlings can usually survive about three days of anoxia, but a null *adh1* mutant can survive only a few hours (Schwartz, 1969). However, comparison of ADH activity among various isogenic lines indicated that a small amount of ADH activity [20 milliunits (nmol NADH produced/min)] is sufficient to maintain a high level of anaerobic fermentation. This suggests that ADH is not the rate-limiting enzyme in this pathway (Roberts et al., 1989; Lemke-Keyes and Sachs 1989). In contrast, over-expression of PDC dramatically increased the flux through the fermentation pathway in transgenic tobacco leaves, suggesting that PDC is the rate-limiting enzyme (Bucher et al., 1994).

Yeast has three highly conserved genes, *pdc1*, *pdc5*, and *pdc6*, that encode PDC. Mutations in these genes cause growth deficiencies on media in which glucose is the sole carbon source (reviewed by Pronk et al., 1996). Multiple *pdc* genes have also been cloned from some plant species; for example, two from tobacco (Bucher et al., 1995), three from rice (Rivoal et al., 1997), and three from maize (Kelley, 1989; Peschke and Sachs, 1993). However, the functions of these plant *pdc* genes have not been well established due to the lack of *pdc* mutants.

The maize *pdc* gene, *pdc1*, was cloned by screening cDNA libraries using oligonucleotides designed from *pdc* sequences of proteobacteria and yeast (Kelley, 1989).

Two more partial maize *pdc* cDNA clones, *pdc2* and *pdc3*, were subsequently isolated from libraries constructed from anaerobically treated seedlings using the *pdc1* cDNA as probe. The amino acid sequences of both *pdc2* and *pdc3* have about 85% identity to that of *pdc1*. All three maize *pdc* genes are anaerobically induced, but their induction patterns vary (Peschke and Sachs, 1993). The induction patterns of *pdc1* and *pdc2* are similar in that their expression is not detectable in aerobic seedlings via RNA gel blot analysis, but rapidly increases after two to four hours of anaerobic treatment, followed by gradual reduction. The expression of *pdc3* peaks after four hours of anaerobic treatment and then decreases rapidly. Of the three *pdc* genes, only *pdc3* can be detected in aerobic shoots via RNA gel blot analysis.

The anaerobic fermentation pathway can also function, at least in some tissues, under aerobic conditions. For example, ADH is highly expressed in maize pollen (Schwartz, 1969). Both ADH and PDC are highly expressed during microsporogenesis and pollen germination in tobacco (Tadege and Kuhlemeier, 1997). The fermentation intermediate (acetaldehyde) and product (ethanol) are also detected at high levels in these tissues. Indeed, fermentation accounts for two thirds of the carbohydrate metabolism in tobacco pollen germinated *in vitro* (Bucher et al., 1995). In addition, the flux through this pathway is not influenced by oxygen availability, but rather by sugar concentration in the medium (Bucher et al., 1995; Tadege and Kuhlemeier, 1997). However, the production of ethanol by this pathway is not thought to be essential for pollen development and germination because maize *adh* null mutants do not affect pollen development (Schwartz, 1969).

Due to the lack of *pdc* mutants in any of the plant species, there has been no direct evidence that PDC is necessary for anaerobic tolerance. The study of the relationship

between the fermentation pathway and anther development is also hampered by the lack of *pdc* mutants. Here we present the isolation and characterization of mutants in the maize *pdc3* gene. Significantly, these *pdc3* mutant alleles exhibited reduced tolerance to anaerobic stress. The relationship between the *pdc3* mutants and male fertility is also investigated.

Results

Isolation of *pdc* genes

The cDNA sequence of the maize *pdc1* gene was downloaded from GenBank (GenBank accession number X59546). The cDNA sequences of *pdc2* and *pdc3* were established by sequencing EST clones with high sequence similarity (>95%) to the existing partial cDNA sequences of *pdc2* and *pdc3* (GenBank accession numbers: D14456 and D14457, Peschke and Sachs, 1993). The full-length cDNA sequence of *pdc2* (GenBank accession number: AF370003) was obtained by sequencing a 1.4-kb EST clone (Pioneer clone CHSUB56R) and extending the sequence toward the 5' end via RT-PCR and 5' RACE. The full-length *pdc3* cDNA sequence (GenBank accession number: AF230005) was obtained by sequencing two EST clones and removing the unspliced intron from the full-length clone (Pioneer clone p0102.cerbf14r) based on sequence comparisons with the partial clone (Pioneer clone: CLOPK68R) and RT-PCR products. Sequence comparisons among *pdc1*, *pdc2*, and *pdc3* revealed that relative to *pdc1* and *pdc3*, the *pdc2* gene has two small insertions, 3-bp and 6-bp, in the coding region. The predicted molecular weights of the PDC2 and PDC3 proteins are 63.7 kD and 65.1 kD, respectively, which are very similar to the predicted 65.2 kD PDC1 protein (Kelley 1989).

The genomic sequence of the maize *pdc1* from inbred line W22 (Kelley et al., 1991) was also downloaded from GenBank (GenBank accession number X17555). The genomic sequences of maize *pdc2* (GenBank accession number: AF370004) and *pdc3* (GenBank accession number: AF370006) were obtained by sequencing genomic clones isolated from maize B73 genomic libraries. Sequence comparisons between cDNA and genomic clones established the gene structures for *pdc2* and *pdc3* (Figure 1A). The structure of *pdc1* (Kelley et al., 1991) is shown for comparison. The *pdc2* and *pdc3* genes each contain five introns. The intron/exon junctions are conserved between these two genes. The *pdc1* gene (Kelley, 1989), however, has only three introns. It lacks the second and the third introns of *pdc2* and *pdc3*. Each of its three existing introns has conserved intron/exon junctions with the corresponding introns in *pdc2* and *pdc3*. The structural comparisons among the three *pdc* genes suggest that *pdc2* and *pdc3* are more similar to each other than either of them are to *pdc1*. However, the phylogenetic tree built using the amino acid sequences of three maize *pdc* genes and other full-length plant *pdc* genes in GenBank groups *pdc1* and *pdc3* together (Figure 2). Therefore, the relationship among these three *pdc* genes is not clear.

The number of *pdc* genes

As a consequence of genome duplication (Gaut and Doebley, 1997; Gale and Devos, 1998; Moore, 2000), many maize gene families are expected to have even numbers of members. To date, searches of EST databases have revealed the existence of only three maize *pdc* genes. Hence, if there is a fourth *pdc* gene, it must be expressed at very low levels, in limited cell types, or only under "unusual" conditions. A low-stringency genomic DNA gel blot

hybridization was conducted to determine whether the maize genome contains additional *pdc* genes (Figure 3). Genomic DNA from the inbred line B73 was digested with two restriction enzymes and hybridized at low stringency to a 320-bp fragment from a region of the *pdc2* cDNA that is well conserved among the three *pdc* genes (85% identity among *pdc1*, *pdc2* and *pdc3* DNA sequences). Because the B73 alleles of the three known *pdc* genes do not contain recognition sites for any restriction enzymes used in the digestion within the 320-bp probe region, the appearance of any additional band would represent the existence of an unidentified homolog in the maize genome. At least four bands were visible from each digestion, which indicates that there are at least four *pdc*-hybridizing sequences in the maize genome.

Expression of the *pdc3* gene in *E. coli*

A 65-kD maize protein with PDC activity was previously purified from maize kernels; antisera raised against this protein specifically precipitate the protein synthesized *in vitro* from the *pdc1* gene (Lee and Langston-Unkefer, 1985; Kelley, 1989). To determine whether the *pdc3* gene encodes an active PDC protein, *pdc3* cDNA was cloned into an *E. coli* expression vector, pET-17b and the recombinant protein was expressed and assayed for PDC activity. Initially, the construct, pEPDC3, was transformed into *E. coli* strain BL21(DE3) for expression of recombinant PDC protein. However, this construct was highly unstable in this strain (data not shown). Based on the hypothesis that this instability was a consequence of leaky expression of PDC, pEPDC3 was transformed into another strain of *E. coli*, BL21(DE3)pLysS, in which expression of the T7 promoter is more tightly regulated. In

strain BL21(DE3)pLysS, the stability of pEPDC3 was substantially improved. Following induction with isopropylthio-ß-galactoside (IPTG), crude protein extracts from these BL21(DE3)pLysS clones that harbor the pEPDC3 construct were assayed for PDC activity. PDC activity was detected in one of three protein extracts (Figure 4).

Isolation of *pdc3* mutants

The Trait Utility System for Corn (TUSC) is a reverse genetics system for isolating *Mutator* transposon insertion mutants in genes with known sequences (Bensen et al., 1994). *Mu*-specific primers in combination with primers specific to the *pdc3* sequence (Figure 1) were used to screen a large TUSC population for *Mu*-insertion alleles. Three independent *Mu* insertion alleles, *pdc3-m2015, pdc3-m2012, and pdc3-m2043,* were obtained (Figure 1). Each of these alleles contains an exonic *Mu1* insertion. Due to the difficulties encountered in PCR-genotyping the *pdc3-m2043* allele, this aliele was not used in the further characterizations.

***pdc* mRNA accumulation in *pdc3-m* mutants**

The accumulation of *pdc* mRNAs in *pdc3-m* mutants was compared with that in wild-type controls (the inbred line Ky21), using semi-quantitative RT-PCR (Figure 5). The expression patterns of *pdc1* and *pdc2* in the *pdc3* mutant are similar to those observed in the wild-type control (Figure 5A and 5B). Both genes are expressed in shoots and roots at low or undetectable levels under normal conditions, but at high levels after 7.5-hours of anaerobic treatment. In the wild-type control, the *pdc3* gene is expressed at a low but detectable level

in both shoots and roots under normal conditions, and is also highly induced by the 7.5-hour anaerobic treatment (Figure 5C). In the *pdc3* mutants, the expression of *pdc3* is barely detectable in the anaerobically treated roots and shoots. Because the primers used for the *pdc3* RT-PCR experiment flank the *Mu1* insertion in the *pdc3-m2012* allele (Figure 1), this trace amount of RNA accumulation could arise from somatic excision events of the *Mu1* insertion. To test this hypothesis, these RT-PCR products were purified, subcloned, and sequenced. Sequence comparisons between these RT-PCR products and the *pdc3* gene demonstrated that the *pdc3* mRNA accumulation in seedlings homozygous for *pdc3-m2012* is indeed derived from somatic transposon excision events (data not shown).

PDC enzyme activity in *pdc3* mutants

To determine whether the dramatic reduction of *pdc3* mRNA accumulation in *pdc3-m* mutants reduces the total PDC activity in these plants, PDC activity was measured in crude protein extracts isolated from shoots and roots of five-day-old seedlings. The results are shown in Figure 6. Extracts from shoots of seedlings homozygous for *pdc3-2012* exhibit less PDC activity than those from wild-type Ky21 controls, regardless of whether or not these seedlings were subjected to anaerobic treatment (Figure 6A). These data also suggest that although the expression of PDC3 is reduced in *pdc3* mutants, the expression of PDC1 and PDC2 is not dramatically elevated in these mutants (Figure 5). When compared within genotypes, PDC activity is higher in anaerobically treated seedlings (12 hr) than that in untreated seedlings (0 hr) in both wild-type Ky21 and *pdc3-m2012* mutant seedlings. This result is consistent with the anaerobic induction of the *pdc* genes (Figure 5). A similar

pattern was obtained from seedling roots, except that the PDC activity is much lower in *pdc3* mutant seedlings than that in wild-type control seedlings, suggesting that *pdc3* accounts for a larger portion of PDC activity in seedling roots than shoots (Figure 6B). PDC activity assays with seedlings homozygous for another *pdc3* mutant allele, *pdc3-m2015*, gave similar patterns for both shoots and seedling roots (data not shown).

Reduced anaerobic survival of *pdc3* mutant alleles

Since PDC is the rate-limiting enzyme in the anaerobic fermentation pathway (Bucher et al., 1994), and mutations of the *pdc3* gene affect levels of PDC activity, these mutations might affect tolerance to anaerobic stresses. Two *pdc3* mutant alleles, *pdc3-m2012* and *pdc3-m2015*, were tested for their ability to confer tolerance to anaerobic stress. The results are shown in Figure 7. Both mutant alleles start to succumb after six hours of anaerobic treatment and no *pdc3* mutant seedlings survived 12 hours of treatment. In contrast, all wild-type controls survived over 36 hours. Both roots and shoots of *pdc3* mutant seedlings became flaccid after six hours of anaerobic treatment, while those of the wild-type controls remained turgid even after 36 hours of anaerobic treatment. Unlike the wild-type controls after 24 hours of recovery under light at room temperature, mutant shoots did not develop chlorophyll. Instead, the mutant seedlings turned brown and died.

After a shorter period (four to six hours) of anaerobic treatment, the mutant seedling shoots remain turgid; however, after the subsequent 12-hour recovery period under aerobic conditions, some of the shoots exhibited a small area of damage located in the vicinity of the coleoptilar node. Following a longer recovery period (over 24 hours) this region underwent

desiccation. When observed under a light microscope, cells in this region show damage and deformation after a 12-hour recovery period (Figure 8). To test whether the anaerobic induction of *pdc3* at this region is stronger than in the remainder of the shoot, 3mm-thick cross sections of the shoot that included the coleoptilar node were separated from the remainder of the shoot. Semi-quantitative RT-PCR assays for *pdc3* expression demonstrated that the induction level at this region is similar to the remainder of the shoot after a four-hour anaerobic treatment (Figure 9). Hence, the reason for the coleoptilar node's hypersensitivity to anaerobic stress in the *pdc3* mutants is not known.

Correlation between homozygosity of *pdc3* mutants and reduced survival to anaerobic stress

To establish the correlation between loss of *pdc3* function and reduced anaerobic tolerance, seedlings from a segregating population resulted from the test cross, *pdc3-m2015/pdc3-m2015* x *pdc3-m2012/Pdc3*, were treated with anaerobic stress for 12 hours and then allowed to recover for 24 hours. Out of 76 seedlings treated, 40 survived. The progeny from this cross are expected to segregate 1:1 for homozygous mutant seedlings and those that carry a functional *Pdc3* allele. If homozygosity for *pdc3* mutant alleles confers reduced resistance to anaerobic stress, the surviving seedlings should be predominantly heterozygotes. The surviving seedlings were genotyped for *pdc3* via PCR and the results are shown in Table 2. Of the 40 seedlings that survived the anaerobic treatment, 39 carried a functional *Pdc3* allele (i.e. *pdc3-m2015/Pdc3*). The single exceptional homozygous mutant was transplanted to soil in parallel with *pdc3-m2015/Pdc* controls. This *pdc3-m2012/pdc3-m2012* plant never

emerged from the soil while the controls grew well during a 3-week observation period. Similar results were obtained for the *pdc3-m2015* allele (Table 2).

The *pdc3* mutants do not affect male fertility

It has been hypothesized that the conversion of pyruvate to acetate by PDC and ALDH might be involved in anther and pollen development in maize (Cui et al., 1996; Tadege et al., 1999; Liu et al., 2001). If this were true, mutations in *pdc3* might be expected to affect anther development. The *pdc3* mutant alleles, *pdc3-m2012* and *pdc3-m2015*, were crossed as males onto the inbred line Ky21, which carries normal cytoplasm (N). The resulting progeny were self-pollinated. Plants that were homozygous for the two *pdc3* alleles were identified by PCR. All such plants had fully developed tassels and were male fertile (data not shown). This result indicates that mutations of *pdc3* do not affect male fertility in plants that carry normal cytoplasm.

Maize T cytoplasm accumulates a novel protein, URF13, in its mitochondrial inner membrane, that damages the mitochondria. The *rf2* gene is one of the two nuclear restorer genes of T cytoplasm (Wise et al., 1999). Mutant alleles of the *rf2* gene condition male sterility in plants that carry T cytoplasm, while they only cause anther arrest in the lower florets of plants that carry N cytoplasm (Liu et al., 2001). The *pdc3-m* alleles were crossed into a version of the inbred line Ky21 that carries T cytoplasm. The resulting T-cytoplasm heterozyous plants were self-pollinated to produce F_2 families. Six (T) *pdc3-m2015* homozygotes and five (T) *pdc3-m2012* homozygotes were identified in these segregating

families. All such plants had fully developed anthers and were male fertile. These results indicate that *pdc3* mutants do not cause male sterility in T-cytoplasm plants.

It has also been hypothesized that the accumulation of toxic acetaldehyde in the *rf2* mutants could be the cause of male sterility in T-cytoplasm plants. If this were true, mutation of *pdc* genes, and the consequent reduction in PDC activity, might eliminate the accumulation of acetaldehyde, and therefore, complement the *rf2* mutant phenotype. To exclude this possibility, the male fertility of progeny from the test cross: (T) *rf2/rf2 pdc3-m2015/Pdc3* X (N) *rf2/rf2 pdc3-m2015/pdc3-m2015* was observed. If *pdc3* mutants can overcome the *rf2*-induced male sterility, half of the progeny from this test cross would be male fertile. However, all 40 observed progeny were male sterile. PCR genotyping of these plants indicated that 25 of them were homozygous for *pdc3-m2015*. Hence, this result does not support the hypothesis that the toxicity of acetaldehyde accumulated in *rf2* mutants is the cause of male sterility in T-cytoplasm plants. However, a final conclusion as to whether male sterility in (T) *rf2* plants is caused by accumulation of toxic acetaldehyde can not be reached until mutations of the other two *pdc* genes (and the double and even triple mutants) are similarly tested.

Transmission of *pdc3-m* through pollen

Tobacco *pdc* genes are expressed during microsporogenesis and the fermentation pathway accounts for 70% of carbohydrate metabolism in pollen germinated on media (Bucher et al., 1995). Therefore, the loss of PDC activity associated with *pdc3* mutants might affect their ability to be transmitted through pollen. To test this hypothesis, a segregating population

from the test cross, *pdc3-m2015/pdc3-m2015* x *pdc3-m2012/Pdc3* (male parent), was used to test the transmission of *pdc3-m2012* relative to *Pdc3*. Results are shown in Table 1. Out of a total of 79 genotyped seedlings from this cross, 42 had the genotype *pdc3-m2012/pdc3-m2015* and 37 had the genotype *Pdc3/pdc3-m2015*. A χ^2 test showed that this ratio is not significantly different from the expected 1:1. This result indicates that the *pdc3-m2102* allele is transmitted through pollen at the same rate as a non-mutant allele. The *pdc3-m2012* allele is also transmitted through female gametes as efficiently as the non-mutant allele (Table 1).

Discussion

Members of the maize *pdc* gene family and their relationships

The maize genome is a segmental allotetraploid such that most loci have been duplicated once (Gaut and Doebley 1997; Gaut et al., 2000). However, only three maize *pdc* genes have been identified so to date. Although a low-stringency DNA gel blot hybridization with a probe that is well conserved among the three *pdc* genes detected more than three hybridizing bands, the extra band does not necessarily represent an active gene. It could be a fragment of *pdc* sequence duplicated in the genome similar to the 278-bp *pdc* sequence found in a defective retrotransposon element (Christopher and Good, 1999) or a pseudogene such as the rice *pdc3* (Hossain et al., 1994).

One hypothesis to explain the three *pdc* genes in the maize genome is that one of the *pdc* genes underwent duplication or deletion after the alloploidization. According to this hypothesis, two of the three *pdc* genes should be paralogs, and would therefore be located in syntenic regions of the genome. The *pdc1* and *pdc2* genes were mapped 50 cM apart on 8L

and 8S, respectively; the *pdc3* gene was mapped on 1S (Peschke and Sachs 1993). The short arm of chromosome 8 and the short arm of chromosome 1 are syntenic regions (Wilson et al., 1999), which suggests that *pdc2* and *pdc3* may be paralogs. This conclusion is supported by the fact that the gene structures of *pdc2* and *pdc3* are completely conserved, while *pdc1* lacks two introns relative to *pdc2* and *pdc3*. However, the *pdc2* gene has two small insertions, 3-bp and 6-bp, in the coding region compared with *pdc1* and *pdc3*, which indicates that *pdc1* and *pdc3* are more similar. The protein-sequence-based phylogenetic tree also groups *pdc1* and *pdc3* together. Therefore, the evolutionary relationship among the three maize *pdc* genes is still not clear.

Function of the maize *pdc3* gene

Recombinant PDC3 protein exhibits PDC activity *in vitro*. In addition, protein extracts from seedlings homozygous for *pdc3* mutants have less PDC activity than do similar extracts from wild-type seedlings. These results establish that the *pdc3* gene encodes PDC activity.

The expression of recombinant PDC3 was achieved only after the inducible *pdc3* construct was transformed into an *E. coli* strain (BL21(DE3)pLysS) that has tight control over the inducible promoter. Even in this strain PDC activity was detected in only one of three transformation events. The failure of the other two events to exhibit detectable levels of PDC activity may have been due to their cell growth status at the time of their induction by IPTG. The *pdc3* construct was highly unstable in *E. coli* strain, BL21(DE3), which does not tightly control the expression of recombinant proteins in the absence of IPTG. This suggests that *E. coli* may have a low tolerance for even small amounts of PDC activity.

Because *E. coli* does not contain endogenous PDC activity (Pronk et al., 1996) the accumulation of recombinant PDC3 might interfere with pyruvate metabolism or result in the production of toxic levels of aldehyde.

Although all three maize *pdc* genes are all induced by anaerobic stress (Peschke and Sachs, 1993), direct evidence that these genes or similar genes in other plants are involved in anaerobic stress resistance has been lacking. The finding that seedlings homozygous for *pdc3* mutants exhibit dramatically reduced the tolerance to anaerobic stress provides direct evidence for the importance of PDC activity in anaerobic tolerance in plants. The physiological lesion associated with the *pdc3* mutants is first visible at the region surrounding the coleoptilar node. However, although the *pdc3* gene plays a critical role in this region, semi-quantitative PCR experiments established that *pdc3* is not over-expressed at the mRNA level in this region relative to the remainder of the shoot. Interestingly, seedlings homozygous for *pdc3* mutants do not exhibit elevated expression of *pdc1* and *pdc2* either at the level of mRNA or enzyme activity.

The fermentation pathway is also active under aerobic conditions in anthers during microsporogenesis and in germinating pollen (Freeling and Bennett, 1985; Bucher et al., 1995). One hypothesis is that the function of aerobic fermentation in these tissues is to produce acetate from acetaldehyde by aldehyde dehydrogenase (ALDH). Acetate can then be used for lipid biosynthesis or other metabolic pathways, which could be important for the high energy and metabolism requirements in these tissues. Therefore, the production of ethanol from acetaldehyde by ADH might be just a flow control for the production of acetate during microsporogenesis and/or pollen germination. Support for this hypothesis comes from the detection of high levels of ALDH in tobacco pollen and tapetal cells during

microsporogenesis (op den Camp and Kuhlemeier, 1997). In addition, inhibition of ALDH activity hampers tobacco pollen tube growth (Roel et al., 1997). Further evidence comes from the study of the maize *rf2* gene, which encodes a mitochondrial ALDH and is highly expressed in tapetal cells during microsporogenesis (Cui et al., 1996; Liu et al., 2001). Mutation of the *rf2* gene affects anther development in the lower florets (Liu et al., 2001) and male sterility in plants that carry T-cytoplasm (reviewed by Schnable and Wise, 1998; Wise et al., 1999). A direct test of this hypothesis would be to determine whether *pdc* mutants affect anther development in the same fashion as do the *rf2* mutants. The current study established that mutation of *pdc3* does not affect anther development, which indicates that the *pdc3* gene is at least not uniquely involved in this process. This result is not surprising, because either *pdc1* or *pdc2* could presumably substitute for *pdc3*. In fact, the tobacco *pdc* gene that is constitutively expressed in anther (*Tobpdc2*) is not the one (*Tobpdc1*) that responds to anaerobic induction in leaves (Bucher et al., 1995; Tadege and Kuhlemeier, 1997). Another possibility is that the RF2 protein does not function as a restorer of T cytoplasm male sterility through this pathway. Detailed characterization of the mutants of *pdc1*, *pdc2*, and/or the double even the triple mutants of the three *pdc* genes should help to address these questions.

Materials and Methods

Plant materials

Maize (*Zea mays* L.) F_2 families segregating for *Mu*-insertion mutants at *pdc1*, *pdc2* or *pdc3* were obtained from Pioneer Hi-Bred Intl. Inc., Johnston, IA. Plants that carry *pdc* mutant

alleles were crossed to the inbred lines (T) Ky21 and (T) R213. (T) Ky21 carries *Rf1-Ky21* and *Rf2-Ky21* and (T) R213 carries *Rf1-Ky21* and *rf2-R213*.

Cloning of *pdc2* and *pdc3*

The DuPont/Pioneer EST database was searched using a partial *pdc2* cDNA sequence (GenBank accession number D14456) and a partial *pdc3* cDNA sequence (GenBank accession number D14457). Both strands of the resulting *pdc2* (pdc2-A5) and *pdc3* (pdc3-A7 and p0102) EST clones were sequenced. The pdc2-A5 sequence was extended toward the 5' end from mRNA isolated from B73 using a One Step RT-PCR kit (Qiagen, Valencia, CA) with primers pdc2e (5'-GCT CAGGTGCTTCCAGAACG-3') and pdc2d2 (5'-GGTAGGCATCGGCAGACTCG-3') according to the manufacture's instructions. A GeneRacer kit (Invitrogen, Carlsbad, CA) was used to further extend the sequence to the 5' end using primer pdc2f (5'-CGTTCTGGAAGC ACCTGAGC-3') according to the manufacture's instructions.

The partial *pdc2* and *pdc3* EST clones, pdc2-A5 and pdc3-A7, were used to screen two maize B73 genomic libraries. Library screening conditions were as described by XU *et al.* (1997). Two overlapping positive clones, λ1111 and λ10163, were obtained for *pdc2* and two overlapping positive clones, λ9-1 and λ3-6, were obtained for *pdc3*. These positive clones were sequenced using a transposon-based sequencing method (Strathmann et al., 1991).

Expression of *pdc3* cDNA in *E. coli*

The *pdc3* DNA sequence used for expression in *E. coli* was derived from two EST clones, p0102 and pdc3-A7. The 390-bp fragment from the 5' end of p0102 was PCR-amplified using primers, PDC3L (5'ATCCATGGCTA GCCACATCGGATCCGTGAACGGG-3') and PDC3N (5'- CCGATGGTGTGGTGG AGGATGC-3'). The resulting PCR product was digested with *Nhe*I and *Apa*I. The remainder of the *pdc3* cDNA was release from pdc3-A7 using *Apa*I and *Not*I. A three-fragment ligation was performed using the *Nhe*I/*Apa*I fragment from the PCR reaction, the *Apa*I/*Not*I *pdc3* fragment from pdc3-A7 and pET-17b vector (Novagene, Madison, WI) that had been digested with *Nhe*I and *Not*I. The products of this ligation were transformed into *E. coli* strain DH5α and positive clones were identified via PCR. The purified construct was then transformed into other *E. coli* strains, BL21(DE3) and BL21(DE3)pLysS (Novagene), for protein expression. Protein expression was conducted according to the Novagene protocol. Crude protein extracts were obtained as previously described (Liu et al., 2001).

Isolation of *pdc3* mutants

Primers specific for the *pdc3* gene, pdc3-F (5'-ATTGCTGAGACTGGTGACTCCTGGTTC A-3'), and pdc3-R (5'-CCCACCGTGCTA CAGCTTACTATCAC-3'), were designed based on the maize *pdc* sequences in the GenBank (GenBank accession number: D14457). The specificities of these primers were tested by hybridizing the PCR products obtained using these primers in conjuction with maize genomic DNA templates with sequence-confirmed

pdc3 probes isolated from plasmid pPDC3-37. These primers were then used to screen the Pioneer Hi-Bred TUSC population.

Primers specific to the *pdc3* gene and a primer specific to the *Mu* terminal inverted repeats, Mu_TIR [5'-AGAGAAGCCAACGCCA(AT)CGCCTC(CT)ATTTCGTC-3'], were used to amplify from each *pdc3* mutant allele. Sequences of these PCR products were compared with the *pdc3* genomic sequence to identify the *Mu*-insertion site in each *pdc3* mutant allele. Sequences of these PCR products were also compared with the *Mu* transposon sequences in GenBank to determine the identities and orientations of the *Mu* insertions.

Requests for seed of the *pdc3* mutants should be directed to Pioneer Hi-Bred International, Inc. and may require a Materials Transfer Agreement.

Low-stringency DNA gel blotting

Maize genomic DNA was isolated using a 1X CTAB procedure (Saghai-Maroof *et al.* 1984). Approximately 10 µg of DNA was digested with the indicated restriction enzyme in a 30 µl reaction volume for more than three hours and then separated via electrophoresis in a 0.8% agarose gel. DNA was transferred to nylon filters (MSI, Westboro, MA) and hybridized with a 320-bp probe, pdc2YFL-F, labeled with $dCTP^{32}$ (AUSUBEL *et al.* 1999), at 65°C overnight in hybridization solution (6 x SSPE, 0.02% PVP, 0.02% Ficoll, 1% SDS). Washing was performed in Wash I (2 x SSPE, 0.5% SDS) at 50°C for 15 minutes twice and in Wash II (5mM TrisCl, 0.1% SDS) at 65°C for 10 minutes. The 320-bp probe, pdc2YFL-F, was PCR-amplified from λ10163 phage DNA using primers pdc2-YFL (5'-ACTTCA ACCTCACGCTGCTC-3') and pdc2F (5'-CGTTCTGGAAGCACCTGAGC-3'). The PCR

conditions were: preheating at 94° for 2 minutes, denaturing at 94°C for 45 seconds, annealing at 58°C for 1 minute, extension at 72°C for 2 minutes for 34 cycles in the presence of one unit of Taq polymerase (Promega, Madison, WI) and 10% DMSO.

PCR analyses

The allele-specific PCR reactions for genotyping each *pdc* mutant allele or *Mu* insertion determination were conducted using the *Mu*_TIR primer together with the *pdc*-specific primers (Figure 1). The PCR conditions were: preheating at 94° for 2 minutes, denaturing at 94°C for 45 seconds, annealing at 62°C for 1 minute, extension at 72°C for 2 minutes for 34 cycles in the presence of one unit of Taq polymerase (Promega).

RT-PCR was performed according to the 3' and 5' RACE manual provided by GIBCO BRL. About 0.5 ug of total RNA was used for the first strand synthesis using the reverse gene-specific primers, pdc1-i, pdc2-i, pdc3-R, and Act515 (5'-CCGATTGAGCATGGCA TTG-3'). One eighth of the reaction was used for the subsequent PCR using the above reverse primers paired with the forward gene-specific primers, pdcF, pdc2-ii, pdc3-F, and Act326 (5'-ATCGGCAATCCCAGGAAAC-3'), respectively. The PCR conditions were: preheating at 94°C for 2 minutes, denaturing at 94°C for 45 seconds, annealing at 62°C for 1 minute, and extension at 72°C for 2 minutes for 30 cycles at the presence of 2.5 unit of Taq polymerase (Promega). PCR products were separated on 1.0% agarose gel and transferred onto nylon membranes (MSI). The nylon membranes were hybridized with *pdc1*, *pdc2* and *pdc3* cDNA probes released from plasmids pPDC1, pdc2-A5, and pdc3-A7, respectively. The actin RT-PCR products were hybridized with sequence-confirmed PCR product.

PDC enzyme activity assay

The PDC enzyme activity assay was performed according to Bucher et al., (1994) with minor modifications. In this assay, PDC activity is detected via the oxidation of NADH to NAD^+ when the product, acetaldehyde, is converted to ethanol by ADH. The protein concentrations of crude extracts from seedling shoots and roots were determined using the Bio-Rad Protein Assay (Catalog No. 500-0006, Bio-Rad Laboratories, Hercules, CA). Thirty μg of shoot protein, 20 μg of root protein or 30 μg of *E. coli* protein were used in a 333-μl reaction. NADH concentrations were measured using a plate reader, Spectra MAX Plus (Molecular Devices, Sunnyvale, CA), at OD_{340} over a 15-minute period. Yeast PDC (Promega, Catalog No. p-6810) was used as a positive control. The PDC activity was calculated according to Bucher et al. (1994).

Anaerobic tolerance test

The anaerobic tolerance test was performed according to the methods of Lemke-Keyes and Sachs (1989) with modifications. Sterilized seeds were rolled in wet germination paper (Anchor Paper, St. Paul, MN). The bottom of the paper rolls were soaked in water and kept in a 28°C stationary incubator. Twenty seedlings that were 5- to 8-cm long and had closed coleoptiles were sealed in a Magenta plant cell culture vessel (Sigma, St. Louis, MO) filled with 5mM TRIS-HCl, 200mg/L ampicillin, pH 7.0 for various lengths of time. The seedlings were rolled into fresh germination paper after the anaerobic treatment and allowed to recover for 12 to 24 hours under light at room temperature.

To test the correlation between loss of *pdc3* function and reduced anaerobic tolerance, five-day-old seedlings were subjected to 24-hour anaerobic treatment and allowed to recover for 24 hours. The surviving seedlings (green) were divided into groups of five for pooled DNA isolation. The DNA sample from each seedling group was genotyped via PCR using primer pdc3-F (for family 98g1462 /1444-5) or pdc3-R (for family 98g1458 /1445-2) in combination with the Mu_TIR primer. Seedlings from the groups that contained *pdc3-m2015/pdc3-m2012* DNA were genotyped individually. The survived *pdc3-m2015/pdc3-m2012* seedlings were transplanted into soil together with four controls and allowed to grow under greenhouse conditions for three weeks.

Light microscopy

Maize seedling shoots and roots were fixed in FAA (50% ethanol, 5% acetic acid and 3.7% formaldehyde) at room temperature for 24 hours. Fixed tissues were dehydrated, infiltrated, and embedded in paraffin (Sylvester and Ruzin, 1994). Cross sections of 10 to 20 μm were deparaffinized and stained with Toluidine Blue for observation via bright field microscopy.

DNA sequencing and analysis

DNA sequencing was performed at the Iowa State University DNA Sequencing and Synthesis Facility on an automated sequencer (ABI 373A, Applied Biosystems) using DyeTerminator technology, and on a 4200 LiCor sequencer at the USDA-ARS-NPURU using labeled primers (Amersham Pharmacia Biotech). Sequence assembly and analyses at Iowa State University were performed using the Wisconsin GCG software package (Version

10.0-UNIX) from the Genetics Computer Group, Inc. Sequence assembly and analyses at USDA-ARS-NPURU were performed using Lasergene from DNASTAR.

For the genomic sequence, overlapping fragments for both *pdc2* and *pdc3* were cloned into the vector pCSOS-72 and transposon mutagensis, using a modified TN1000 element (provided by S. Case, University of Mississippi Medical Center, Jackson, MS), was performed according to the protocol of Strathmann et al. (1991). Insertion sites were confirmed by PCR and the selected clones (spaced at approximately 500 bp intervals) were sequenced using standard M13 universal and reverse primers.

Acknowledgments

We thank Dr. Martin Sachs (University of Illinois at Urbana-Champaign, Urbana, IL) for the partial *pdc1* cDNA clone pPDC1 and Dr. Pam Close (University of Missouri, Columbia, MO) and John Tossberg (Pioneer Hi-Bred, Intl. Inc., Johnston, IA) for the B73 genomic libraries. We also thank David Skibbe for his assistance in library screening and Tim Fox from Marc Albertson's group (Pioneer Hi-Bred, Intl. Inc., Johnston, IA) for his assistance in searching the Pioneer EST database. This research was supported in part by competitive grants from the USDA-NRI program to P.S.S. (98001805 and 0001478) and from the Human Frontiers in Science Program (RG0067) to Cris Kuhlemeier (Institute of Plant Physiology, University of Berne, Switzerland) and P.S.S. Journal paper No. 19307 of the Iowa Agriculture and Home Economics Experiment Station, Ames, IA 50011; Project No: 3554 and supported by Hatch Act and State of Iowa funds.

Literature Cited

Ausubel FM, Brent R, Kingston R E, Moore DD, Seidman JG, *et al.* (1999) *Current protocols in molecular biology.* John Wiley & Sons, New York.

Bensen RJ, Johal GS, Crane VC, Tossberg JT, Schnable PS, et al. (1995) Cloning and characterization of the maize *An1* gene. Plant Cell 7: 75-84

Bucher M, Brandle R, Kuhlemeier C (1994) Ethanolic fermentation in transgenic tobacco expressing Zymomonas mobilis pyruvate decarboxylase. EMBO J. 13: 2755-2763

Bucher M, Brander KA, Sbicego S, Mandel T, Kuhlemeier C (1995) Aerobic fermentation in tobacco pollen. Plant Mol Biol 28: 739-750

Christopher M.E, Good AG (1996) Characterization of hypoxically inducible lactate dehydrogenase in maize. Plant Physiol 112: 1015-1022

Christopher M.E, Good AG (1999) Evolution of a functionally related lactate dehydrogenase and pyruvate decarboxylase pseudogene complex in maize. Genome 42: 1167-75

Cui X, Wise RP, Schnable PS (1996) The *rf2* nuclear restorer gene of male sterile T-cytoplasm maize. Science 272: 1334-1336

Dennis ES, Sachs MM, Gerlach WL, Finnegan EJ, Peacock WJ (1985) Molecular analysis of the *Alcohol dehydrogenase 2* (*Adh2*) gene of maize. Nucleic Acids Research 13: 727-743

Drew MC (1997) Oxygen deficiency and root metabolism: injury and acclimation under hypoxia and anoxia. Annu. Rev Plant Mol Biol 48: 223-250

Freeling M (1973) Simultaneous induction by anaerobiosis or 2,4-D of multiple enzymes specified by two unlinked genes: differential *adh1-adh2* expression in maize. Mol Gen Genet 127: 215-227

Freeling M, Bennett DC (1985) Maize *Adh1*. Annu Rev Genet 19: 297-323

Freeling M, Schwartz D (1973) genetic relationships between the multiple alcohol dehydrogenases of maize. Biochem Genet 8:27-36

Gale MD, Devos K.M (1998) Comparative genetics in the grasses. Proc Natl Acad Sci USA 95: 1971-1974

Gerlach WL, Pryor AJ, Dennis ES, Ferl RJ, Sachs MM, Peacock WJ (1982) cDNA cloning and induction of the *alcohol dehydrogenase* gene (*Adh1*) of maize. Proc Nat Acad Sci 79: 2981-2985

Gaut BS, Doebley JF (1997) DNA sequence evidence for the segmental allotetraploid origin of maize. Proc Natl Acad Sci USA 94: 6809-6814

Gaut BS, Le Thierry d'Ennequin M, Peek AS., Sawkins MC (2000) Maize as a model for the evolution of plant nuclear genomes. Proc Natl Acad Sci USA 97: 7008-7015

Hossain MA, McGee JD, Grover A, Dennis ES, Peacock WJ, Hodges TK, Dennis E (1994) Nucleotide sequence of a rice genomic pyruvate decarboxylase gene that lacks introns: a pseudo-gene? Plant Physiol 106: 1697-8

Kelley PM (1989) Maize pyruvate decarboxylase mRNA is induced anaerobically. Plant Mol Biol. 13: 213-222

Kelley PM, Godfrey K, Lal SK, Alleman M (1991) Characterization of the maize pyruvate decarboxylase gene. Plant Mol Biol 17: 1259-1261

Kennedy RA, Rumpho ME, Fox TC (1992) Anaerobic metabolism in plants. Plant Physiol 100: 1-6

Lee TC, Langston-Unkefer PJ (1985) Pyruvate decarboxylase from *Zea mays* L. I. Purification and partial characterization from mature kernels and anaerobically treated roots. Plant Physiol 79: 242-247

Lemke-Keyes CA, Sachs MM (1989) Genetic variation for seedling tolerance to anaerobic stress in maize germplasm. Maydica 34: 329-337

Liu F, Cui X, Horner HT, Weiner H, Schnable PS (2001) Mitochondrial aldehyde dehydrogenase activity is required for male fertility in maize. Plant Cell, 13: 1063-1078

Moore G (2000) Cereal chromosome structure, evolution, and pairing. Annu Rev Plant Physiol Plant Mol Biol 51: 195-222

op den Camp RG, Kuhlemeier C (1997) Aldehyde dehydrogenase in tobacco pollen. Plant Mol Biol 35: 355-365

Peschke VM, Sachs MM (1993) Multiple pyruvate decarboxylase genes in maize are induced by hypoxia. Mol Gen Genet 240: 206-212

Pronk JT, Yde Steensma H, Van Dijken JP (1996) Pyruvate metabolism in Saccharomyces cerevisiae. Yeast 12: 1607-33

Rivoal, J, Thind S, Pradet A, Ricard B (1997) Differential induction of pyruvate decarboxylase subunits and transcripts in anoxic rice seedlings. Plant Physiol 114: 1021-9

Roberts JKM, Chang K, Webster C, Callis J, Walbot V (1989) Dependence of ethanolic fermentation, cytoplasmic pH regulation, and viability on the activity of alcohol dehydrogenase in hypoxic maize root tips. Plant Physiol 89: 1275-1278

Roel G L, op den Camp R G, Kuhlemeier C (1997) Aldehyde dehydrogenase in tobacco pollen. Plant Molecular Biology 35: 355-365

Sachs MM (1993) Molecular genetic basis of metabolic adaptation to anoxia in maize and its possible utility for improving tolerance of crops to soil waterlogging. In MB Jackson and CR Black eds, Interacting Stresses on Plants in a Changing Climate, NATO ASI Series Vol 116, Springer-Verlag Berlin Heidelberg, pp. 375-393

Saghai-Maroof MA, Soliman KM, Jorgensen RA, Allard RW (1984) Ribosomal DNA spacer-length polymorphisms in barley: mendelian inheritance, chromosomal location, and population dynamics. Proc Natl Acad Sci USA 81: 8014-8018

Schnable PS, Wise RP (1998) The molecular basis of cytoplasmic male sterility and fertility restoration. Trends in Plant Science 3: 175-180

Schwartz D (1969) An example of gene fixation resulting from selective advantage in suboptimal conditions. Am Not 103: 479-481

Strathmann M, Hamilton BA, Mayeda CA, Simon MI, Meyerowitz EM, Palazzolo MJ (1991) Transposon-facilitated DNA sequencing. Proc Natl Acad Sci USA 88:1247-50

Sylvester AW, Ruzin SE (1994) Light Microscopy I: Dissection and Microtechnique. In M Freeling, V Walbot Eds, the Maize Handbook, Springer-Verlag New York, Inc., New York, pp. 89-92

Tadege M, Kuhlemeier C (1997) Aerobic fermentation during tobacco pollen development. Plant Mol Biol 35: 343-354

Tadege M, Dupuis I, Kuhlemeier C (1999) Ethanolic fermentation: new functions for an old pathway. Trends Plant Sci 4: 320-325

Wilson WA, Harrington SE, Woodman WL, Lee M, Sorrells ME, McCouch SR (1999) Inferences on the genome structure of progenitor maize through comparative analysis of rice, maize and the domesticated panicoids. Genetics 153: 453-73

Wise RP, Bronson CR, Schnable PS, Horner HT (1999) The genetics, pathology, and molecular biology of T-cytoplasm male sterility in maize. Advances in Agronomy 65: 9-130

Xu, X, Dietrich CR, Delledonne M, Xia Y, Wen TJ, Robertson DS, Nikolau BJ, Schnable PS (1997) Sequence analysis of the cloned *glossy8* gene of maize suggests that it may code for a

beta-ketoacyl reductase required for the biosynthesis of cuticular waxes. Plant Physiol 115: 501-510

Tables

Table 1. The transmission of *pdc3-m2012* through male and female gametes.

Row Numbers	Crosses [a]	No. of Progeny with Indicated Genotypes				χ^2 (1:1)
		pdc3-m2012 /pdc3-m2015	*Pdc /pdc3-m2015*	*Pdc3/ pdc3-m2012*	*Pdc3 /Pdc3*	
98g1463 /1444-5	*pdc3-m2015/pdc3-2015* x *pdc3-m2012 /Pdc3*	42	37	NA	NA	0.16 [ns]
987720-7 /6307	*pdc3-m2012/Pdc3* x *Pdc3/Pdc3*	NA	NA	32	34	0.06 [ns]

Seeds resulted from two crosses were germinated and seedlings were genotyped using PCR. The PCR products were hybridized with a partial *pdc3* cDNA probe. [a] genotypes of the crosses are written as female parent x male parent and the tested allele is underlined; NA, not applicable; ns, not significant.

Table 2. Correlation between *pdc3-m* homozygosity and reduced tolerance to anaerobic stress

Families	Crosses	No. of seedlings			
		Died	Survived		
			pdc3-m2015 /Pdc3	*pdc3-m2015/ pdc3-m2012*	*pdc3-m2012/ Pdc3*
98g1462 /1444-5	*pdc3-m2015/pdc3-m2015* x *pdc3-m2012/Pdc3*	36	39	1[a]	
98g1458 /1445-2	*pdc3-m2012/pdc3-m2012* x *pdc3-m2015/Pdc3*	35		1[b]	45

[a] Did not emerge from soil after planted; [b] emerged but died within one week. The wild-type controls grew well in the 3-week observation.

Figure Legends

Figure 1. Gene structures of three *pdc* genes and the positions of the *Mu* transposons responsible for *pdc3* mutants isolated via the TUSC system. Genomic and cDNA sequences are indicated by solid lines and filled boxes, respectively. The dashed lines indicate the corresponding introns and exons in three *pdc* genes. Transposon insertions are represented by triangles. The identified transposon orientations are indicated by the horizontal arrows inside the triangles with the arrow heads pointing to the 3' ends of the transposon sequences in the GenBank.

Figure 2. Phylogenetic tree of plant *pdc* genes. The tree was constructed using neighbor-joining methods based on alignments derived from ClustalX. Felsenstein's Bootstrap test scores (>50%) from 1000 replicates were indicated at nodes. At, *Arabidopsis thaliana*; Nt, *Nicotiana tobacum* (tobacco); Fa, *Fragaria ananassa* (strawberry); Os, *Oryza sativa* (rice); Ps, *Pisum sativum* (garden pea); Zm, *Zea mays* (maize). The GenBank accession numbers of the sequences in the tree: At PDC1, U71121; AtPDC2, U71122; AtPDC1-like1, CAB18915.1; AtPDC1-like2, CAB81916.1; NtPDC1, X81854; NtPDC2, X81855; FaPDC, AF193791; PsPDC1, Z66543; OsPDC1, U26660; OsPDC2, U27350; OsPDC3 (pseudo), U07338; OsPDC4; ZmPDC1, X17555; ZmPDC2, AF370003; ZmPDC3, AF230005.

Figure 3. Low-stringency DNA gel blot hybridization. B73 genomic DNA was digested with indicated enzymes and hybridized with a 320-bp highly conserved probe, pdc2YFL-F.

Figure 4. PDC enzyme activity of recombinant PDC3 protein. Protein was extracted from *E. coli* strains that harbor a *pdc3* expression construct. PDC activity was measured by monitoring the oxidation of NADH (see Materials and Methods). pEPDC3-3, pEPDC3-7, and pEPDC3-32 are different transformation events containing the same construct

Figure 5. The anaerobic induction of *pdc1*, *pdc2*, *pdc3* mRNAs. RT-PCR products were hybridized with probes from each gene. Hours of anaerobic treatment are indicated above each panel. The inbred line Ky21 is homozygous for the functional *Pdc3-Ky21* allele. RT, root; ST, shoot.

Figure 6. PCD enzyme activity of *pdc3* mutant. Protein was extracted from roots and shoots of Five-day old seedlings. PDC activity was measured by monitoring the oxidation of NADH (see Materials and Methods). One unit (U) of PDC converts 1.0 μmol of pyruvate to acetaldehyde per minute at pH 6.0 at 25°C.

Figure 7. The reduced anaerobic tolerance of *pdc3* mutants. Five-day-old-seedlings from each genotype were tested for anaerobic tolerance (see Materials and Methods). Each data point represents the percentage of seedlings (N=20) that survived the indicated anaerobic treatment.

Figure 8. The physiological lesion associated with *pdc3* mutants. Seven-day-old *pdc3* mutant seedlings were subjected to anaerobic stress for four hours and allowed to recover under light for 12 hours (A) or 24 hours (B). Roots and shoots subjected to anaerobic stress for seven hours followed by a 12-hour recovery period were fixed with FAA and embedded in paraffin. 10-μm-thick sections were stained with toluidine blue and observed under a light microscope. No obvious differences were observed between wild-type roots (C) and *pdc3* mutant roots (D). Damaged cells were observed in *pdc3* shoots (E) compared with wild type (G). F and H are higher magnification of E and G, respectively. Magnification: 40X in C, D, E and G; 200X in F and H.

Figure 9. The anaerobic induction of *pdc3* mRNA. RT-PCR products were hybridized with probes from *pdc3* and *actin*. Hours of anaerobic treatment are indicated above each panel.

The inbred line Ky21 is homozygous for the functional *Pdc3-Ky21* allele. C, coleoptilar node region; R, remainder of the shoot.

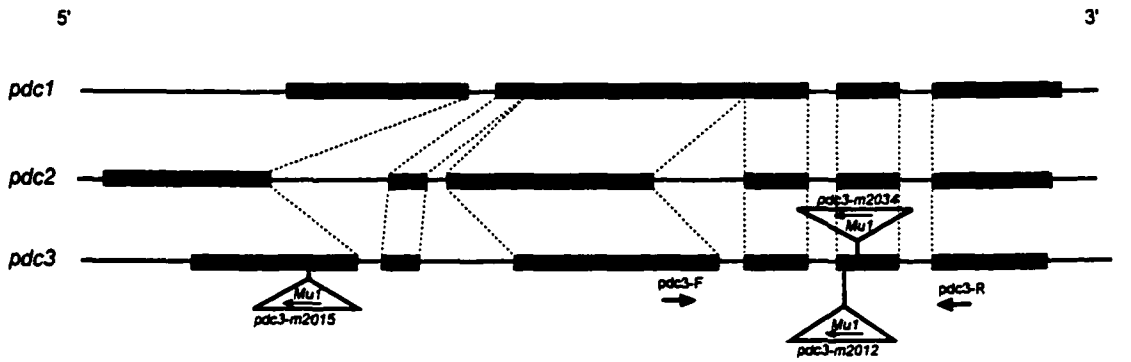

Cui et al., Figure 1

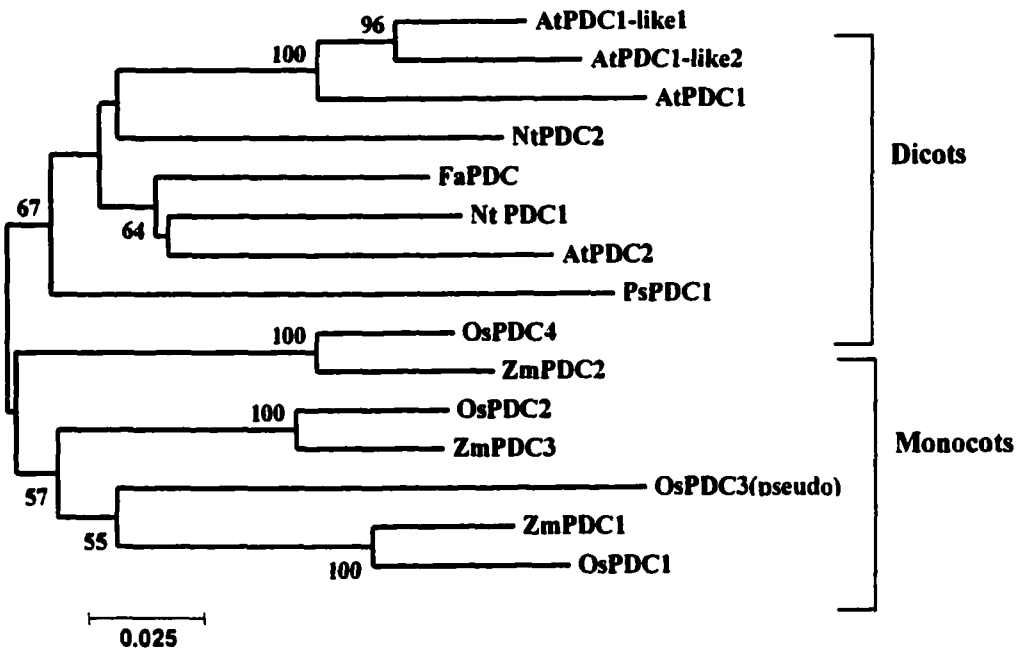

Cui et al., Figure 2

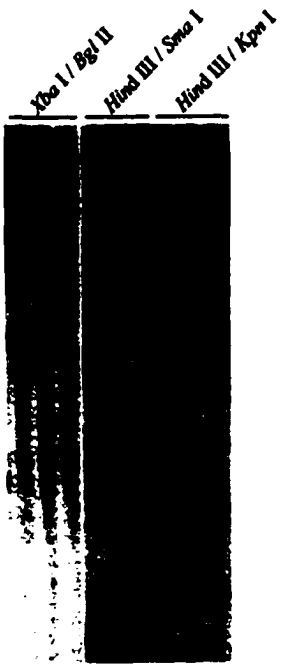

Cui et al., Figure 3

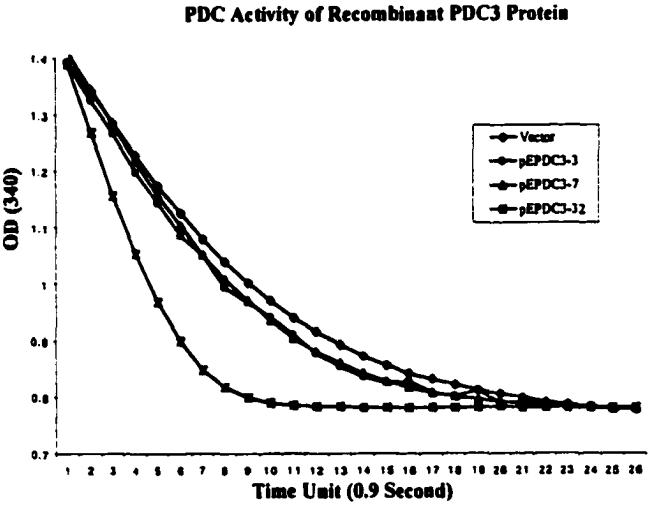

Cui et al., Figure 4

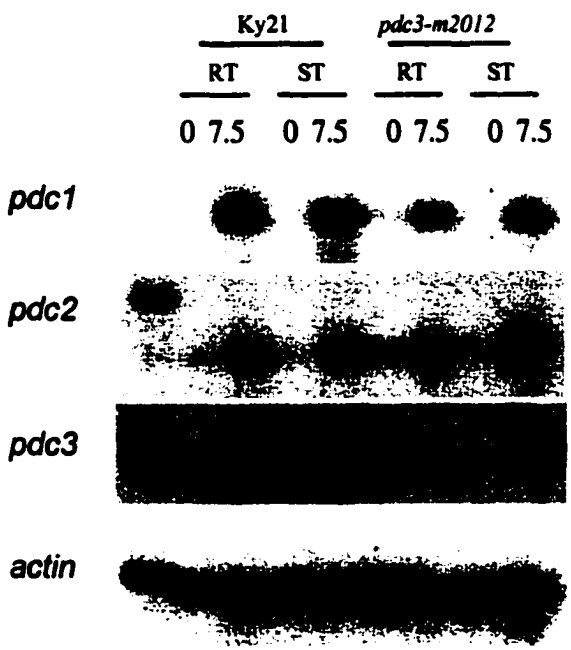

Cui et al., Figure 5

A

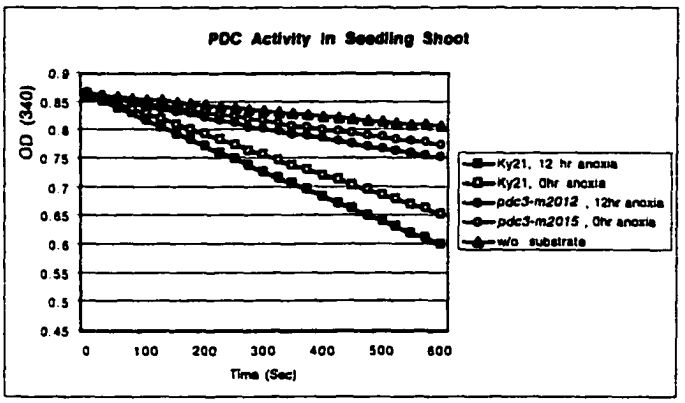

B

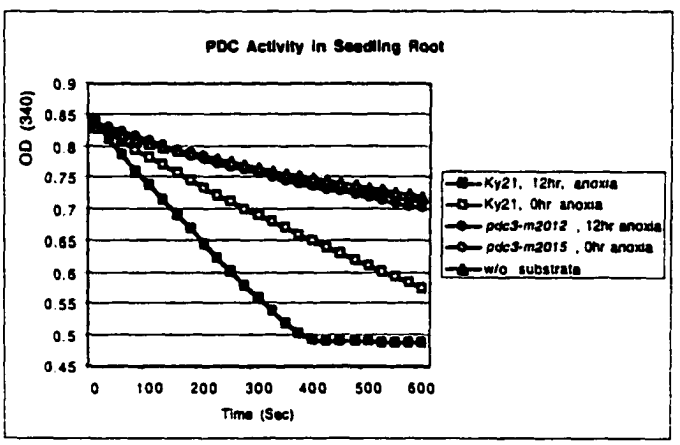

PDC activity (mU) represented in panel A and B

Genotype	Ky21	Ky21	*pdc3-m2012*	*pdc3-m2012*
Anaerobic Treatment	(12 hr)	(0 hr)	(12 hr)	(0 hr)
Shoot	35.4	26.3	10.6	6.5
Root	91.6	38.1	5.7	4.5

Cui et al., Figure 6

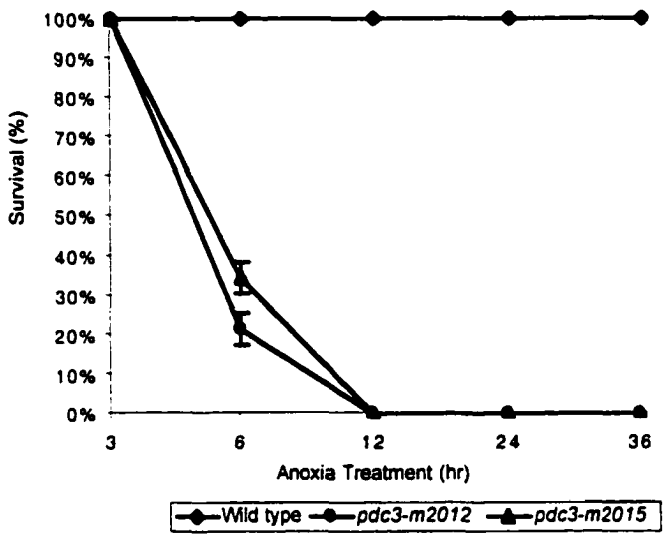

Cui et al., Figure 7

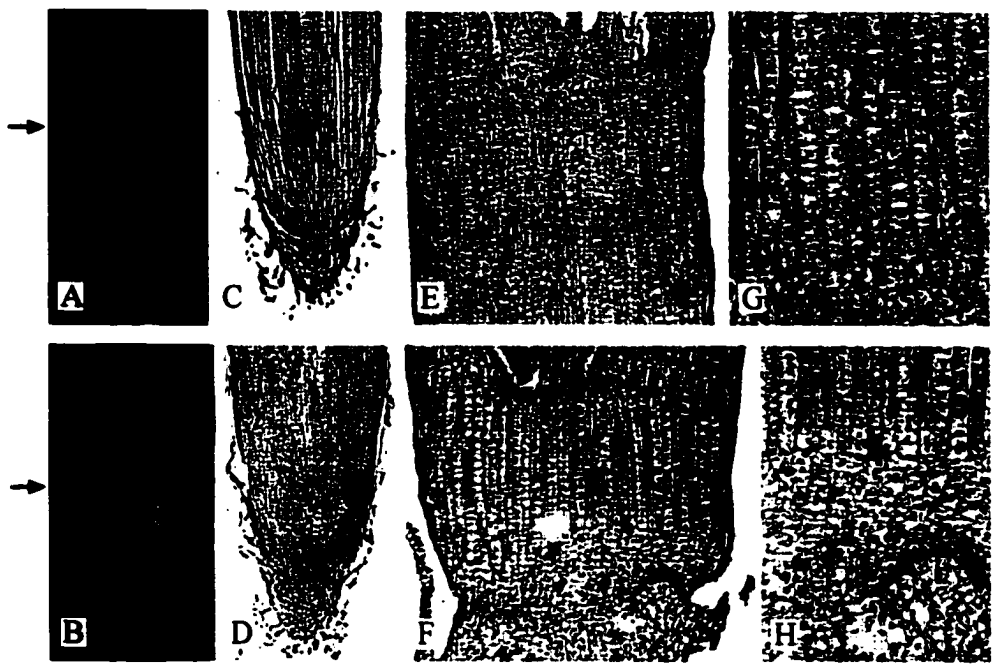

Cui et al., Figure 8

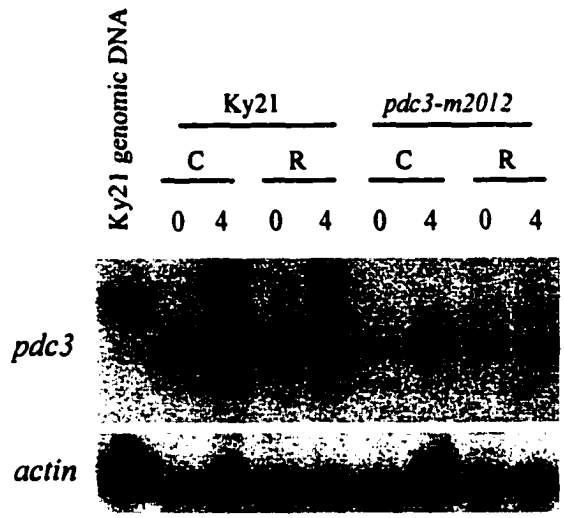

Cui et al., Figure 9

CHAPTER 5. ALTERNATIVE TRANSCRIPTION INITIATION SITES AND POLYADENYLATION SITES ARE RECRUITED DURING *Mu* SUPPRESSION AT THE *rf2* LOCUS OF MAIZE

A paper submitted to Genetics

Xiangqin Cui,[1] An-Ping Hsia,[2] Daniel A. Ashlock,[3] Roger P. Wise,[4] and Patrick S. Schnable[5]

Abstract

Even in the absence of excisional loss of the associated *Mu* transposons, some *Mu*-induced mutant alleles of maize can lose their capacity to condition a mutant phenotype. Three of the five existing *Mu*-induced *rf2* alleles are susceptible to *Mu* suppression. The suppressible *rf2-m9437* allele has a novel *Mu* transposon insertion (*Mu10*) in its 5' untranslated region (UTR). The suppressible *rf2-m9390* allele has a *Mu1* insertion in its

[1] Interdepartmental Genetics Program and Department of Zoology & Genetics

[2] Department of Agronomy

[3] Department of Mathematics

[4] Corn Insects and Crop Genetics Research, U.S. Department of Agriculture-Agricultural Research Service (USDA-ARS), Department of Plant Pathology

[5] Department of Agronomy and Department of Zoology & Genetics

5' UTR. During suppression, alternative transcription initiation sites flanking the *Mu1* transposon yield functional transcripts. The suppressible *rf2-m8110* allele has an *rcy:Mu7* insertion in its 3' UTR. Suppression of this allele occurs via a previously unreported mechanism; sequences in the terminal inverted repeats of *rcy:Mu7* function as alternative polyadenylation sites such that the suppressed *rf2-m8110* allele yields functional *rf2* transcripts. The nucleotide compositions of these alternative polyadenylation sites were compared with 94 other maize polyadenylation sites. No significant difference was found at the 95% confidence level (χ^2 =3.67). In contrast to earlier reports, this study revealed only a weak correlation between hyper-methylation of *Mu* transposons and *Mu* suppression.

Introduction

There are two broad categories of DNA transposons, autonomous and nonautonomous. Autonomous transposons encode all non-host factors required for their own transposition. In contrast, the transposition of nonautonomous transposons is dependent upon factors encoded by autonomous transposons of the same family. Hence, only in the presence of factors encoded by the autonomous *Spm/En*, *Ac*, and *MuDR* maize transposons, can the nonautonomous *dSpm/I*, *Ds*, and *Mu* transposons undergo excision and transposition (reviewed by MASSON *et al.* 1991; BENNETZEN *et al.* 1993; KUNZE 1996; BENNETZEN 1996; FEDOROFF 1999). However, autonomous and nonautonomous transposons can both cause mutations when they insert into genes. The *Mutator* (*Mu*) transposon family (ROBERTSON 1978) has been widely used for gene mutagenesis and

cloning (BENNETZEN *et al.* 1993; BENNETZEN 1996). Its 4.9-kb autonomous member, *MuDR*, mediates the transposition of the nonautonomous transposons, *Mu1* through *Mu8* (SCHNABLE and PETERSON 1986; ROBERTSON and STINARD 1989; HERSHBERGER *et al.* 1991; CHOMET *et al.* 1991; QIN *et al.* 1991; HSIA and SCHNABLE 1996). *MuDR* contains two open reading frames, *mudrA* and *mudrB* (HERSHBERGER *et al.* 1991; JAMES *et al.* 1993). The *mudrA* gene encodes a DNA-binding protein with sequence similarity to bacterial transposases (EISEN *et al.* 1994; BENITO and WALBOT 1997). The *mudrA* gene is necessary and sufficient for somatic excision of *Mu* transposons (LISCH *et al.* 1999; RAIZADA and WALBOT 2000). The *mudrB* gene may be involved in suppression (DONLIN *et al.* 1995; LISCH *et al.* 1999).

Many transposon-induced mutants exhibit unstable phenotypes due to DNA rearrangements such as excision. In addition, some transposon-induced alleles also exhibit instabilities that occur in the absence of DNA rearrangements. For example, in the presence of an autonomous *Spm/En* transposon, the *a1-m1* allele conditions a colorless kernel phenotype with colored clonal sectors due to excision of the resident *dSpm/I* insertion (McCLINTOCK 1967). However, in the absence of an autonomous *Spm/En* transposon, both this colorless phenotype and excision are suppressed such that the *a1-m1* allele conditions a uniform pale kernel phenotype. *Ac/Ds* and *Mu* transposon families are also subject to similar phenomena (McCLINTOCK 1964; MARTIENSSEN *et al.* 1989). However, the mechanisms underlining these phenomena are not well understood.

The loss of a *Mu*-induced allele's capacity to condition a mutant phenotype is termed *Mu* suppression. *Mu* suppression was first reported at the *hcf106::Mu1* mutant allele, which has

a *Mu1* insertion in its 5' untranslated region (UTR) (MARTIENSSEN *et al.* 1989). In the presence of active *MuDR* transposons, this allele conditions a pale-green seedling. However, in the absence of *MuDR*, the *hcf106::Mu1* allele conditions a non-mutant phenotype (MARTIENSSEN *et al.* 1989; MARTIENSSEN *et al.* 1990). In this suppressed state, alternative transcription initiation sites are used to generate functional *hcf106* transcripts that are not present in plants that carry active *MuDR*. These alternative transcription initiation sites are in the 5' terminal inverted repeat (TIR) of *Mu1* and regions of the *hcf106* gene's 5' UTR that are 3' of the *Mu1* insertion site (BARKAN and MARTIENSSEN 1991).

Mu suppression has also been observed in several other *Mu*-induced mutants. Two suppressible *Knotted1* (*Kn1*) alleles arose via *Mu1* and *Mu8* insertions in the junction region of the *Kn1-0* repeats. This junction region contains the promoter region of the downstream copy of *Kn1-0* (LOWE *et al.* 1992). Two other suppressible *Kn1* alleles, *Kn1-mum2* and *Kn1-mum7*, have *Mu8* and *Mu1* insertions in the third intron of the *Kn1* locus (GREENE *et al.* 1994). *Mu* suppression has also been observed with the *Les22-7* mutant allele, which has a *Mu1* insertion in its 5' UTR (HU *et al.* 1998), and the *a1-mum2* allele, which carries a *Mu1* insertion 81-bp upstream of the transcription initiation site (CHOMET *et al.* 1991). Some *Rs1* and *Lg3* alleles, which have *Mu* insertions in 5' UTRs (*Lg3-Or422*, *Lg3-Or102* and *Lg3-Or331*) or introns (*Lg3-Or211* and *Rs1-Or11*) also exhibit suppression (GIRARD and FREELING 2000). Hence, *Mu* insertions in promoter regions, 5' UTRs and introns can all generate suppressible alleles.

The *hcf106::Mu1* mutant and the genetically unlinked *Mu*-induced suppressible mutant *Les28* exhibit coordinated suppression and reactivation. The suppression of both mutant

phenotypes is well correlated with hyper-methylation of *Mu* transposons throughout the entire genome and also hyper-methylation of the region of the *hcf106* locus flanking the *Mu1* insertion (MARTIENSSEN and BARON 1994). As is true for *hcf106::Mu1* and *Les28, Mu* suppression of the four *Kn1* alleles is correlated with genome-wide hyper-methylation of *Mu* transposons (LOWE *et al.* 1992; GREENE *et al.* 1994). At least two of these *Kn1* alleles (*Kn1-mum2* and *Kn1-mum7*) can be reactivated via crossing to *Mu*-active lines (GREENE *et al.* 1994). Since loss of *Mu* activity is correlated with hyper-methylation of *Mu* transposons throughout the genome (reviewed by CHANDLER and HARDEMAN 1992; BENNETZEN *et al.* 1993), these results strongly suggest that *Mu* suppression is caused by an absence of *Mu* activity (MARTIENSSEN and BARKAN 1994).

Mu suppression has the potential to complicate efforts to clone genes via transposon tagging. This is because a critical step in such a project is to identify the particular *Mu*-containing RFLP or PCR fragment responsible for a *Mu*-induced mutation. This step is generally accomplished by identifying *Mu*-containing DNA fragments that co-segregate with the mutant phenotype through meioses. Because suppressed plants exhibit a wild-type phenotype even though they carry a *Mu* transposon in the target gene, suppression can mask the co-segregation between the mutant phenotype and the *Mu*-containing DNA fragment. *Mu* suppression can also lead to the loss of mutant phenotypes during backcrossing programs that are becoming increasingly important with the adoption of new technologies such as RNA profiling and proteomics.

Mu suppression also impacts technologies, such as TUSC (BENSEN *et al.* 1995) and *Mu* rescue (WALBOT 1999), that are important components of maize functional genomics

projects. Each of these projects utilizes *Mu* transposon sequence as bait to obtain *Mu*-insertion mutants through reverse genetics for functional analysis. This selection strategy does not exclude suppressible mutants, which will be unstable and have the potential to complicate the functional analysis of target genes. This is of a particular concern because *Mu* transposons appear to exhibit a strong preference for insertion within the 5' UTRs of at least some genes (C. R. DIETRICH, M. PACKILA, B. J. NIKOLAU, and P. S. SCHNABLE, unpublished data). On the other hand, *Mu* suppression during somatic development can produce clonal sectors on an unsuppressed background. Such chimeric plants provide a unique environment for analyzing mutants (FOWLER *et al.* 1996).

Therefore, understanding the frequency and mechanisms of *Mu* suppression is critical to the use of *Mu* transposons to understand maize biology. Here we report the identification and characterization of three *Mu* suppressible *rf2* alleles. These characterizations have revealed that *Mu* suppression can occur not only at alleles caused by *Mu* insertions in 5' UTRs via the recruitment of alternative transcription initiation sites as reported previously, but also at alleles caused by *Mu* insertions in 3' UTRs. Suppression of this new class of *Mu*-suppressible alleles occurs via the recruitment of alternative polyadenylation sites within the TIRs of the inserted *Mu* transposon. In addition, these studies establish that insertions of two additional classes of *Mu* transposons can generate suppressible alleles.

Materials and Methods

Alleles of the *rf2* gene

The *rf2* gene is one of the two complementary restorers of T-cytoplasm male sterility (reviewed by SCHNABLE and WISE 1998; WISE *et al.* 1999) and encodes a predicted mitochondrial aldehyde dehydrogenase (CUI *et al.* 1996). Plants that carry T cytoplasm and that are homozygous for mutant alleles of either *rf1* or *rf2* are male sterile. All lines used in this study carry *Rf1* and *Rf2* alleles unless otherwise indicated. The reference allele, *rf2-R213*, is a spontaneous mutant carried by the inbred lines, Wf9 and R213. All other described *rf2* mutant alleles were isolated via transposon tagging experiments (SCHNABLE and WISE 1994). Mutant alleles *rf2-m8110*, *rf2-m8122*, *rf2-m9323*, *rf2-m9390*, *rf2-m9385* and *rf2-m9437* were all obtained from a *Mu*-containing population. The wild-type progenitor of *rf2-m8110* and *rf2-m9390* is *Rf2-Q67*. The progenitor of *rf2-m8122* and *rf2-m9323* is *Rf2-Q66*. The progenitor of *rf2-m9437* is *Rf2-B79* (CUI *et al.* 1996). Each of the *rf2-m* alleles used in these experiments was backcrossed to the inbred line Ky21 for at least three generations. The *rf2-m9385* allele was not included in this study because an adequate number of backcrosses had not been completed. The *rf2-m8904* allele was not included in this study because it was isolated from an *Spm/En* population. The inbred line B73 has the genotype *rf1Rf2*.

Backcrosses of the *rf2-m* alleles

Plants heterozygous for each *rf2-m* allele (*rf2-m/Rf2*) carrying T cytoplasm were crossed as females by the inbred line Ky21. Progeny that carried the *rf2-m* alleles were identified via

DNA gel blot analyses or PCR analyses. The 1.2-kb partial or full-length *rf2* cDNA was used as a hybridization probe against *Eco*RV- (for *rf2-m9437*) or *Hin*dIII- (for the rest of the *rf2-m* alleles) digested genomic DNA in DNA gel blot analyses. Genotypes of plants in families segregating for *rf2-m* alleles were often confirmed via testcrosses: (T) *rf2-R213/rf2-R213* x *rf2-m/Rf2-Ky21* (or *Rf2-Ky21/Rf2-Ky21*). Segregation of male-sterile and male-fertile plants (1:1) in the resulting progeny confirmed the presence of a non-suppressed *rf2-m* allele in a particular male parent.

Male fertility ratings

Phenotypes were scored in the morning during the period of pollen shedding for several days according to the rating system of SCHNABLE and WISE (1994). Plants were scored into four categories: male-fertile (F), full fertile with more than 90% of the anthers exerted; semi-fertile ("F"), less than 90% but more than half of the anthers exerted; semi-sterile ("S"), less than 50% of the anthers exerted (usually only a few percent of anthers exerted); male sterile (S), completely male-sterile with no anthers exerted.

***Rf2* genomic clones**

Two overlapping *rf2*-hybridizing genomic clones were obtained by screening B73 libraries. Both libraries were constructed using the λDASHII (Stratagene, La Jolla, CA) vector and were prepared by PAM CLOSE and JOHN TOSSBERG, respectively. Library screening conditions were as described by XU *et al.* (1997). Phage inserts were subcloned into pBluescript SK or KS (Stratagene) vectors for further analysis or direct sequencing. Some of these fragments were sequenced by utilizing the TN1000 transposon system (Gold

Biotechnology, St. Louis, MO, adapted from STRATHMANN *et al.* 1991). These fragments were subcloned into the pMOB vector and transformed into an *E. coli* host (DPWC) that carries a transposon on the F factor. The transposon can fuse with the F' factor and the target plasmid at random positions and form a cointegrated structure. This cointegrated structure was then transferred to a recipient cell (BW26) via conjugation where it resolves into the F factor and a target plasmid containing a transposon insertion at a random position. Primers corresponding to the ends of the transposon were then used to sequence the region of the plasmid flanking the transposon. Both DNA strands were completely sequenced unless otherwise indicated.

The first clone (rf2-DNA1) was obtained using a 900-bp probe (DD1, see Figure 1C of CUI *et al.* 1996) that includes the last 2 introns (9 and 10) and exons (10 and 11) of the *rf2* gene. An alignment of the sequence of the entire 20072-bp insert of rf2-DNA1 with the full-length *rf2* cDNA (GenBank accession number U43082) revealed that 353 bp from the 5' end of the cDNA clone was not included in clone rf2-DNA1. Hence, another *rf2* genomic clone (rf2-DNA2-65) was isolated from the second B73 genomic library using the full-length *rf2* cDNA as probe. Sequencing and restriction mapping experiments revealed that the two *rf2* genomic clones differ in the region 5' of exon 2 but not in the region defined by exons 2 and 11. Furthermore, data from PCR amplification of B73 genomic DNA using various primer pair combinations and genomic mapping via DNA gel blot analyses indicate that the structure of rf2-DNA2-65, but not of rf2-DNA1, reflects the structure of the *Rf2-B73* allele. Based on these results we believe that clone rf2-DNA1 is chimeric such that although the region 3' of intron 1 is derived from the *rf2* gene, the region 5' of intron 1 is not. Hence, to generate the complete genomic sequence of the *Rf2-B73* allele, 5.2 kb of sequence from the

5' end of clone rf2-DNA2-65 was combined with 12.6 kb of sequence from the 3' end of clone rf2-DNA1 and deposited in GenBank (accession number AF215823).

Mapping transposon insertion sites and identifying *Mu* transposons

The transposon insertion site in the *rf2-m8122* allele was established during the cloning of the *rf2* gene (CUI *et al.* 1996). Genomic restriction mapping was conducted on *rf2-m8110*, *rf2-m9323*, *rf2-m9390*, *rf2-m9437*, and *rf2-m8904* alleles using a variety of restriction enzymes. These DNA gel blots were hybridized with the *rf2*-specific probes: rf2-5m, C4-C6, B461-xq and C1-C2. Using this method, it was possible to map the *Mu* insertions in four of the five alleles analyzed (*rf2-m8110*, *rf2-m9390* and *rf2-m9437*, *rf2-m8904*) to specific regions of the *rf2* gene.

PCR reactions were also conducted on DNA from plants homozygous for each of the *rf2-m* alleles to map and identify *Mu* transposons. Each PCR reaction included a *Mu*-TIR primer and one of many *rf2*-specific primers. As expected, most PCR reactions did not yield *rf2*-specific products. After some of the transposon insertion sites were mapped via genomic restriction mapping, appropriate *rf2*-specific primers were used (RF2C6 for *rf2-m9390* and *rf2-m9437*, RF2C1 for *rf2-m8110*) to amplify these *rf2-m* alleles (Figure 1). In these instances the transposon insertion sites were physically mapped via sequence comparisons between the resulting PCR products and the sequence of the *rf2* gene (GenBank accession number AF215823). The junction between the *rf2* and *Mu* TIR sequences in these PCR products defines the *Mu* insertion site. The transposon insertion in the *rf2-m8904* allele was identified by PCR amplification using primers rf2a-3320 and RF2C5UTRR, which flank the

transposon insertion. The identity of the transposon was revealed by sequence comparison between this transposon and the *Ds1* transposon in GenBank (GenBank accession number: AF010445).

Since the TIRs of each class of *Mu* transposon contain diagnostic polymorphisms, it was possible to determine the identities of the *Mu* transposons inserted in *rf2-m* alleles by comparing the *Mu*-TIR sequence contained in the allele-specific PCR products to the TIRs of all known *Mu* transposons. In addition, since the sequences of the two TIRs of most *Mu* transposons have one or more polymorphisms relative to each other, the orientations of the *Mu* insertions in *rf2-m* alleles could also be determined.

To confirm the identity of the transposon inserted in the *rf2-m9390* allele, genomic DNA samples from plants that were homozygous for *rf2-m9390* and its progenitor Q67 were digested with *Eco*RV, *Hin*dIII, *Xba*I, *Eco*RV + *Hin*dIII, *Eco*RV + *Xba*I and *Hin*dIII + *Xba*I and then hybridized with the *rf2*-specific probe, rf2-5m. The same filter was stripped (AUSUBEL *et al.* 1999) and hybridized with a *Mu1*-specific probe. In each restriction digest the *rf2*-hybridizing fragments were the same size as *Mu1*-hybridizing fragments, which provided further support for the view that the transposon inserted in *rf2-m9390* is *Mu1*. The identity of the *rcy:Mu7* transposon in *rf2-m8110* was confirmed similarly with *rf2*-specific probe C1-C2 and a *rcy:Mu7*-specific probe. To further confirm the identity and orientation of the *rcy:Mu7* transposon insertion in *rf2-m8110*, an *rf2*-specific primer, RF2C2, which is about 0.1-kb 3' of the *rcy:Mu7* insertion site in this allele, and an *rcy:Mu7* internal primer, Mu7-R, were used to amplify a 1.7-kb fragment from the 5' end (i.e., the right-most end in Figure 1) of the *rcy:Mu7* transposon in *rf2-m8110*. This PCR product was subcloned into a pGEM-T vector (Promega, Madison, WI) and over 80% of this fragment

was sequenced. Sequence comparisons between this PCR product and *rcy:Mu7* (Genbank accession number X15872) revealed only a few nucleotide polymorphisms.

Genotyping *rf2-m* alleles via PCR

To determine which plants in a segregating family carry an *rf2-m* allele, PCR amplifications were conducted using a *Mu*-TIR primer in combination with an appropriate *rf2*-specific primer. Various primers that anneal to *Mu*-TIRs, such as XX153, were used in these PCR reactions. The *rf2*-specific primers used for genotyping *rf2-m* alleles include RF2C1 (for *rf2-m8110* and *rf2-m8122*) and RF2C6 (for *rf2-m9390* and *rf2-m9437*) (Figure 1). PCR reactions were performed for 34 cycles under the following conditions: denature at 94° for 40 seconds; anneal primers for 40 seconds at 55°-58° (depends upon the Mu-TIR primer used); extend at 72° for 2 minutes at the presence of 2.5 units of Taq polymerase (Promega) per reaction.

Primer sequences

Mu7-R: $^{5'}$TTCTCCGCCGTTGCCATCTC$^{3'}$

RF2C1: $^{5'}$GCGTCGTTGGTGATCCGTTC$^{3'}$

RF2C2: $^{5'}$CCAGGCTAGGGCAAATCTTAT$^{3'}$

RF2C4: $^{5'}$AGCGGGAGACGAGCGAGGAC$^{3'}$

RF2C5: $^{5'}$ATGCTGCGATTCCGTTTGGTG$^{3'}$

RF2C6: $^{5'}$TCCTCACTCCCACACCAACC$^{3'}$

RF2C8: $^{5'}$GCAGCAGGAGAAGCGGCAGGCAG$^{3'}$

RF2C9: $^{5'}$GTGATGGGCTCCTCTACT$^{3'}$

XX153: $^{5'}$CGCCTCCATTTCGTCGAATCC$^{3'}$

rf2-B461: $^{5'}$ACAGATCTAAAGCTCCTCATTAAT$^{3'}$

rf2-xq: $^{5'}$CCAACTTTCCAGGCATACATCA$^{3'}$

rf2a-3320: $^{5'}$GAGGAACCAGTAGCGGAGGC$^{3'}$

RF2C5UTRR: $^{5'}$GCTCCCGTTCGCAGTCG$^{3'}$

DNA and RNA gel blot analyses

Maize genomic DNA was isolated using a 1X CTAB procedure (SAGHAI-MAROOF *et al.* 1984). About 10 μg of DNA was digested with the indicated restricted enzyme in a 30 μl reaction volume for more than 3 hours and then separated via electrophoresis through a 0.8% agarose gel. DNA was transferred to nylon filters (MSI, Westboro, MA) and hybridized with probes labeled with dCTP^{32} (AUSUBEL *et al.* 1999).

Total RNA from immature tassels (still in the whorl) was isolated according to DEAN *et al.* (1985). Approximately 10 μg of total RNA was subjected to electrophoresis using a MOPS buffer system (AUSUBEL *et al.* 1999) and transferred onto GeneScreen filters (NEN Research Products Inc., Boston, MA). The filters were hybridized with probes labeled with dCTP^{32} (AUSUBEL *et al.* 1999).

Probes

DNA fragments used as probes in this study were obtained as follows. The 2.2-kb full-length *rf2* cDNA fragment was obtained from plasmid prf273-11 with the restriction

enzymes *Xho*I and *Eco*RI. The 1.2-kb partial *rf2* cDNA was obtained from plasmid prf2a-1.2 with the restriction enzyme *Eco*RI. Plasmids prf273-11 and prf2a-1.2 contain the 1.2-kb and 2.2-kb *rf2* cDNAs as described in CUI *et al.* (1996). The *rf2* 5' 0.15-kb probe, rf2-5m, was PCR-amplified from plasmid prf273-11 using primers RF2C6 and RF2C8 (Figure 1). Another *rf2* 5' probe, C4-C6, was PCR-amplified from plasmid prf273-11 using primers RF2C4 and RF2C6. Probes B461-xq (from 461 to 927 bp in GenBank U43082) and C1-C2 (from 1374 to 2029 bp in GenBank U43082) were PCR-amplified from plasmid prf273-11 using primers rf2-B461 and rf2-xq or primers RF2C1 and RF2C2 (Figure 1). A 0.96-kb *Mu1*-specific fragment was isolated from plasmid pRB1 (ROBERTSON *et al.* 1988) using the restriction enzyme *Mlu*I. The 0.16-kb *rcy:Mu7* probe was isolated from plasmid pSB9-in (SCHNABLE *et al.* 1989) using restriction enzymes *Bam*HI and *Eco*RI. Maize GAPDH cDNA (GenBank accession number X07156) was isolated from pGAPDH with the restriction enzymes *Eco*RI and *Hin*dIII. All probes were labeled with $dCTP^{32}$ using a random primer labeling protocol (AUSUBEL *et al.* 1999).

3' and 5' RACE (Rapid Amplification of cDNA Ends)

RNA was isolated from immature tassels (still in the whorl) using the Trizol reagent (GIBCO BRL, Rockville, MD) and treated with PCR-grade DNaseI (GIBCO BRL) according to the manufacture's instructions. Five µg and 100 ng of RNA were used for 3' and 5' RACE experiments using kits provided by GIBCO BRL. The *rf2*-specific primers RF2C5 and RF2C9 (Figure 1) were used for 3' and 5' RACE, respectively. RF2C9 was positioned in exon 2 so that inadvertent amplification of genomic DNA could be detected. Primer RF2C4was used as a nested primer for the 5' RACE experiments. RACE products

were subcloned into the pGEM-T vector (Promega) and transformed into the *E. coli* strain DH5α. Colonies were lifted onto nylon filters (MSI) and hybridized with the full-length *rf2* cDNA. Plasmid DNAs from positive clones were extracted using an alkaline lysis miniprep protocol (AUSUBEL *et al.* 1999) and then sequenced.

Sequencing

DNA sequencing was performed at the Iowa State University DNA Sequencing and Synthesis Facility on an automated sequencer (ABI 373A, Applied Biosystems). Sequence assembly and analyses were performed using the Wisconsin GCG software package Version 10.0-UNIX from the Genetics Computer Group, Inc.

Analysis of polyadenylation sites

All GenBank records for which the organism was *Zea mays* (excluding chloroplast and mitochondrial genes), that had the feature of "polyA_site" were downloaded on March 22nd, 2000. This data set was then parsed for the feature of polyadenylation site. The few records that lacked sequence data downstream of the reported polyA site or that had only "A" bases downstream of this site were excluded. Only the most recent GenBank submission was used for multiple submissions of the same sequence. χ^2 homogeneity tests were performed according to STEEL and TORRIE (1980).

Results

Unusual observations in families segregating for *rf2-m8110* and *rf2-m9390*

Seven independent *rf2* mutant alleles (*rf2-m*) were obtained via transposon tagging in a previous investigation (SCHNABLE and WISE, 1994). Six of these were derived from *Mu* tagging populations and one from an *Spm/En* tagging population. As expected, testcross progenies of plants heterozygous for these tagged alleles, (T) *rf2-m/Rf2* x *rf2-R213/rf2-R213*, segregated for male-fertile and male-sterile plants. However, in one family (92 2123) segregating for the *rf2-m8110* allele the ratio of male-fertile to male-sterile plants was significantly higher than the expected 1:1. In this family, only four out of 26 plants exhibited complete male sterility (Table 1), a ratio that is significantly different from the expected 1:1. In contrast, the corresponding ratio in a related family (92 2124) that was also segregating for *rf2-m8110* was not significantly different from the expected ratio.

Aberrant phenotypic ratios were also observed in a family (92 2148) segregating for the *rf2-m9390* allele (Table 2). Because at the time these studies were conducted an *rf2* probe was not available, plants were genotyped with a probe derived from the *wx1* gene which is genetically linked to *rf2*. Based on this RFLP analysis, two of the five fully male-fertile plants in this family were predicted to have the genotype *rf2-m9390/rf2-R213* (Table 2). These could have arisen via crossovers between the *wx1* and the *rf2* genes (if so, their actual genotype would have been *Rf2/rf2-R213*), but the ratio of 2/5 is high relative to the 8.3 cM that exists between the *rf2* and *wx1* genes (SNYDER and DUVICK 1969; WISE and

SCHNABLE 1994). However, in the absence of a *rf2* clone, it was not possible to more precisely determine the genotypes of these exceptional male-fertile plants.

Structure of the *rf2* gene

More recently the *rf2* gene was cloned. The *rf2* cDNA is about 2 kb in length and encodes a predicted mitochondrial aldehyde dehydrogenase (CUI *et al.* 1996). Two overlapping genomic clones (rf2-DNA1 and rf2-DNA2-65) were obtained by screening B73 genomic libraries (MATERIALS AND METHODS). Sequence comparisons of 17.8-kb derived from these genomic clones (GenBank accession number AF215823) and the full-length *rf2* cDNA clone (GenBank accession number U43082) defined 11 exons and 10 introns (Figure 1). The extreme 5' end of the genomic sequence (base positions 102 to 740) is 81.5% and 80.7% identical to the 3' long terminal repeat (LTR) (GenBank accession number AF050449) and the 5' LTR (GenBank accession number U68407) of the maize Milt retrotransposon. In addition, a member of a newly defined class of retrotransposons, *DON QUIXOTE*, that is present in intron 5 (base positions 6763 to 13927 of GenBank accession number AF215823) contains a characteristic nucleic acid binding site, which serves as the primer site for reverse transcription, and an uninterrupted ORF of about 4 kb (positions 8335 to 12129) that encodes predicted proteins with high degrees of sequence similarity to the reverse transcriptase, protease, integrase, and endonuclease typical of copia-like retrotransposons (KONIECZNY *et al.* 1991). Two other regions of the *rf2* gene (base positions 2065 to 3096, 5' of the transcription initiation site and positions 4875 to 5270 in intron 1) exhibit about 88% and 85% sequence similarity, respectively, to the non-coding

regions of various maize genes (GenBank accession numbers X06333, L40803, AF030385, AF031569, AF041044; and AJ005343, Z22760, AF043346, Z26824, AJ223471). However, these regions of sequence similarity have not been assigned any putative functions and do not exhibit characteristics of DNA transposons or retrotransposons. A 0.6 kb region that is about 140 bp 5' of exon 2 in rf2-DNA2-65 exhibits 91% sequence identity to the LTR of Grande1-4 retrotransposon (GenBank accession number X97604).

Positions of transposons in *rf2-m* alleles

The positions of transposon insertions responsible for four of the five *Mu* -tagged *rf2-m* alleles (*rf2-m8110*, *rf2-m8122*, *rf2-m9390*, and *rf2-m9437*) were mapped via genomic restriction mapping and sequence comparisons between PCR products obtained using *rf2-m* DNA templates in conjunction with *Mu*-TIR- and *rf2*-specific primer pairs and the sequence of the *rf2* gene. The specific class of *Mu* transposon responsible for each mutant and its orientation were determined via sequence analysis of the *Mu* TIRs obtained from these PCR products. The *rf2-m9390* allele has a *Mu1* transposon inserted in its 5' UTR, 105-bp 5' of the translation start codon. The orientation of this *Mu1* transposon is 3' to 5' relative to the *rf2* gene. The identity of this *Mu1* transposon was confirmed by DNA gel blot analysis (MATERIALS AND METHODS). The *rf2-m9437* allele contains a novel *Mu* transposon insertion in its 5' UTR, 35-bp 5' of the translation start codon. The TIR of this transposon differs from those of all other described *Mu* transposons. Therefore, this *Mu* transposon has been designated *Mu10* (GenBank accession number AF231940). The *rf2-m8904* allele contains a *Ds1* transposon a few base pairs down stream of the translation start codon. This

395-bp *Ds1* has three single nucleotide polymorphisms with the GenBank record (GenBank accession number: AF010445). The *rf2-m8110* allele arose via an *rcy:Mu7* insertion in the 3' UTR, 30-bp 3' of the translation stop codon. The identity of this *rcy:Mu7* transposon was confirmed by sequence analysis of a 1.7-kb fragment of it and DNA gel blot analyses. This transposon is inserted 3' to 5' relative to the *rf2* gene (Figure 1). The *rf2-m8122* allele is the only allele in this collection that has a transposon insertion (*Mu1*) within the coding region (9^{th} exon) (CUI *et al.* 1996). This transposon is inserted 5' to 3' relative to the *rf2* gene. It has not yet been possible to identify the molecular lesions associated with the *rf2-m9323* and *rf2-m9385* alleles.

Reanalysis of data from SCHNABLE and WISE, 1994

After the *rf2* gene was cloned and the positions of the *Mu* insertions responsible for many of the *rf2-m* alleles determined, genomic DNA samples from plants presented in Tables 1 and 2 were regenotyped via PCR (MATERIALS AND METHODS). The results of these analyses are presented in Table 3. Families segregating for *rf2-m8110* (92 2123) and *rf2-m9390* (92 2148) contain three and six male-fertile plants with the genotype of *rf2-m/rf2-R213*, respectively. Hence, these two alleles display 70% and 40% penetrance, respectively in these families. In contrast, a similar family but segregating for the *rf2-m8122* allele, which has a *Mu1* insertion in the coding region, exhibited 100% penetrance (family 92 2126 in Table 3). Another allele, *rf2-m9437* (family 92 2153), with a *Mu10* insertion in the 5' UTR, also exhibited 100% penetrance in this generation. However, after three generations of

backcrossing to the inbred line Ky21, this allele also began to show evidence of *Mu* suppression (data not shown).

Reactivation of suppressible *rf2-m* alleles

The above genotyping established that neither a high rate of crossing over nor *Mu* excision is responsible for the aberrant ratios observed in the previous analysis of SCHNABLE and WISE (1994). Instead, the loss of these alleles' capacity to condition mutant phenotypes without excisional loss of their associated *Mu* transposons could be due to *Mu* suppression. Since reactivation is one of the hallmarks of *Mu* suppression, crosses were conducted to determine whether the incomplete penetrance of *rf2-m8110* and *rf2-m9390* could be reversed. Various rates of male-sterile (i.e., reactivated) progeny were obtained when *Mu*-active lines were crossed to suppressed plants carrying either *rf2-m8110* or *rf2-m9390* (Table 4). As a control, some suppressed (i.e., male-fertile) plants that contain these two alleles were self-pollinated. No male-sterile (i.e., reactivated) plants appeared among the resulting progenies (96g 6104-05 and 98 6336 in Table 4).

The stability of the reactivation of *rf2-m8110* was tested by crossing a reactivated heterozygous plant, (T) *rf2-m8110/rf2-R213*, by (N) *rf2-m8904/rf2-m8904*. The *rf2-m8904* allele was used for this cross instead of *rf2-R213* because unlike *rf2-R213* it does not accumulate a detectable amount of *rf2* mRNA (CUI *et al.* 1996). About one hundred of the resulting progeny were scored for male fertility (data not shown). Most were male sterile. Seven of 16 random male-sterile plants carried the *rf2-m8110* allele. Hence, *rf2-m8110* can be transmitted through meiosis in the reactivated state.

Due to the early suppression of the *rf2-m9390* allele during backcrossing, unsuppressed plants homozygous for *rf2-m9390* were not initially available for mRNA accumulation analyses. To generate unsuppressed stocks homozygous for this allele, some original unsuppressed heterozygous plants, (T) *rf2-m9390/rf2-R213*, were crossed by suppressed (i.e., male fertile) plants with the genotype (T) *rf2-m9390/rf2-m9390*. About three hundred progeny were screened for male-sterile (i.e., unsuppressed) plants. Only 19 were obtained. When these 19 plants were genotyped, it was found that they all had the genotype *rf2-m9390/rf2-R213*, i.e., no male-sterile *rf2-m9390* homozygous plants were obtained. The reason for this unbalanced result is not known, but perhaps plants that carry two doses of *rf2-m9390* require higher levels of *Mu* activity to maintain the unsuppressed (i.e., male sterile) state.

Accumulation of *rf2* mRNA in suppressed *rf2-m* plants

Prior RNA gel blot analysis identified a plant homozygous for *rf2-m9390* that accumulated *rf2* mRNA at the same level as wild-type plants (CUI *et al.* 1996). Since the entire young tassel of this plant had been collected for RNA in that analysis, the male fertility status of this plant could not be determined. To overcome this problem in subsequent experiments, only a few branches of each young tassel were collected from plants homozygous for the *rf2-m9390* or *rf2-m8110* alleles. An RNA gel blot analysis of these individuals is shown in Figure 2. Hybridization with a full-length *rf2* cDNA detected an mRNA that accumulated to the same or only slightly lower levels in fertile plants (i.e., suppressed) that were homozygous for either *rf2-m8110* or *rf2-m9390* as accumulated in the

wild-type controls. In addition, these mRNAs were indistinguishable in size from those that accumulated in the wild-type controls.

Native transcription initiation sites are not used in suppressed *rf2-m9390* plants

Because the *rf2-m9390* allele contains a *Mu1* insertion in its 5' UTR, the *rf2* transcripts that accumulate in the suppressed *rf2-m9390* plants (Figure 2) could be derived from alternative transcription initiation sites downstream of the native sites (i.e., in the *Mu1* and/or its flanking region) as has been reported in the case of *hcf106::Mu1* (BARKAN and MARTIENSSEN 1991). Alternatively, these transcripts could arise via read-through transcription of the *Mu1* transposon followed by the splicing of the *Mu1* from the transcripts. To distinguish between these two possibilities, a probe (rf2-5m) upstream of the *Mu1* transposon (Figure 1) was hybridized to RNA from suppressed plants homozygous for *rf2-m9390*. The results of this experiment are shown in Figure 3. Because *rf2-m9390* transcripts could not be detected with the rf2-5m probe (Figure 3, panel B), it can be concluded that transcription initiation in suppressed *rf2-m9390* does not occur from the native *rf2* transcription initiation sites. Instead, transcription of this allele must initiate downstream of the position of probe rf2-5m (Figure 1), likely from the 5' TIR (i.e., the right-most TIR in Figure 1) of *Mu1* and/or an *rf2* flanking region.

Transcription initiation sites in *rf2-m9390*

Initially 5' RACE experiments were conducted on RNA extracted from the inbred line Q67, which is homozygous for the wild-type progenitor of *rf2-m9390* (CUI *et al.* 1996). The

primer (RF2C9) used for the first strand synthesis was located at position +182 relative to the start of translation; the nested primer (RF2C4) at position +37. DNA gel blot analysis revealed that the resulting RACE products were approximately 290 bp in size, a result that is consistent with the size of the longest *rf2* cDNA clone isolated to date (prf273-11) which begins at position –253.

Cloned 5' RACE products obtained using RNA extracted from a plant homozygous for suppressed *rf2-m9390* were considerably smaller than those obtained from the inbred line Q67. Sequence analysis of nine of the RACE products from *rf2-m9390* revealed multiple transcription initiation sites, all of which were located between the position of the *Mu1* insertion (-105) and the translation start codon (Figure 4).

Alternative polyadenylation sites in the TIR of *rcy:Mu7* are used during suppression of *rf2-m8110*

The *rf2-m8110* allele contains an *rcy:Mu7* insertion in its 3' UTR. As it is true for *rf2-m9390*, suppressed plants homozygous for *rf2-m8110* accumulate *rf2* mRNA that is indistinguishable from wild-type via RNA gel blot analyses (Figure 2). Based on the analysis of cDNA clones, two *Rf2* alleles (*Rf2-B73* and *Rf2-W22*) use polyadenylation sites over 140-bp 3' of the site of the *rcy:Mu7* insertion in the *rf2-m8110* allele (Figure 5). In addition, 3' RACE experiments have established that this is also true for the *Rf2-Q67* allele, which is the wild-type progenitor of *rf2-m8110* (Figure 5). These results indicate that either the *rf2-m8110* allele uses the native polyadenylation sites but that the *rcy:Mu7* transposon is subsequently spliced out or that this allele uses alternative polyadenylation sites. 3' RACE

was used to identify the actual polyadenylation sites used by *rf2-m8110* and to thereby distinguish between these two possibilities. As shown in Figure 5, five alternative polyadenylation sites were detected in two independent 3' RACE experiments. Some sites were recovered in both experiments. All identified sites are within the 3' TIR (i.e., left-most TIR in Figure 5) of the *rcy:Mu7* transposon insertion in *rf2-m8110*.

Polyadenylation sites are preferentially located at the 3' end of a YA (i.e., UA, CA, or GA) sequence in at least some eukaryotes (reviewed by ROTHNIE 1996; WAHLE and RUEGSEGGER 1999). To determine whether this pattern holds for maize, the polyadenylation sties associated with *Zea mays* records in GenBank were examined. Fifty-eight records with a total of 94 polyadenylation sites were obtained. Of these 94 sites, 73 fit the YA rule (Table 5). Similarly, six of the seven polyadenylation sites within the 3' UTR of the *rf2* gene are YA. In contrast, only two out of the five alternative polyadenylation sites within *rcy:Mu7* (GA, GA, UC, AC and CC) fit this pattern. However, a χ^2 homogeneity test (χ^2 =3.67) revealed that the rate of YA polyadenylation sites in *rcy:Mu7* is not significantly different at the 95% confidence level from that in other maize genes.

Methylation and *Mu* suppression of *rf2-m* alleles

The correlation between the methylation of *Mu* TIRs and *Mu* activity has been well established (reviewed by BENNETZEN 1996). In all previously reported studies of *Mu* suppression, hyper-methylation of *Mu* transposons throughout the genome was generally well correlated with *Mu* suppression, although a few exceptions were found in some studies (MARTIENSSEN *et al.* 1990; LOWE *et al.* 1992). In the current study, methylation status

was determined by the hybridization of a *Mu1*-specific probe (Figure 6, panel C) to *Hin*fI-digested genomic DNA (CHANDLER and WALBOT 1986). In this analysis, *Mu1*-hybridizing fragments larger than 1.34-kb (except for the 1.7-kb *Mu2*-related fragment) are derived from methylated *Mu1* transposons (Figure 6, panel A). In contrast to previous reports, only minimal correlation was found between the suppression of *rf2-m9390* and the hyper-methylation of other *Mu* transposons throughout the genome. For example, although 17 suppressed plants (male-fertile (F), semi-fertile ("F") and semi-sterile ("S")) carried methylated *Mu1* transposons, five carried hypo-methylated *Mu1* transposons (Table 6). Similarly, although four nonsuppressed (i.e., male sterile) plants carried hypo-methylated *Mu1* transposons, two carried methylated *Mu1* transposons (Figure 6 and Table 6).

MARTIENSSEN *et al.* (1990) reported that suppression is also correlated with hyper-methylation of the *Mu1* transposon inserted in the *hcf106::Mu1* allele. To detect the methylation status of the *Mu1* insertion in *rf2-m9390*, an *rf2* probe (rf2-5m), was hybridized to *Hin*fI-digested genomic DNA from suppressed and unsuppressed plants. This probe hybridizes to a 1.1-kb fragment bounded by the *Hin*fI site 5' of the probe in the *rf2* promoter region and the *Hin*fI site in the 3' end (i.e., left-most end in figure 6) of the *Mu1* transposon. The methylation status of the *Mu1* inserted in *rf2-m9390* was scored by determining the signal strength of the 1.1-kb *rf2*-hybridizing fragment relative to the 2.4-kb and 2.8-kb *rf2*-hybridizing fragments. If the 3' *Hin*fI site in the *Mu1* transposon is susceptible to *Hin*fI digestion (i.e., it is unmethylated), a 1.1-kb *rf2*-hybridizing fragment will be detected (e.g., see the right-most four lanes of category S in Panel B of Figure 6). If this site is not susceptible to *Hin*fI digestion (i.e., it is methylated), either the 2.4-kb (the 5' *Hin*fI site in the *Mu1* transposon is digested) or the 2.8-kb (neither of the two *Hin*fI sites in the *Mu1*

transposon is digested) *rf2*-hybridizing fragment will be detected (e.g., see the "F" and "S" category in Panel B of Figure 6). Table 7 reveals that there is little correlation between suppression and methylation of the *Mu1* transposon in *rf2-m9390*. However, a strong correlation was observed between the methylation status of the *Mu1* transposon in *rf2-m9390* and the methylation status of other *Mu1* transposons in the genome (Compare panels A and B in Figure 6).

Discussion

Mu suppression occurs at a high frequency

Mu transposons are widely used for the functional analysis of the maize genome, including gene tagging, gene discovery and reverse genetics. It has been known for over a decade that even in the absence of gross changes in their DNA sequences, some *Mu*-insertion alleles lose the capacity to condition a mutant phenotype (MARTIENSSEN *et al.* 1989) in the absence of *Mu* activity. This phenomenon, *Mu* suppression, has important implications for the use of *Mu* transposons to understand maize biology.

Although enough suppressible alleles have been identified to demonstrate that this is a widespread phenomenon, the proportion of *Mu*-insertion alleles that are susceptible to suppression has not been well established. In this study a collection of five *Mu*-induced *rf2* mutant alleles originally obtained via a phenotypic screen was backcrossed to a non-*Mu* inbred line (Ky21) for at least three generations. By the end of this program three of the five *Mu*-insertion alleles exhibited evidence of suppression. Hence, it is clear that suppressible alleles arise frequently enough that they can seriously impact the outcome of genetic

experiments. In retrospect, suppression probably accounts for our lack of success in identifying a *Mu*-containing DNA fragment that co-segregated with any of the five *Mu*-induced *rf2* alleles except *rf2-m8122* (CUI *et al.* 1996). An even greater proportion of suppressible alleles might exist in a collection of alleles derived from reverse genetic screens, because such alleles would not have been prescreened via phenotypic selection as was true for this collection of *rf2-m* alleles.

It has previously been established that the insertion of *Mu* transposons into promoter regions, 5' UTRs and introns can generate suppressible alleles. By determining the structure of the *Rf2-B73* allele and the insertion sites of the *Mu* transposons responsible for four of five *rf2-m* alleles, this study not only identified two suppressible alleles with *Mu* insertions in the 5' UTR of the *rf2* gene (*rf2-m9390* and *rf2-m9437*), but also for the first time demonstrated that a *Mu* insertion into a 3' UTR can result in a suppressible allele (*rf2-m8110*). Only the apparently non-suppressible *rf2-m8122* allele arose via a *Mu* insertion in an exon.

The *Rf2-B73* allele spans over 17-kb (Figure 1) and contains many small exons and introns as well as two large introns (the largest of which is over 7-kb). It is worth noting that if a reverse genetic screen that depends upon PCR-based detection of *Mu* insertions (BENSEN *et al.* 1995) were to be conducted on the *rf2* gene, it is likely that most of the *rf2-m* alleles described in this report would have been missed. This is because as a result of the presence of two large introns, only *rf2* primers from a small portion of the gene can amplify the *rf2-m* alleles. For example, *Mu*- and *rf2*-specific (such as RF2C6, Figure 1) primers from the 5' end of the *rf2* gene fail to amplify DNA templates from plants that carry *rf2-m8122* or *rf2-m8110* (data not shown). Similarly, under all PCR conditions, *Mu* and *rf2* primers from the 3' end of the gene fail to amplify DNA from plants that carry *rf2-m9390* and *rf2-m9437*.

Instead, such a reverse genetic screen would most likely identify *Mu* insertions in introns that would be unlikely to confer a mutant phenotype. These results point to the importance of having a gene structure available before performing reverse genetics and/or using a large number of primer pairs when conducting reverse genetic screens in species such as maize that often have large introns.

Suppressible alleles described previously arose via the insertion of a variety of *Mu* transposons: *Mu1*, *Mu3*, *Mu8* and *MuDR* deletion derivatives (BARKAN and MARTIENSSEN 1991; LOWE *et al.* 1992; GREENE *et al.* 1994; HU *et al.* 1998; GIRARD and FREELING 2000). Three *rf2-m* suppressible alleles, *rf2-m9390*, *rf2-m8110* and *rf2-m9437*, are *Mu1*-, *rcy:Mu7*- and *Mu10*-induced, respectively. These results indicate that insertions of at least six different classes of *Mu* transposons can generate suppressible alleles.

_Mu_ suppression occurs to alleles that have a _Mu_ insertion in the 5' UTR

Three mutant alleles that arose via *Mu* transposon insertions in 5' UTRs recruit alternative transcription initiation sites during suppression. The *hcf106::Mu1*, *Lg3-Or422* and *rf2-m9390* alleles have *Mu1*, *Mu3* and *Mu1* insertions at positions -34 (BARKAN and MARTIENSSEN 1991), -238 (GIRARD and FREELING 2000), and –105 relative to the presumed translation start codons, respectively. The alternative transcription sites recruited during suppression of *hcf106::Mu1* and *rf2-m9390* exhibit a significant difference in relation to their *Mu1* insertions. In the suppressed *hcf106::Mu1* allele, alternative transcription sites are recruited from both the downstream TIR of the inserted *Mu1* transposon and the region of the 5' UTR that is 3' of this *Mu1* insertion. In contrast, all of the transcription initiation sites

recruited during suppression of *rf2-m9390* are located 3' of the *Mu1* insertion, i.e., there is no evidence that this allele recruits transcription initiation sites from within *Mu1*. This difference is not due to the orientation of the transposons; the *Mu1* transposons responsible for the *hcf106::Mu1* allele and the *rf2-m9390* allele are inserted in the same relative orientation. However, the positions of all these alternative transcription initiation sites are similar relative to the presumed translation start sites; *hcf106::Mu1* uses positions -7 to -80 and *rf2-m9390* uses positions -6 to -91. This observation suggests that there may be a downstream *cis*-acting signal which interacts with the promoter to determine the locations of transcription initiation sites.

The *rf2-m9437* allele also arose via a *Mu* insertion in the 5' UTR. Unlike *rf2-m9390* which exhibited evidence of suppression very early in the backcrossing program, *rf2-m9437* did not begin to exhibit evidence of suppression until after three generations of backcrossing to the inbred line Ky21 (Table 3 and data not shown). Interestingly, the position of the *Mu10* insertion responsible for *rf2-m9437* (base pair -35 relative to the presumed translation start codon) precludes the use of all but one of the alternative transcription initiation sites used by *rf2-m9390.*

_Mu_ suppression affects alleles that have _Mu_ insertions in their 3' UTRs

Analysis of *rf2-m8110* revealed a novel mechanism of *Mu* suppression. This allele has an *rcy:Mu7* transposon insertion 30-bp downstream of the stop codon in the 3' UTR. Sequence analysis of cloned 3' RACE products revealed that during suppression the *rf2-m8110* allele recruits novel polyadenylation sites from within the TIR of the *rcy:Mu7*

transposon. This is the first report that *rcy:Mu7* contains polyadenylation sites. Because the TIRs of the 10 classes of *Mu* transposons are well conserved, analysis of the *rf2-m8110* allele suggest that the recruitment of alternative polyadenylation sites might be a general mechanism by which mutants containing other classes of *Mu* insertions in their 3' UTRs could be suppressed.

Polyadenylation sites in *Mu1* were identified previously following the analysis of truncated transcripts produced by the *adh1-s3034* allele, which contains a *Mu1* insertion in its first intron (ORTIZ and STROMMER 1990). However, these alternative polyadenylation sites differ from those in the current report in that they are located in the central (i.e., non-TIR) region and the 3' TIR of the *Mu1* transposon.

In eukaryotes, genetic information is first transcribed from DNA into RNA, one of which is hnRNA, in the nuclear during gene expression. The hnRNA is then processed into messenger RNA (mRNA) by adding a 7-methyl guanosine cap to its 5' end, splicing out its introns and polyadenylating its 3' end. Polyadenylation occurs following the cleavage of the hnRNA, producing a 3' –OH, to which are added multiple adenines. The positions at which cleavage, and hence polyadenylation, occur are controlled by cis-acting elements that are usually located between the stop codon and the cleavage site. In mammals, the polyadenylation signals consist of the AAUAAA positioning element (PE) and the U- or UG-rich downstream element (DE) (Figure 7, ZHAO *et al.* 1999; WAHLE and RUEGSEGGER 1999). Plant and yeast genes contain AAUAAA-like PEs and U- or UG-rich upstream elements (UEs), which resemble the DEs of mammals (reviewed by WAHLE and RUEGSEGGER 1999; ROTHNIE 1996; HUNT and MESSING 1998). In addition, the

polyadenylation sites of rice and Arabidopsis genes are often located in U-rich regions (GRABER *et al.* 1999).

Seven polyadenylation sites were detected in *Rf2* alleles (VI to XII in Figure 5). Each of these sites is 20-50 bases downstream of an AAUAAA-like PE and in the vicinity of a U-rich flanking region (each approximately 50% U). No obvious UE was detected in the *rf2* gene. Similarly, all five polyadenylation sites in the TIR of *rcy:Mu7* (I to V in Figure 5) are located in the vicinity of U-rich regions and 20- to 50-bp downstream of one of the three AAUAAA-like PE elements that exist in this TIR.

The fact that only the TIR polyadenylation sites are used in suppressed *rf2-m8110* plants indicates either that transcription does not proceed through the *rcy:Mu7* transposon to the native polyadenylation sites, or that the TIR sites are preferred over the native sites by the polyadenylation machinery. One hypothesis to explain such a preference would be the presence of as yet unidentified polyadenylation signal upstream of the position of the *rcy:Mu7* insertion. The spatial separation between this upstream signal and the native sites caused by the 2.2-kb *rcy:Mu7* insertion in the *rf2-m8110* allele might cause such an upstream signal to interact more efficiently with the nearby TIR sites than with the native sites.

In vitro and *in vivo* polyadenylation experiments demonstrated that cleavage occurs preferentially at the 3' end of a YA (i.e., UA, CA, or GA) sequence (reviewed by ROTHNIE 1996; WAHLE and RUEGSEGGER 1999). In mammals, this YA consensus was observed in about 70 of 100 polyadenylation sites (SHEETS *et al.* 1990). YA was also found to be the most frequent sequence at the polyadenylation sites in the yeast *cyc1* gene (GUO and

SHERMAN 1995) and several plant genes (WU *et al.* 1995). Our analysis of 94 polyadenylation sites from 58 maize genes confirmed that this rule also holds for maize; 73 out of 94 polyadenylation sites fit the YA pattern (Table 5). In contrast, only two out of five polyadenylation sites in the TIR of the *rcy:Mu7* transposon inserted *in rf2-m8110* follow this rule.

In mammals, the preferred bases at the first position of the YA consensus are C>>U>G, where C accounts about 60% of sites (SHEETS *et al.* 1990). In contrast, our analysis of 94 maize polyadenylation sites showed that UA is most common (45%) while CA and GA account for 34% and 21% respectively (Table 5). Exceptions to the YA rule exist. In mammals, 30% of the polyadenylation sites are non-A sites. The preference is in the order of U>C>>G (SHEETS *et al.* 1990). Our analysis of the 94 maize polyadenylation sites revealed that approximately 22% do not follow the YA rule (Table 5) and the frequencies at which specific non-A bases are used are similar to those in mammals.

_Mu_ suppression and hyper-methylation

It has been reported that there is a strong correlation between hyper-methylation of the TIRs of *Mu* transposons and suppression of *Mu*-induced alleles (MARTIENSSEN *et al.* 1990; MARTIENSSEN and BARON 1994; LOWE *et al.* 1992; GREENE *et al.* 1994). However, the current analysis revealed many exceptions to this relationship (Table 6).

Analyses of *hcf106::Mu1* and *Les28* indicate that suppression progresses acropetally. Hence, the young leaves from which DNA samples were extracted in the current study may have been less suppressed and less methylated than the tassels on the same plants. Therefore,

in some plants the *rf2* allele may have been suppressed in tassels even though the DNA extracted from young leaves of the same plants were not methylated. However, this would explain only one category of exceptions, plants that were suppressed (i.e., male fertile) and had hypo-methylated DNA. The other category of exceptions, unsuppressed (i.e., male sterile) but which had methylated DNA, is more difficult to reconcile with a suppression mechanism that is dependent upon DNA methylation.

Acknowledgements

We thank Ms. Weijun Chen for assistance sequencing the rf2-DNA1 genomic clone; Feng Liu for assistance in identifying the transposon insertion in the *rf2-m8904* allele; Steve Briggs, who while at Pioneer Hi-Bred International Inc., provided the two B73 genomic libraries; and Alfons Gierl (Technische Universitat Munchen, Germany) for the GAPDH clone. This research was partially supported by a USDA/NRI grant (9600804) to PSS and RPW, a USDA/NRI grant (98001805) to PSS, a Human Frontiers in Science Program grant (RG0067) to Cris Kuhlemeier (Institute of Plant Physiology, University of Berne, Switzerland) and PSS, an NSF grant (DBI-9975868) to PSS and DA, and Hatch Act and State of Iowa funds. This is Journal Paper No. J-18707 of the Iowa Agriculture and Home Economics Experiment Station, Ames, IA 50011; Project Nos. 3554, 3390, 3485, and 3368.

Literature Cited

AUSUBEL, F. M., R. BRENT, R. E. KINGSTON, D. D. MOORE, J. G. SEIDMAN, *et al.*, 1999 *Current protocols in molecular biology*. John Wiley & Sons, New York.

BARKAN, A., and R. A. MARTIENSSEN, 1991 Inactivation of maize transposon *Mu* suppresses a mutant phenotype by activating an outward-reading promoter near the end of *Mu1*. Proc. Natl. Acad. Sci. USA. **88:** 3502-3506.

BENNETZEN, J. L., 1996 The *Mutator* transposable element system of maize. Curr Top Microbiol Immunol. **204:** 195-229.

BENNETZEN, J. L., P. S. SPRINGER, A. D. CRESSE, and M. HENDRICKX, 1993 Specificity and regulation of the *Mutator* transposable element system of maize. Crit. Rev. Plant Sci. **12:** 57-95.

BENITO, M. I., and V. WALBOT, 1997 Characterization of the maize *Mutator* transposable element MURA transposase as a DNA-binding protein. Mol. Cell. Bio. **17:** 5165-5175.

BENSEN, R. J., G. S. JOHAL, V. C. CRANE, J. T. TOSSBERG, P. S. SCHNABLE *et al.*, 1995 Cloning and characterization of the maize An1 gene. Plant Cell **7:** 75-84.

CHANDLER, V. L., and K. J. HARDEMAN, 1992 The *Mu* elements of *Zea mays*. Adv. Genet. **30:** 77-122.

CHANDLER, V. L., and V. WALBOT, 1986 DNA modification of a maize transposable element correlates with loss of activity. Proc Natl Acad Sci U S A **83:** 1767-1771.

CHOMET, P., D. LISCH, K.J. HARDEMAN, V.L. CHANDLER, and M. FREELING, 1991 Identification of a regulatory transposon that controls the *Mutator* transposable element system in maize. Genetics **129:** 261-270.

CUI, X., R. P. WISE, and P. S. SCHNABLE, 1996 The *rf2* nuclear restorer gene of male sterile T-cytoplasm maize. Science **272:** 1334-1336.

DEAN, C., VAN DEN ELZEN P., TAMAKI S., DUNSMUIR P., and J. BEDBROOK, 1985 Differential expression of the eight genes of the petunia ribulose bisphosphate carboxylase small subunit multi-gene family. EMBO J. **4:** 3055-3061.

DONLIN, M. J., D LISCH, and M. FREELING, 1995 Tissue-specific accumulation of MURB, a protein encoded by *MuDR*, the autonomous regulator of the *Mutator* transposable element family. Plant Cell **7:** 1989-2000.

EISEN J. A., M. I. BENITO, and V. WALBOT, 1994 Sequence similarity of putative transposases links the maize *Mutator* autonomous element and a group of bacterial insertion sequences. Nucleic Acids Res. **22:** 2634-6.

FEDOROFF, N. V., 1999 The *suppressor-mutator* element and the evolutionary riddle of transposons. Genes Cells **4:** 11-19.

FOWLER, J. E., G. J. MUEHLBAUER, and M. FREELING, 1996 Mosaic analysis of the *liguleless3* mutant phenotype in maize by coordinate suppression of *Mutator*-insertion alleles. Genetics **143:** 489-503.

GIRARD, L., and M. FREELING, 2000 *Mutator*-suppression alleles of *rough sheath1* and *liguleless3* in maize reveal multiple mechanisms for suppression. Genetics **154:** 437-446.

GRABER J. H., C. R. CANTOR, S. C. MOHR, and T. F. SMITH, 1999 In silico detection of control signals: mRNA 3'-end-processing sequences in diverse species. Proc. Natl. Acad. Sci. USA **96:** 14055-60.

GREENE, B., R. WALKO, and S. HAKE, 1994 *Mutator* insertions in an intron of the maize *knotted1* gene result in dominant suppressible mutations. Genetics **138:** 1275-1285.

GUO Z., and F. SHERMAN, 1995, 3'end-forming signals of yeast mRNA. Mol. Cell. Biol. **15:** 5983-5990.

HERSHBERGER, R. J., C. A. WARREN, and V. WALBOT, 1991 *Mutator* activity in maize correlates with the presence and expression of the *Mu* transposable element *Mu9*. Proc. Natl. Acad. Sci. USA **88:** 10198-10202.

HSIA, A. P., and P. S. SCHNABLE, 1996 DNA sequence analyses support the role of interrupted cap repair in the origin of internal deletions of the maize transposon, *MuDR*. Genetics **142:** 603-618.

HU, G., N. YALPANI, S. P. BRIGGS, and G. S. JOHAL, 1998 A porphyrin pathway impairment is responsible for the phenotype of a dominant disease lesion mimic mutant of maize. Plant Cell **10:** 1095-1105.

Hunt A. G., and J. Messing, 1998 mRNA polyadenylation in plants, pp. 29-39 in *A look beyond transcription: mechanisms determining mRNA stability and translation in plants,* edited by J. BAILEY-SERRES and D. R. GALLIE. American Society of Plant Physiologists, Rockville, MD.

JAMES, M. G., M. J. SCANLON, M. QIN, D. S. ROBERTSON, and A. M. MYERS, 1993 DNA sequence and transcript analysis of transposon *MuA2*, a regulator of *Mutator* transposable element activity in maize. Plant Mol. Biol. **21:** 1181-1185.

KONIECZNY, A., D.F. VOYTAS, M.P. CUMMINGS and F.M. AUSUBEL, 1991 A superfamily of *Arabidopsis thaliana* retrotransposons. Genetics **127:** 801-809.

KUNZE, R., 1996 The maize transposable element *activator* (*Ac*). Curr Top Microbiol Immunol. **204:** 161-194.

LISCH , D., L. GIRARD, M. DONLIN and M. FREELING, 1999 Functional analysis of deletion derivatives of the maize transposon *MuDR* delineates roles for the MURA and MURB proteins. Genetics **151:** 331-341.

LOWE, B., J. MATHERN, and S. HAKE, 1992 Active *Mutator* elements suppress the Knotted phenotype and increase recombination at the *Kn1-0* tandem duplication. Genetics **132:** 813-822.

MARTIENSSEN, R., and A. BARON, 1994 Coordinate suppression of mutations caused by Robertson's *Mutator* transposons in maize. Genetics **136:** 1157-1170.

MARTIENSSEN, R. A., A. BARKAN, M. FREELING, and W. C. TAYLOR, 1989 Molecular cloning of a maize gene involved in photosynthetic membrane organization that is regulated by Robertson's *Mutator*. EMBO J. **8:** 1633-9.

MARTIENSSEN, R., A. BARKAN, W. C. TAYLOR, and M. FREELING, 1990 Somatically heritable switches in the DNA modification of *Mu* transposable elements monitored with a suppressible mutant in maize. Genes Dev. **4:** 331-343.

MASSON, P., J. A. BANKS, and N. FEDOROFF, 1991 Structure and function of the maize *Spm* transposable element. Biochimie. **73:** 5-8.

McCLINTOCK, B., 1964 Aspects of gene regulation in maize. Carnegie Inst. Washington Year Book **63:** 592-602.

McCLINTOCK, B., 1967 Genetic systems regulating gene expression during development. pp. 84-112 in *Developmental Biology,* supplement 1, the 26th Symposium of the Society for Developmental Biology, "Control Mechanisms in Developmental Processes." Academic Press, USA.

ORTIZ, D. F., and J. N. STROMMER, 1990 The *Mu1* maize transposable element induces tissue-specific aberrant splicing and polyadenylation in two *Adh1* mutants. Mol. Cell. Bio. **10:** 2090-2095.

QIN M., D. S. Robertson and A. H. Ellingboe, 1991 Cloning of the *Mutator* transposable element *MuA2*, a putative regulator of somatic mutability of the *a1-Mum2* allele in maize. Genetics **129:** 845-854.

RAIZADA M. N., and V. WALBOT, 2000 The late developmental pattern of *Mu* transposon excision is conferred by a cauliflower mosaic virus 35S-driven MURA cDNA in transgenic maize. Plant Cell **12:** 5-21.

ROBERTSON, D. S., 1978 Characterization of a *mutator* system in maize. Mutat. Res. **5:** 21-28.

ROBERTSON, D. S., and P. S. STINARD, 1989 Genetic analyses of putative two-element system regulating somatic mutability in *mutator*-induced aleurone mutants of maize. Dev. Genet. **10:** 482-506.

ROBERTSON, D. S., D. W. MORRIS, P. S. STINARD, and B. A. ROTH, 1988 Germline and somatic *Mutator* activity: are they functionally related? pp. 17-42, In *Plant Transposable elements*, edited by O. Nelson. Plenum Press, New York and London.

ROTHNIE H. M., 1996 Plant mRNA 3'-end formation. Plant Mol. Biol. **32:** 43-61.

SAGHAI-MAROOF, M. A., K. M. SOLIMAN, R. A. JORGENSEN, and R. W. ALLARD, 1984 Ribosomal DNA spacer-length polymorphisms in barley: mendelian inheritance, chromosomal location, and population dynamics. Proc. Natl. Acad. Sci. USA **81:** 8014-8018.

SCHNABLE, P. S., and P. A. PETERSON, 1986 Distribution of genetically active *Cy* elements among diverse maize lines. Maydica **31:** 59-82.

SCHNABLE, P. S., and R. P. WISE, 1994 Recovery of heritable, transposon-induced, mutant alleles of the *rf2* nuclear restorer of T-cytoplasm maize. Genetics **136:** 1171-1185.

SCHNABLE, P. S., and R. P. WISE, 1998 The molecular basis of cytoplasmic male sterility and fertility restoration. Trends in Plant Science **3:** 175-180.

SCHNABLE, P. S., P. A. PETERSON and H. SAEDLER, 1989 The *bz-rcy* allele of the *Cy* transposable element system of *Zea Mays* contains a *Mu*-like element insertion. Mol. Gen. Genet. **217:** 459-463.

SHEETS M. D., S. C. OGG, and M. P. WICKENS, 1990 Point mutations in AAUAAA and the poly (A) addition site: effects on the accuracy and efficiency of cleavage and polyadenylation *in vitro*. Nucleic Acids Research **18:** 5799-5805.

SNYDER, R. J., and D. N. DUVICK, 1969 Chromosomal location of *Rf2*, a restorer gene for cytoplasmic pollen sterile maize. Crop Sci. **9:** 156-157.

STEEL R. G., and J. H. TORRIE, 1980 Principles and procedures of statistics, a biometrical approach. McGraw-Hill Book Company, New York.

STRATHMANN, M., B. A. HAMILTON, C. A. MAYEDA, M. I. SIMON, E. M. MEYEROWITZ, *et al.*, 1991 Transposon-facilitated DNA sequencing. Proc. Natl. Acad. Sci. USA **88:** 1247-1250.

WAHLE E., and U. RUEGSEGGER, 1999 3'-End processing of pre-mRNA in eukaryotes. FEMS Microbiol. Rev. 1999 **23:** 277-95.

WALBOT, V., 1999 Genes, genomes, genomics. What can plant biologists expect from the 1998 National Science Foundation Plant Genome Research Program? Plant Physiol. **119:** 1151-1156.

WISE, R. P., and P. S. SCHNABLE, 1994 Mapping complementary genes in maize: positioning the *rf1* and *rf2* nuclear-fertility restorer loci of Texas (T) cytoplasm relative to RFLP and visible markers. Theor. Appl. Genet. **88:** 785-795.

WISE, R. P., C. R. BRONSON, P. S. SCHNABLE, and H. T. HORNER, 1999 The genetics, pathology, and molecular biology of T-cytoplasm male sterility in maize. Advances in Agronomy **65:** 9-130.

WU L., T. UEDA, and J. MESSING, 1995 The formation of mRNA 3'-ends in plants. The Plant Journal **8:** 323-329.

XU, X., C. R. DIETRICH, M. DELLEDONNE, Y. XIA, T. J. WEN, *et al.*, 1997 Sequence analysis of the cloned *glossy8* gene of maize suggests that it may code for a beta-ketoacyl reductase required for the biosynthesis of cuticular waxes. Plant Physiol. **115:** 501-510.

ZHAO J., L. HYMAN, and C. MOORE, 1999 Formation of mRNA 3' ends in eukaryotes: mechanism, regulation, and interrelationships with other steps in mRNA synthesis. Microbiol. Mol. Biol. Rev. **63:** 405-45.

TABLE 1

Fertility status of progeny segregating for *rf2-m8110*

Family	No. of Plants			Total No.	χ^2 (1:1)
	F	"S"	S		
92 2123	19	3	4	26	5.53*
92 2124	12	0	14	26	0.154 ns

These data were extracted from Table 2 of SCHNABLE and WISE (1994). Families were derived from the test cross: (T) *rf2-m8110/Rf2-Ky21* x *rf2-R213/rf2-R213*. Plant phenotypes: F, fully male fertile; "S", some anthers exerted; S, completely male sterile with no anthers exerted. *, significant at 0.05 level; ns, not significant at 0.05 level.

TABLE 2

Correlation between male sterility and *rf2* genotype in a family (92 2148) segregating for *rf2-m9390*

Phenotype [a]	No. of Plants [b]		Total
	rf2-m/rf2-R213	*Rf2/rf2-R213*	No.
S	3	0	3
"S" + "F"	6	2	8
F	2	3	5
Total	11	5	16

These data were extracted from Table 3 of SCHNABLE and WISE (1994). The segregating population was from the test cross (T) *rf2-m9390/Rf2-Ky21* x *rf2-R213/rf2-R213*.

[a] Plant phenotypes: F, fully male fertile; "F", more than half of the anthers exerted; "S", some anthers exerted; S, completely male sterile with no anthers exerted.

[b] The *rf2* genotypes were predicted based on RFLP analysis with the *wx1* marker, which is 8.3 cM from the *rf2* gene (WISE and SCHNABLE 1994).

TABLE 3

Comparison of the penetrance of suppressible and non-suppressible *rf2-m* alleles

		No. of Plants					
		F + "F"		S + "S"		Total	
Families	Alleles	*Rf2/rf2*	*rf2-m/rf2*	*rf2-m/rf2*	*Rf2/rf2*	No.	Penetrance [a]
92 2123	*rf2-m8110*	16	3	7	0	26	70%
92 2148	*rf2-m9390*	4	6	4	0	14	40%
92 2126	*rf2-m8122*	4	0	14	0	19	100%
92 2153	*rf2-m9437*	13	0	12	0	25	100%

Random plants from the cross: (T) *rf2-m/Rf2-Ky21* x *rf2-R213/rf2-R213*, were genotyped via PCR using *rf2*-specific and *Mu*-specific primers (MATERIALS AND METHODS). The number of suppressed mutant plants in each family is underlined. Plant phenotypes: F, fully male fertile; "F", more that half of the anthers exerted; "S", some anthers exerted; S, completely male sterile with no anthers exerted.

[a] Penetrance was calculated as the ratio of sterile plants (S + "S") with the genotype *rf2-m/rf2-R213* to the total number of plants with the genotype *rf2-m/rf2-R213*.

TABLE 4

Reactivation of suppressed *rf2-m* alleles

Families	Alleles	Crosses	No. of Fertile Progeny	No. of Sterile Progeny	Reactivation Ratio [a]
97 5432	*rf2-m9390*	(T) *rf2-m/rf2-m* (*Mu* off) x *rf2-R213/ Rf2* (*Mu* on)	36	20	71%
97 5433-34	*rf2-m9390*	same as above	114	21	29%
96g 6104-05	*rf2-m9390*	(T) *rf2-m/rf2-m* (*Mu* off) self	20	0	0%
97 5435-36	*rf2-m8110*	(T) *rf2-R213/rf2-R213* (*Mu* on) x *rf2-m/rf2-R213*	18	95	68%
97 5437	*rf2-m8110*	same as above	1	9	80%
975446	*rf2-m8110*	(T) *rf2-m/rf2-R213* (*Mu* on) x *rf2-m/rf2-m*	55	50	48%
98 6336	*rf2-m8110*	(T) *rf2-m/rf2-m* (*Mu* off) self	15	0	0%

Mu-active lines were crossed to plants carrying suppressed *rf2-m* alleles. The resulting progenies were scored for male-fertile plants. Each row in the table is from a single reactivation cross. (*Mu* on) indicates that the plant contains active *Mu* transposons.

[a] The reactivation ratio was calculated by dividing the number of male-sterile plants by the number of male-sterile plants expected if the *rf2-m* alleles displayed 100% penetrance. This formula was adjusted to account for the segregation of homozygous *rf2-R213* plants in families 97 5435-36 and 97 5437.

TABLE 5

Summary of 94 polyadenylation sites from 58 maize genes in GenBank.

5' Base [a]	Polyadenylation Site [b]				Total
	A	U	C	G	No.
A	0	3	0	0	3
U	33	3	4	2	42
C	25	2	2	1	30
G	15	1	2	1	19
Total	73	9	8	4	94

[a] Base immediate 5' of the polyadenylation site.

[b] Polyadenylation sites were determined as: 1) The "U", "C", and "G" sites annotated in the GenBank records unless they are followed by an "A", in which case this "A" was assumed to be the polyadenylation site; 2) The "A" sites annotated in GenBank unless they are proceeded by an "A", in which case the 5'-most "A" was designated as the polyadenylation site.

TABLE 6

Correlation between methylation status of *Mu1* transposons in the genome and the male fertility in (T) *rf2-m9390/rf2-R213* plants.

	No. of Plants	
Phenotype [a]	Methylated [b]	Hypo-methylated [c]
F	12	4
"F"	2	0
"S"	3	1
S	2	4

[a] Plant phenotypes: F, fully male fertile; "F", more that half of the anthers exerted; "S", some anthers exerted; S, completely male sterile with no anthers exerted.

[b] Plants were scored as "Methylated" if their DNA did not contain a 1.34-kb band that hybridized to the *Mu1*-specific probe, but did contain many larger *Mu1*-hybridizing bands.

[c] Plants were scored as "Hypo-methylated" if their DNA contained a strong 1.34-kb *Mu1*-hybridizing band (e.g., right-most four lanes of the S category in panel A of Figure 6).

TABLE 7

Correlation between methylation status of the *Mu1* transposon in the *rf2-m9390* allele and the male fertility of (T) *rf2-m9390/rf2-R213* plants

	No. of Plants	
Phenotype[a]	Methylated[b]	Hypo-methylated[c]
F	7	2
"F"	2	0
"S"	3	1
S	3	4

[a] Plant phenotypes: F, fully male fertile; "F", more that half of the anthers exerted; "S", some anthers exerted; S, completely male sterile with no anthers exerted.

[b] Plants were scored as "Methylated" if their DNA contained no or only a weakly hybridizing 1.1-kb band and strongly hybridizing 2.4-kb and/or 2.8-kb bands (e.g., two left-most lanes of the F category in panel B of Figure 6).

[c] Plants were scored as "Hypo-methylated" if their DNA contained a strongly hybridizing 1.1-kb band (i.e., the 5' *Hin*fI site relative to *rf2* was unmethylated therefore digested), and weakly hybridizing 2.4-kb and/or 2.8-kb bands (e.g., four right-most lanes of the S category in panel B of Figure 6).

Figure Legends

FIGURE 1. The structure of the *rf2* gene (GenBank accession number AF215823). Filled and open boxes represent coding regions and 5' or 3' UTRs, respectively. Hatched box represents a *copia*-like retrotransposon, *DON QUIXOTE*. The positions of the transposon insertions responsible for the indicated alleles are indicated by triangles (not to scale). Triangles that represent *Mu* insertions responsible for suppressible alleles are filled. The arrows inside the triangles indicate the orientations of the transposons relative to the transposon sequences in GenBank. The position of probe rf2-5m within exon 1 is shown as a bar underneath the 5' UTR. The positions of PCR primers are indicated by arrows. Bm, *Bam*HI; Bg, *Bgl*II; Xb, *Xba*I.

FIGURE 2. The accumulation of *rf2* mRNA in suppressed plants is as high as or only slightly lower than in wild type. An RNA gel blot containing RNA isolated from young tassels of the indicated genotypes was hybridized with a full-length *rf2* cDNA probe (A) and the loading control maize GAPDH (B). All plants were homozygous for the indicated *rf2* alleles unless otherwise noted. The inbred line Q67 is homozygous for the wild-type progenitor (*Rf2-Q67*) of *rf2-m8110* and *rf2-m9390*. All plants in this analysis were male fertile. (T), T cytoplasm; (N) N cytoplasm.

FIGURE 3. RNA gel blot analysis reveals that the suppressed *rf2-m9390* allele does not utilize native transcription initiation sites. About 10 μg of RNA from young tassels was loaded in each lane. Full-length *rf2* cDNA (A) and rf2-5m, a 5' fragment (see Figure 1) of

the *rf2* gene, (B) were used as hybridization probes. All plants were homozygous for the indicated alleles.

FIGURE 4. Alternative transcription initiation sites in the suppressed *rf2-m9390* allele. The open and solid boxes indicate the 5' UTR and coding regions of exons 1 and 2, respectively. Horizontal arrows indicate the primers used for the 5' RACE experiments. Sequence is provided for the *rf2* 5' UTR and the beginning of the coding region. The translation start codon is boxed. The triangle indicates the position of the *Mu1* insertion in *rf2-m9390*. The vertical arrows indicate the transcription initiation sites revealed by 5' RACE using tassel RNA from a male-fertile plant homozygous for the *rf2-m9390* allele. Alternative transcription initiation sites are designated by Roman numbers. The number of clones isolated with each initiation site is indicated.

FIGURE 5. Polyadenylation sites used in suppressed *rf2-m8110* plants and in wild-type *Rf2* plants. The solid and open boxes indicate the translated and 3' UTR regions of the last exon of the *rf2* gene, respectively. The triangle represents the *rcy:Mu7* transposon insertion responsible for the *rf2-m8110* mutation. The two hatched boxes containing horizontal arrows represent the TIRs of the *rcy:Mu7* transposon. The vertical arrows above the TIRs indicate the polyadenylation sites used in the suppressed plants as revealed by 3' RACE experiments. Each arrow represents one event unless otherwise indicated. The solid and dashed arrows indicate the events revealed in the first and the second 3' RACE experiments, respectively. The primer used in the 3' RACE experiment is indicated as a horizontal arrow labeled as RF2C5. The *rcy:Mu7* TIR sequence in which the polyadenylation sites were revealed is

shown above the transposon. The 3' UTR sequence of *Rf2-B73* is shown below. The arrows below the gene structure represent the polyadenylation sites used by the *Rf2-B73* (solid arrows), *Rf2-W22* (gray arrow) and *Rf2-Q67* (dashed arrows) alleles as determined by sequence analysis of cDNA clones (B73 and W22) or 3' RACE (Q67). Polyadenylation sites are designated by Roman numbers. The translation stop codon, TAG, is boxed. The AAUAAA-like PE elements are shaded. U-rich regions flanking polyadenylation sites are underlined.

FIGURE 6. Methylation status in suppressed and nonsuppressed plants with the genotype *rf2-m9390/rf2-R213*. DNA was isolated from young leaves and digested with *Hin*fI. A, a DNA gel blot was hybridized with the *Mu1*-specific probe illustrated in panel C. B, the same blot was stripped and hybridized with the *rf2*-specific probe rf2-5m (panel C). C, a diagram of the *Mu1* insertion and *Hin*fI sites in the *rf2-m9390* allele. The DNA samples in the left-most two lanes are from plants homozygous for the indicated alleles. All plants carry T cytoplasm and their phenotypes are indicated as: F, fully male fertile; "S", with some anthers exerted; S, completely male sterile with no anthers exerted. H, *Hin*fI; distances between restriction sites are indicated in kb.

FIGURE 7. Models for polyadenylation signals. This figure is adapted and modified from GRABER *et al.* (1999). Polyadenylation signals are boxed. UE, upstream element; PE, positioning element; CS, cleavage site (i.e., polyadenylation site); U-rich, U-rich region flanking CS in plant and yeast; DE, downstream element.

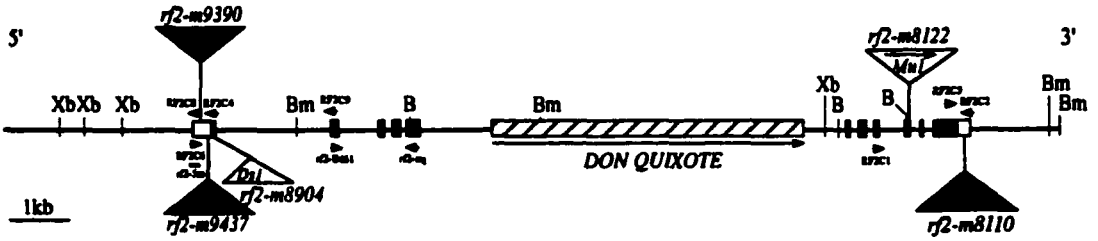

Cui et al., Figure 1

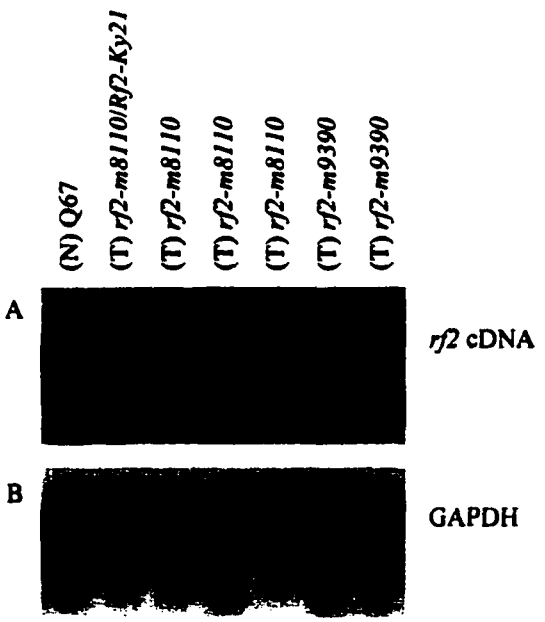

Cui et al., Figure 2

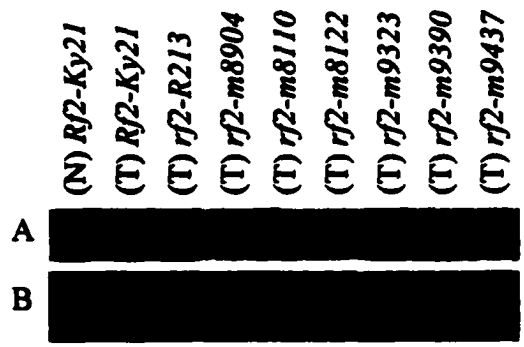

Cui et al., Figure 3

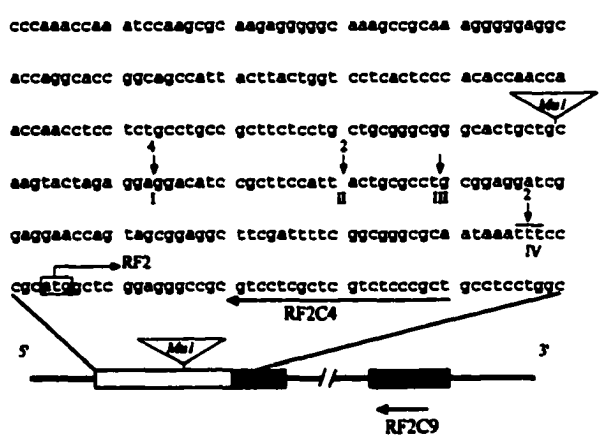

Cui et al, Figure 4

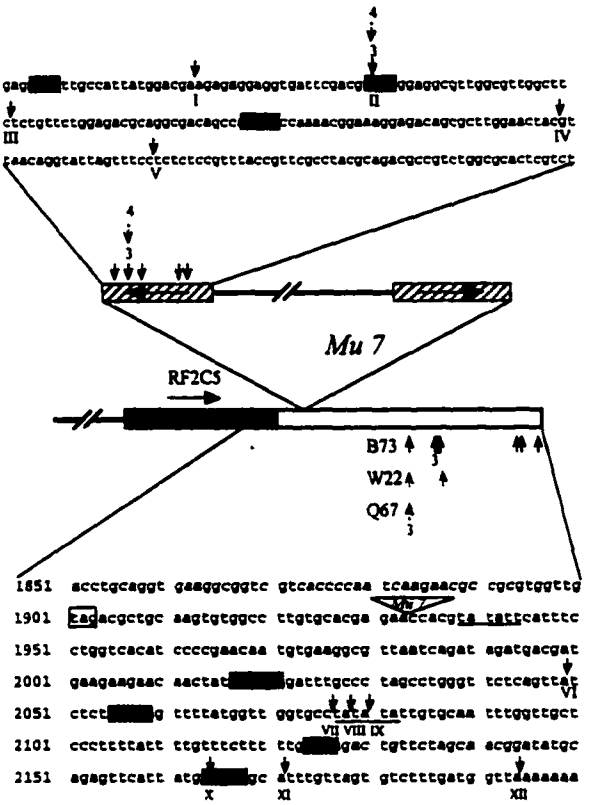

Cui et al., Figure 5

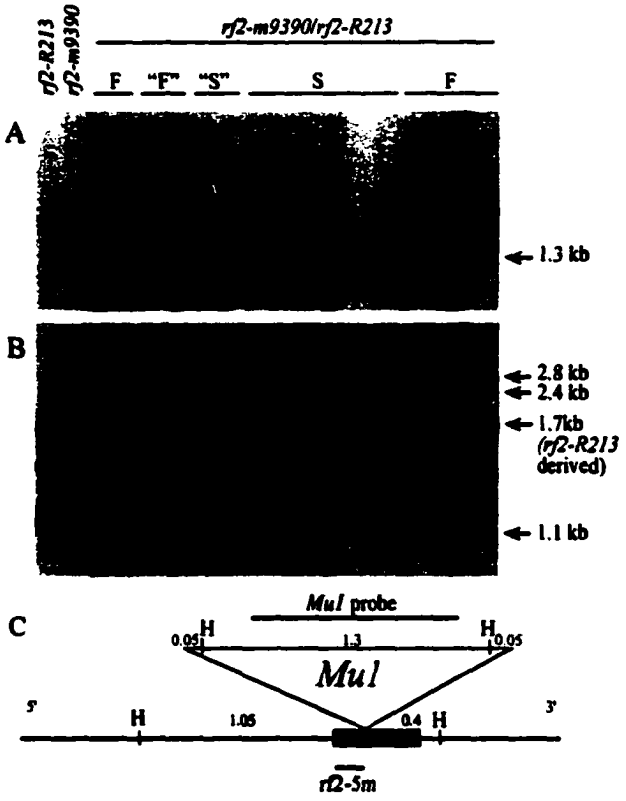

Cui et al., Figure 6

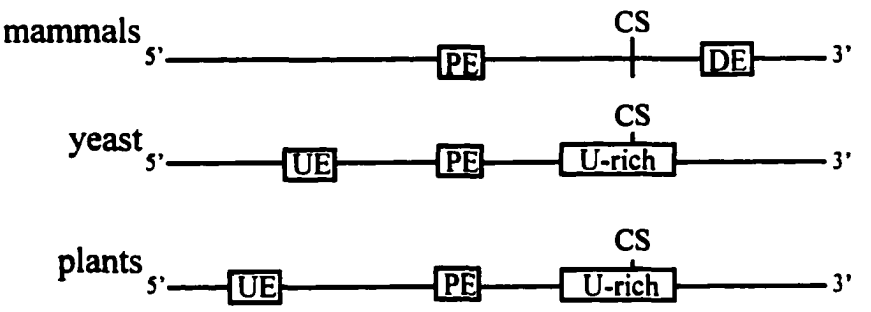

Cui et al., Figure 7

CHAPTER 6. GENERAL CONCLUSIONS

General Conclusions

Maize T-cytoplasm male sterility (cms-T) plays an important role as a model system for studying gene interactions between the nuclear and the mitochondria. This system also has commercial applications in the production of hybrid seeds (Wise et al., 1999). The causal factor of cms-T, URF13, is encoded by the mitochondrial genome and accumulates in the mitochondrial inner membrane (Dewey et al., 1986; Wise et al., 1987). *Rf2* is one of the two complementary nuclear restorers of cms-T (Duvick, 1965). Although a functional *Rf2* allele does not affect the expression of T-*urf13*, it is necessary for male fertility in plants that carry T cytoplasm (Dewey et al., 1987). Most maize inbred lines contain functional *rf2* alleles, even though they have never been exposed to T cytoplasm (Duvick, 1965; Wise et al., 1999). The overall goal of the *rf2* project was to clone the *rf2* gene and to dissect the underlying mechanism of fertility restoration mediated by *Rf2*.

This dissertation describes the early efforts toward understanding the mechanism by which *rf2* restores male fertility to cms-T. The *rf2* gene was cloned via a transposon tagging strategy, and sequence analysis indicated that it has high sequence similarity with mammalian mitochondrial aldehyde dehydrogenases (mtALDHs). One of the functions of mtALDHs in mammals is during ethanol detoxification, whereby ethanol-derived acetaldehyde is converted to acetate in the liver (Lindahl and Petersen, 1991).

The RF2 protein was confirmed to be a mtALDH by a combination of approaches, including subcellular localization, protein expression, and biochemical analyses conducted by Feng Liu in the Schnable laboratory. Detailed genetic analyses of *rf2 Mu*-insertion

mutant alleles established that the mutation of *rf2* not only causes male sterility in T-cytoplasm plants, but also causes anther arrest in the lower florets of N-cytoplasm plants. This result confirmed an earlier hypothesis that the *rf2* gene has a physiological function during anther development independent of its role as cms-T restorer (Schnable and Wise, 1994). This hypothesis was based on the observation that most maize inbred lines carry a functional *Rf2* gene, even though they have never been exposed to T cytoplasm (Duvick, 1965; Wise et al., 1999). Therefore, it appears that the *rf2* gene has been newly recruited to cope with T-cytoplasm male sterility.

To investigate the underlying mechanism, by which functional *Rf2* alleles restore male fertility, the relationship between male fertility and ALDH activity was tested. The spontaneous *rf2* mutant allele, *rf2-R213*, accumulates mRNA and protein at the same levels as those in plants carrying wild-type alleles; however, the mitochondrial protein extracts from plants homozygous for *rf2-R213* has no detectable ALDH activity. Sequence analysis of the *rf2-R213* allele revealed three single nucleotide polymorphisms, one of which caused Pro^{323}-to-Ser substitution in one of the two catalytic domains predicted by the Motif function in the GCG software package. This amino acid substitution likely abolishes the ALDH activity in RF2-R213.

One hypothesis for the role of RF2 in fertility restoration involves the anaerobic fermentation pathway. This pathway converts pyruvate to acetaldehyde via pyruvate decarboxylase (PDC), which could serve as the substrate for RF2. In addition, some enzymes and intermediates of this pathway have been detected in anthers during microsporogenesis and germinating pollen in tobacco (Bucher et al., 1995). To test this hypothesis, mutants in three genes that encode PDC were isolated using the TUSC (Trait

Utility System for Corn) reverse genetic system (Bucher et al., 1994; Bensen et al., 1995). The relationship between the mutant alleles of the *pdc3* gene, cms-T, and *rf2* was extensively characterized. Results indicate that the mutation of *pdc3* does not affect male fertility in either T- or N-cytoplasm plants; however, this experiment provided the first direct evidence that *pdc3* is essential for seedlings to survive anaerobic stresses regardless of the cytoplasm system.

During the analyses of *rf2 Mu*-insertion alleles, instances of *Mu* suppression were observed. Detailed analyses revealed that *Mu* suppression occurs at a high frequency in alleles that carry *Mu* insertions in the 5' UTR or 3' UTR of the *rf2* gene. These results confirmed the previous hypothesis that suppression of alleles that contain a *Mu* insertion in the 5' UTR occurs via the recruitment of alternative transcription start sites for functional transcripts (Barkan and Martienssen, 1991). In addition, it was demonstrated for the first time that the suppression at the 3' UTR occurs via the recruitment of alternative polyadenylation sites from the *Mu*-TIR sequence.

Future Research

The cloning and characterization of *rf2* has enhanced our understanding of mechanisms by which fertility restoration can occur. It has been widely reported that most of the cms restorer genes function by altering the accumulation of transcripts encoded by the mitochondrial novel open reading frames. Other restorers have been shown to delete the novel open reading frame from the mitochondrial genome or alter the mitochondrial RNA editing status (reviewed by Schnable and Wise, 1998). This study on *rf2* revealed that a

fundamental enzyme, such as a mtALDH, could be recruited as a restorer to combat the malfunction in the mitochondria of T cytoplasm.

Since it has been established that *rf2* is a mtALDH, the next question is how does this mtALDH function as a restorer of cms-T? There are several approaches to address this question. One approach involves testing the candidate pathways. Chapter 4 describes a reverse genetic approach to test whether RF2 functions in the fermentation pathway by isolating mutants in the *pdc* genes. This approach was complicated by the fact that there are at least three *pdc* genes in the maize genome (Peschke and Sachs, 1993), therefore, to completely eliminate PDC enzyme function, it will be necessary to knockout all three *pdc* genes. The triple mutant may have to be analyzed to draw a regarding the relationship between the fermentation pathway, *rf2* and male fertility. Since this approach is time-consuming, candidate pathways should first be narrowed down using various complementary approaches, such as global gene expression analyses.

Another approach to characterize the mechanism by which RF2 functions as a restorer of cms-T is to identify the endogenous substrate(s) of RF2 in T and N cytoplasms, determine the source of this substrate, and determine the relationship between this substrate and male fertility. Experiments using this approach are currently being conducted in the Schnable laboratory. In addition, mutant screens are being conducted to isolate enhancers and suppressors of the *rf2* gene.

Finally, comparing *rf2* mutants and wild type plants at various levels may provide critical information leading to the mechanism by which *rf2* functions in cms-T. 1) Comparing the development of anthers from (T) *Rf1rf2* and (T) *rf1Rf2* plants may help to determine whether the restoration by *rf2* is similar to that by *Rf1*. 2) Identifying nuclear

genes that that are differently expressed using microarray and comparing mitochondrial protein accumulations using proteomics between (T) *Rf1rf2* and (T) *Rf1Rf2* may help to identify genes or pathways related to *rf2*. 3) Comparing the lipid or other compositions of the mitochondria between (T) *Rf1rf2* and (T) *Rf1Rf2* might also be helpful.

The anther arrest phenotype observed in *rf2* mutant plants that carry N cytoplasm indicates that RF2 has a physiological function during anther development independent of its role as a restorer of cms-T. The *rf2* mutation specifically affects the anthers in the lower florets. This raises an interesting question: what makes the *rf2* gene essential in the anthers of the lower but not the upper floret? The upper and lower florets within a spikelet have the same structure. The only difference appears to be that the lower floret develops approximately three days after the upper floret (Hsu and Peterson, 1991). This question could be addressed using global gene expression technologies, such as microarray and proteomics. By comparing the patterns of gene expression between anthers from the upper and lower florets at the same stage of development, genes that are differentially involved in the development of these two types of florets could be identified. In combination with reverse genetics, functions of the genes could be analyzed. In addition, detailed microscopic comparisons of anthers from the upper and lower florets of (N) *rf2* could also provide direct evidence on which stages and tissues mtALDH is required. Electron microscopy observations of mitochondria in *rf2* mutants carrying T and N cytoplasms could test whether the *rf2* mutation affects mitochondria in the same way in both cytoplasms.

Literature Cited

Barkan A, Martienssen RA (1991) Inactivation of maize transposon *Mu* suppresses a mutant phenotype by activating an outward-reading promoter near the end of *Mu1*. Proc. Natl. Acad. Sci. USA. 88: 3502-3506

Bensen RJ, Johal GS, Crane VC, Tossberg JT, Schnable PS, Meeley RB, Briggs SP (1995) Cloning and characterization of the maize *An1* gene. Plant Cell 7: 75-84

Bucher M, Brandle R, Kuhlemeier C (1994) Ethanolic fermentation in transgenic tobacco expressing *Zymomonas mobilis* pyruvate decarboxylase. EMBO J. 13: 2755-2763

Bucher M, Brander KA, Sbicego S, Mandel T, Kuhlemeier C (1995) Aerobic fermentation in tobacco pollen. Plant Mol. Biol. 28: 739-750

Dewey RE, Levings CS III, Timothy DH (1986) Novel recombinations in the maize mitochondrial genome produce a unique transcriptional unit in the Texas male-sterile cytoplasm. Cell 44: 439-49

Dewey RE, Timothy DH, Levings CS III (1987) A mitochondrial protein associated with cytoplasmic male sterility in the T cytoplasm of maize. Proc. Natl. Acad. Sci. USA 84: 5374-5378

Duvick DN (1965) Cytoplasmic pollen sterility in corn. In EW Caspari, JM Thoday, Eds, Advances in Genetics Vol. 13. Academic Press, New York, pp. 1-56

Hsu SU, Peterson PA (1991) The upper and lower florets of spikelets in maize. J. Genet. & Breed. 45: 215-222

Lindahl R, Petersen DR (1991) Lipid aldehyde oxidation as a physiological role for class 3 aldehyde dehydrogenases. Biochem. Pharmacol. 41: 1583-1587

Peschke VM, Sachs MM (1993) Multiple pyruvate decarboxylase genes in maize are induced by hypoxia. Mol. Gen. Genet. 240: 206-212

Schnable PS, Wise RP (1994) Recovery of heritable, transposon-induced, mutant alleles of the *rf2* nuclear restorer of T-cytoplasm maize. Genetics 136: 1171-1185

Wise RP, Bronson CR, Schnable PS, Horner HT (1999) The genetics, pathology, and molecular biology of T-cytoplasm male sterility in maize. Adv. Agron. 65: 79-130

Wise RP, Pring DR, Gengenbach BG (1987) Mutation to male fertility and toxin insensitivity in Texas (T)-cytoplasm maize is associated with a frameshift in a mitochondrial open reading frame. Proc. Natl. Acad. Sci. USA 84: 2858-2862

ACKNOWLEDGEMENTS

I would like to thank my major advisor, Dr. Patrick S. Schnable, for his guidance through my dissertation research. Many thanks also go to Dr. Roger Wise for his advice. I thank all my committee members for providing critical comments on my research. The friendship and collaboration within the *rf2* group and the whole Schnable lab made this research possible. Finally, I want to thank my husband, Zhihua Li, for his loving support.